The Role of Mechanics, Degradability, and Topography on Oligodendrocyte Precursor Cell Fate in a 3D Poly(Ethylene Glycol)-Based Hydrogel

---

A Dissertation

Presented to

the faculty of the School of Engineering and Applied Science

University of Virginia

---

in partial fulfillment
of the requirements for the degree

Doctor of Philosophy

by

Lauren N Russell

May 2019

APPROVAL SHEET

This Dissertation
is submitted in partial fulfillment of the requirements
for the degree of
Doctor of Philosophy

Author Signature: _____

This Dissertation has been read and approved by the examining committee:

Advisor: Kyle Lampe

Committee Member: Steven Caliari

Committee Member: Giorgio Carta

Committee Member: Rachel Letteri

Committee Member: Hui Zong

Committee Member: _____

Accepted for the School of Engineering and Applied Science:

Craig H. Benson, School of Engineering and Applied Science

May 2019

Abstract

The myelin sheath is a critical tissue component in the central nervous system (CNS) enabling the fast and efficient communication of neurons. This myelin sheath is the primary tissue component damaged in demyelinating diseases such as multiple sclerosis. Oligodendrocyte precursor cells (OPCs) give rise to myelin forming cells, oligodendrocytes, however current *in vitro* tissue models fail to adequately represent OPC and oligodendrocyte phenotypes, preventing the development of therapeutic strategies to reverse demyelinating diseases. Traditional tissue culture methods in 2D polystyrene dishes fail to mimic the 3D dimensionality of cells in native tissue as well as the stiffness and mechanical properties of native extracellular matrix. 3D hydrogel biomaterials are an attractive alternative to traditional 2D cell culture because they can be engineered to more closely mimic native tissue in terms of mechanics, degradability, or topography. In particular, poly(ethylene glycol)-based (PEG) hydrogels are an exciting avenue for neural tissue engineering due to their ability to recapitulate the highly hydrated and compliant native tissue. In this work, PEG-dimethacrylate (PEG-DM) hydrogels were engineered to create an *in vitro* tissue model that enables OPCs to proliferate and differentiate into oligodendrocytes, and investigate conditions suitable for the ultimate goal of an *in vitro* myelination model.

First, the effects of hydrogel mechanics were investigated to determine their impact on OPC proliferation. When OPC- like cells were encapsulated in the most compliant hydrogels with the largest mesh sizes, cells proliferated more than cells in the stiffer hydrogels, as shown through higher values of ATP and DNA and a greater propensity for EdU staining. In the least compliant materials, cells expressed more PDGFRα, platelet derived growth factor receptor-α, suggesting that cells in the least compliant materials may de-differentiate into a more proliferative cell type.

Hydrogels that degrade over the course of weeks were made by incorporating polylactic acid (PLA) into the hydrogel by mixing ratios of PEG-DM with PEG-PLA-DM. PLA was chosen as the degradable unit due to the mild antioxidant properties of lactic acid, which is released upon hydrolytic degradation. OPC-like cells encapsulated in the degradable hydrogels were able to extend processes due to the degradation, but did not respond metabolically to the release of lactic acid. These results are not surprising given the differing role of lactic acid in

metabolism between cancer cells and primary OPCs. Primary OPCs were also investigated for preliminary differences between metabolism and degradable macromer content, however minimal metabolic differences were found, likely due to general poor cell viability from the OPC isolation process.

In the CNS, OPCs are known to respond to neuronal topography to differentiate and create the electrically insulating myelin sheath, thus the differentiation of OPCs in fiber containing hydrogels was also assessed. Electrospun fibers, engineered to mimic the high aspect ratio and diameter of neuronal axons, were encapsulated in the degradable PEG hydrogels. When cells and fibers were co-encapsulated, OPC-like cells remained more viable compared to cells in hydrogels without fibers. Additionally, OPC-like cells were observed extending processes towards and along fibers, similar to native OPCs or oligodendrocytes in the brain. However, gene expression results from primary rat OPCs showed minimal differences in both OPC and oligodendrocyte genes, indicating that differentiation may not occur from the introduction of topographical cues alone.

Finally, an important observation is that primary rat OPCs encapsulated in PEG hydrogels remained more viable over 7 days when compared to traditional 2D cell culture, measured through apoptosis and viability quantification assays. Together these results suggest the importance of hydrogel mechanics, degradability, and topography on OPC fate and the potential biomaterials have in developing better myelination models. Despite these strides, more work remains to fully develop an *in vitro* myelination model.

Acknowledgements

First and foremost, I would like to acknowledge my advisor Dr. Kyle Lampe. I really appreciate your dedication and patience the first couple of years in setting up the lab. Without you pushing me to apply to things, my resume wouldn't look half as impressive. You have been a great mentor over these last six years and I'm excited to see the great science to come from your lab.

I would like to thank all the members of my committee for all their time, input, and resources: Dr. Stephen Caliari, Dr. Giorgio Carta, Dr. Alban Gaultier, Dr. Rachel Letteri, and Dr. Hui Zong. Thank you to all of the Chemical Engineering staff for putting up with my orders to restock the lab and their lost shipping labels, making sure I got paid, and installing/fixing random things around the lab: Ricky Buchanan, Jennifer Davis, Vickie Faulconer, Jen Lamb, Teresa Morris, April Spencer, and Ryan Thompson.

This work was funded by the UVA Biotechnology Training Grant and the Metro Washington Chapter of ARCS.

Thank you, Dr. Periasamy for the use of the Keck Center for Cellular Imaging microscopes and your mentorship and help over the years.

I would like to thank all the past and present members of the Lampe Lab. In particular, Chelsea Harris and Sarah Shamsie for helping start up the lab, the other graduate students during my time- Edi Meco, Nick Murphy, Deniz Unal, James Tang, and Zhiqi Zhang. To all of my wonderful undergrads- Felipe Barraza, Marika Gutzman, Patryck Michalik, Meghan Pinezich, Ethan Purnell, & Julia Shanno- thank you for all your hard work. Special shout out to Meghan for my 2nd paper cake, Ethan for all your contributions to our fiber project, and Julia and Patryck for directly contributing to the data included in my dissertation.

To all my friends I've made in Charlottesville through the University of Virginia, C'ville Social, and my trivia team—I am grateful for all the fun times we had. Special Thanks to Dr. Arch Creasy, Dr. Sabra Hanspal, Dr. Jason Reck, and Dr. Laura Sipe for sharing the frustrations of grad school with me. Thanks to Dr. Katy Wilson, Meghan Dunegan, and Nik Hays for all the fun times at our apartment and to Dr. Phil Shivokevich for all the sunrise hikes.

To all my old friends- Lee Grove, Tyler and Sherrie Flint, Jacob Bean, and Gretchen Lee. Thanks for all the fun weekend trips and understanding when I had to bring along my work.

I would like to thank my dad for all his support throughout the years. You have been the best role model I could ask for. Thank you for all of the love, football games, and restaurant weeks along the way.

Finally, I would like to thank Tyler. Thank you for being my best friend, for popping bubbles with me on late lab days, and for getting tacos every Saturday. Without you my last year would have been unbearable.

Abbreviations

AkT	Protein kinase B
ATP	Adenosine Triphospate
BDNF	Brain-Derived Neurotrophic Factor
bFGF	Basic Fibroblast Growth Factor
CNS	Central Nervous System
CNTF	Ciliary Neurotropic Factor
DNA	Deoxyribonucleic acid
DM	Dimethacrylate
ECM	Extracellular Matrix
GSH	Glutathione
GSSG	Glutathione disulfide
H_2O_2	Hydrogen peroxide
L1	Laminin type 1
MapK	Mitogen-Activated Protein Kinases
MBP	Myelin Basic Protein
MS	Multiple Sclerosis
NMDA	N-Methyl-D-Aspartate
NPC	Neural Progenitor Cell
Nrf2	Nuclear Factor-Like 2
NSC	Neural Stem Cell
NT-3	Neurotrophin-3
OPC	Oligodendrocyte Precursor Cell
PDGF	Platelet-Derived Growth Factor
PEG	Polyetheylene Glycol
PLA	Polylactic Acid
PLGA	Poly(lactic acid-co-glycolic acid)
PLL	Poly(L-Lysine)
PLL+LN	Poly(L-Lysine) with Laminin
qPCR	Quantitative Polymerase Chain Reaction
SHH	Sonic Hedgehog

Table of Contents

Table of Figures

Index of Tables

1 Introduction

1.1 Oligodendrocyte Precursor Cells and Oligodendrocytes in the CNS

Oligodendrocyte precursor cells (OPCs) are capable of proliferating and differentiating into the myelinating oligodendrocytes in the brain and spinal cord. These OPCs are highly migratory cells that move along the CNS vasculature[1]. OPCs then begin extending processes towards neuronal axons where they begin to generate the electrically insulating myelin sheath as they differentiate into oligodendrocytes. In this role, each oligodendrocyte electrically insulates many neuronal axons and together, they contribute a significant amount to the CNS stiffness[2].

In normal brain development most myelination occurs after birth, and continues for the first 20 years of life in humans[3]. Despite the long timescale for complete myelination in the CNS, each OPC matures into a myelinating oligodendrocyte as quickly as 5 hours[4]. The highly organized formation of myelin is a complicated process that involves many factors. Vasculature or axonal signaling molecules, neuronal topography, and neuronal activity have all been shown to play a role in OPC maturation[5]. Neuregulin-1 (NRG-1) is a signaling molecule secreted by neurons or expressed on the surface of axons. This molecule has been shown to either enhance OPC survival through activation of the AkT pathway or guide differentiation in the presence of laminin-2a through the activation of the MAPK pathway[6]. Additionally, electrical activity, experience, and the functional use of neurons have been shown to further guide maturation[5]. Notably, myelination of new brain regions correlates with cognitive ability and developmental milestones such as speech in children, while social isolation has been shown to result in myelination deficits[7]. Furthermore electrical signaling and the associated release of glutamate along neurons have been shown to increase the number of myelinating segments along the axon *in vitro*[8]. Function of an important glutamate receptor, NMDA, was further shown to promote OPC differentiation[9]. However, despite the benefit in development, NMDA receptor knockout mice were found to have normal myelination[10], indicating that many factors simultaneously guide and enhance differentiation.

In healthy adult brain tissue, OPCs remain in large amounts, 2% in gray matter and 8-9% in white matter, and are able to continually replenish myelin through normal maturation[11]. However in injury or diseases, such as multiple sclerosis, OPCs face significant challenges in maturing and replenishing damaged myelin[12]. Multiple sclerosis in particular involves an

immune response as well as a pathology marked by active, demyelinating lesions. These lesions have numerous inhibitory factors, from low molecular weight hyaluronan[13] to interferon-γ[14]. Reactive T-cells in the injury environment express inflammatory cytokines and secrete reactive oxygen species (ROS) to assist in debris clean up. However, these cytokines and ROS hinder the ability of OPCs to differentiate and remyelinate the demyelinated axons.

1.2 OPC and Oligodendrocyte Response to Reactive Oxygen Species

In the injury environments such as MS, oxidative stress is thought to play a large role in the debilitating disease progression[15]. Activated microglia and infiltrating macrophages antagonize this disease phenotype through their release of large amounts of reactive oxygen species[16]. Hydrogen peroxide, in particular, is a known oxidizer found in injury environments that causes lipid peroxidation and oxidizes important cellular redox pairs, such as lactate or glutathione[17]. This exposure to oxidative stress in OPCs and oligodendrocytes causes the activation of the transcription factor Nrf2 as an anti-oxidative stress response[18]. The activation of Nrf2 results in the oxidation of glutathione to GSSG and a more oxidized intracellular redox state[19].

Both OPCs and oligodendrocytes are both highly susceptible to damage due to oxidative stress. It is well understood that the intracellular redox state of a cell directly correlates with the proliferation or differentiation potential[20]. In OPCs, a more reduced intracellular redox state suggests the ability to proliferate while a more oxidized intracellular redox state demonstrates a move towards a more differentiated oligodendrocyte phenotype[20]. This intracellular redox state can be tuned by incorporating many soluble factors, from antioxidants[21] to growth factors such as PDGF[20]. However, when OPCs are subjected to oxidative stress from buthionine sulfoximine or tert-butyl hydrogen peroxide, OPCs lose the ability to differentiate[22]. In these environments, maturation inhibitory genes are upregulated while mature oligodendrocyte markers are downregulated. Furthermore, mature oligodendrocytes undergo lipid peroxidation and begin apoptosis, or programed cell death, when exposed to large amounts of hydrogen peroxide[23].

1.3 Topography and OPCs

Many cell types respond to topography, but in the CNS, OPCs are highly responsive to numerous topographical cues. Oligodendrocytes have recently been found to migrate along the

brain vasculature[1], where they respond to numerous secreted factors such as platelet derived growth factor (PDGF) [24], vascular endothelial growth factor[25], or fibroblast growth factor[26]. Furthermore, the brain vasculature, fibrous extracellular matrix proteins, and topography provide important biophysical signaling cues. Most importantly, OPCs are known to extend processes toward neuronal axons where they then respond to axonal topography by their ultimate role of differentiating and becoming functional myelinating oligodendrocytes. [27]

Neuronal axon diameter is highly variable across brain and spinal cord regions, with a 100-fold variation of 0.1 to 10 μm[28]. This wide variation in axon diameter leads to significant differences in OPC and oligodendrocyte morphology[29]. Oligodendrocytes in the spinal cord, where neurons have a large diameter, often are seen only myelinating one neuronal axon, while oligodendrocytes found in the corpus callosum are capable of myelinating as many as 50 axons[30]. These large axons often have thicker myelin sheaths indicating that oligodendrocytes respond to the aspect ratio and curvature to ensure optimal insulation[30a].

Recently, a promising myelination model was developed that utilizes electrospun fibers to act as axon mimics[31]. These fibers were spun from either polylactic acid or polystyrene and were generated over a range of 0.2 to 4 μm[31a]. While this model enables myelination on some fibers there appears to be a critical fiber diameter. Optimal myelination and myelin basic protein (MBP) expression appeared on fibers in the range of 2-4 μm[31a]. *In vivo,* oligodendrocytes in a region with small axon diameters would myelinate many neurons[30b], however in this model OPCs seeded on fibers with a small diameter (0.2-0.8 μm) were not found to myelinate or mature. This model yielded only a small amount of myelin positive OPCs suggesting the need for additional cell signaling components or 3D dimensionality.

1.4 OPCs and Their Interaction with Native ECM

The CNS extracellular matrix is unique compared to other tissues in that it is comprised of significantly less structural matrix proteins[32]. In the CNS, most of the common structural proteins such as laminin, collagen, or fibronectin, are found primarily in the basement membrane along the blood vasculature[33]. The main component of the extracellular matrix is hyaluronic acid, which form the backbone of the ECM along with proteoglycans and glycoproteins[33]. This unique makeup causes the characteristic properties of CNS tissue, namely their hydrophilicity and complaint nature.

OPCs in the brain are known to have significantly greater contact with extracellular matrix proteins than mature oligodendrocytes as they migrate along the vasculature[1]. OPCs have even been shown to deposit extracellular matrix proteins, while mature oligodendrocytes are known to only have brief encounters with extracellular matrix proteins as most ECM proteins are only colocalize with oligodendrocytes following injury[34]. OPCs and oligodendrocytes respond differently to all types of ECM proteins, in particular collagen has been shown to inhibit OPC migration[34]. While OPC growth cones actively avoid collagen, oligodendrocytes lack collagen binding receptors[34]. The same trend is found for laminin. OPCs have a high expression of laminin receptors while mature oligodendrocytes have a significantly lower expression[35].

1.5 Objectives of This Work

The overall objective of this work is to develop a three-dimensional, *in vitro*, myelination model that can be further used to either gain a basic understanding of OPC maturation into oligodendrocytes or develop novel therapeutics for demyelinating diseases, such as multiple sclerosis. In particular, this work targets using a PEG based hydrogel due to its ability to mimic the highly hydrated native neural tissue and further investigate PEG hydrogel material properties on OPC maturation. Here, we investigate the effect of hydrogel compositions from molecular weight to degradability and incorporation of topographical cues. The specific objectives are outlined below:

1. Investigate the effect of hydrogel stiffness and mesh size on the proliferation and differentiation of OPC-like cells.
2. Determine the role of degradability and lactic acid release from a PEG-PLA hydrogel on intracellular redox state of OPC-like cells.
3. Incorporate electrospun fibers into the PEG hydrogel to guide differentiation of OPCs into mature myelinating oligodendrocytes.
4. Assess the ability of the PEG hydrogel as an artificial extracellular matrix to increase the long-term viability of OPCs in culture.

Cells were cultured in hydrogels over the course of a week at 37°C with 5% CO_2 and 100% relative humidity. Viability was assessed at discrete time points through the use of the

Live/Dead assay and confocal microscopy or quantitative ATP and DNA assays in a plate reader. Metabolic activity was assessed through the ATP assay or alamarBlue assay, while intracellular redox state was measured through either a glutathione quantitative assay or Mitotracker Orange stain. Additionally, maturation was assessed through the use of quantitative polymerase chain reaction (qPCR) for mature, oligodendrocyte markers or immature, OPC markers. Immunostaining for various markers was also preformed to confirm qPCR. These results all combine to increase our understanding on how OPCs respond to their surrounding extracellular matrix to mature and differentiate into mature, myelinating oligodendrocytes. Furthermore, from this knowledge, a more advanced myelination model can be derived to not only develop better therapies for demyelinating diseases, but also broaden our basic understanding of oligodendrocyte biology.

1. Tsai, H.-H.; Niu, J.; Munji, R.; Davalos, D.; Chang, J.; Zhang, H.; Tien, A.-C.; Kuo, C. J.; Chan, J. R.; Daneman, R.; Fancy, S. P. J., Oligodendrocyte precursors migrate along vasculature in the developing nervous system. *Science* **2016,** *351* (6271), 379-384.
2. Weickenmeier, J.; de Rooij, R.; Budday, S.; Steinmann, P.; Ovaert, T. C.; Kuhl, E., Brain stiffness increases with myelin content. *Acta biomaterialia* **2016,** *42*, 265-272.
3. Andersen, S. L., Trajectories of brain development: point of vulnerability or window of opportunity? *Neuroscience & Biobehavioral Reviews* **2003,** *27* (1-2), 3-18.
4. Czopka, T.; Ffrench-Constant, C.; Lyons, D. A., Individual oligodendrocytes have only a few hours in which to generate new myelin sheaths in vivo. *Dev Cell* **2013,** *25* (6), 599-609.
5. Hughes, E. G.; Appel, B., The cell biology of CNS myelination. *Curr Opin Neurobiol* **2016,** *39*, 93-100.
6. (a) Taveggia, C.; Thaker, P.; Petrylak, A.; Caporaso, G. L.; Toews, A.; Falls, D. L.; Einheber, S.; Salzer, J. L., Type III neuregulin-1 promotes oligodendrocyte myelination. *Glia* **2008,** *56* (3), 284-93; (b) Mitew, S.; Hay, C. M.; Peckham, H.; Xiao, J.; Koenning, M.; Emery, B., Mechanisms regulating the development of oligodendrocytes and central nervous system myelin. *Neuroscience* **2014,** *276*, 29-47.
7. (a) Liu, J.; Dietz, K.; DeLoyht, J. M.; Pedre, X.; Kelkar, D.; Kaur, J.; Vialou, V.; Lobo, M. K.; Dietz, D. M.; Nestler, E. J.; Dupree, J.; Casaccia, P., Impaired adult myelination in the prefrontal cortex of socially isolated mice. *Nat Neurosci* **2012,** *15* (12), 1621-3; (b) Makinodan, M.; Rosen, K.; Ito, S.; Corfas, G., A Critical Period for Social Experience- Dependent Oligodendrocyte Maturation and Myelination. *Science* **2012,** *337*, 1357-1360.
8. Wake, H.; Lee, F. R.; Fields, R. D., Control of Local Protein Synthesis and Initial Events in Myelination by Action Potentials. *Science* **2011,** *333* (6049), 1647-1651.
9. Li, C.; Xiao, L.; Liu, X.; Yang, W.; Shen, W.; Hu, C.; Yang, G.; He, C., A functional role of NMDA receptor in regulating the differentiation of oligodendrocyte precursor cells and remyelination. *Glia* **2013,** *61* (5), 732-49.

10. Guo, F.; Maeda, Y.; Ko, E. M.; Delgado, M.; Horiuchi, M.; Soulika, A.; Miers, L.; Burns, T.; Itoh, T.; Shen, H.; Lee, E.; Sohn, J.; Pleasure, D., Disruption of NMDA receptors in oligodendroglial lineage cells does not alter their susceptibility to experimental autoimmune encephalomyelitis or their normal development. *The Journal of neuroscience : the official journal of the Society for Neuroscience* **2012,** *32* (2), 639-45.
11. Dawson, M.; Polito, A.; Levine, J.; Reynolds, R., NG2-expressing glial progenitor cells: an abundant and widespread population of cycling cells in the adult rat CNS. *Molecular and Cellular Neuroscience* **2003,** *24* (2), 476-488.
12. Wolswijk, G., Chronic Stage Multiple Sclerosis Lesions Contain a Relatively Quiescent Population of Oligodendrocyte Precursor Cells. *Journal of Neuroscience* **1998,** *18* (2), 601-609.
13. Sloane, J.; Batt, C.; Ma, Y.; Harris, Z.; Trap, B.; Vartanian, T., Hyaluronan blocks oligodendrocyte progenitor maturation and remyelination through TLR2. *Proceedings of the National Academy of Sciences of the United States of America* **2009,** *107* (25), 11555-11560.
14. Heine, S.; Ebnet, J.; Maysami, S.; Stangel, M., Effects of interferon-beta on oligodendroglial cells. *J Neuroimmunol* **2006,** *177* (1-2), 173-80.
15. Ohl, K.; Tenbrock, K.; Kipp, M., Oxidative stress in multiple sclerosis: Central and peripheral mode of action. *Exp Neurol* **2016,** *277*, 58-67.
16. Luo, C.; Jian, C.; Liao, Y.; Huang, Q.; Wu, Y.; Liu, X.; Zou, D.; Wu, Y., The role of microglia in multiple sclerosis. *Neuropsychiatr Dis Treat* **2017,** *13*, 1661-1667.
17. Lee, D. H.; Gold, R.; Linker, R. A., Mechanisms of oxidative damage in multiple sclerosis and neurodegenerative diseases: therapeutic modulation via fumaric acid esters. *Int J Mol Sci* **2012,** *13* (9), 11783-803.
18. (a) Licht-Mayer, S.; Wimmer, I.; Traffehn, S.; Metz, I.; Bruck, W.; Bauer, J.; Bradl, M.; Lassmann, H., Cell type-specific Nrf2 expression in multiple sclerosis lesions. *Acta neuropathologica* **2015,** *130* (2), 263-77; (b) Keough, M. B.; Yong, V. W., Remyelination therapy for multiple sclerosis. *Neurotherapeutics* **2013,** *10* (1), 44-54.
19. Harvey, C. J.; Thimmulappa, R. K.; Singh, A.; Blake, D. J.; Ling, G.; Wakabayashi, N.; Fujii, J.; Myers, A.; Biswal, S., Nrf2-regulated glutathione recycling independent of biosynthesis is critical for cell survival during oxidative stress. *Free Radic Biol Med* **2009,** *46* (4), 443-53.
20. Smith, J.; Ladi, E.; Mayer-Proschel, M.; Noble, M., Redox state is a central modulator of the balance between self-renewal and differentiation in a dividing glial precursor cell. *Proceedings of the National Academy of Sciences of the United States of America* **2000,** *97* (18), 10032-7.
21. Li, Z.; Dong, T.; Proschel, C.; Noble, M., Chemically Diverse Toxicants Converge on Fyn and c-Cbl to Disrupt Precursor Cell Function. *PloS Biol* **2007,** *5* (2), 0212-0231.
22. French, H. M.; Reid, M.; Mamontov, P.; Simmons, R. A.; Grinspan, J. B., Oxidative stress disrupts oligodendrocyte maturation. *Journal of neuroscience research* **2009,** *87* (14), 3076-87.
23. Jana, A.; Pahan, K., Oxidative stress kills human primary oligodendrocytes via neutral sphingoyelinase: implications for multiple sclerosis. *J Neuroimmune Pharmacol* **2007,** *2* (2), 184-193.
24. Tang, D. G.; Tokumoto, Y. M.; Raff, M. C., Long Term Culture of Purified Postnatal Oligodendrocyte Precursor Cells: Evidence for an Intrinsic Maturation Program that Plays out over Months. *The Journal of Cell Biology* **2000,** *148* (5), 971-984.

25. Hayakawa, K.; Pham, L. D.; Som, A. T.; Lee, B. J.; Guo, S.; Lo, E. H.; Arai, K., Vascular endothelial growth factor regulates the migration of oligodendrocyte precursor cells. *The Journal of neuroscience : the official journal of the Society for Neuroscience* **2011,** *31* (29), 10666-70.
26. Noble, M.; Barnett, S.; Bogler, O.; Land, H.; Wolswijk, G.; Wren, D., Control of Division and Differentiation in Oligodendrocyte - Type - 2 Astrocyte Progenitor Cells. 2007; pp 227-249.
27. Snaidero, N.; Simons, M., Myelination at a glance. *J Cell Sci* **2014,** *127* (Pt 14), 2999-3004.
28. Liewald, D.; Miller, R.; Logothetis, N.; Wagner, H. J.; Schuz, A., Distribution of axon diameters in cortical white matter: an electron-microscopic study on three human brains and a macaque. *Biol Cybern* **2014,** *108* (5), 541-57.
29. Simons, M.; Nave, K. A., Oligodendrocytes: Myelination and Axonal Support. *Cold Spring Harb Perspect Biol* **2015,** *8* (1), a020479.
30. (a) Murray, J.; Blakemore, W., The relationship between internodal length and fibre diameter in the spinal cord of the cat. *Journal of the Neurological Sciences* **1980,** *45*, 29-41; (b) Hilderbrand, C.; Hahn, R., Relation between myelin sheath thickness and axon size in spinal cord white matter of some vertebrate species. *Journal of the Neurological Sciences* **1978,** *38*, 421-434.
31. (a) Lee, S.; Leach, M. K.; Redmond, S. A.; Chong, S. Y.; Mellon, S. H.; Tuck, S. J.; Feng, Z. Q.; Corey, J. M.; Chan, J. R., A culture system to study oligodendrocyte myelination processes using engineered nanofibers. *Nature methods* **2012,** *9* (9), 917-22; (b) Lee, S.; Chong, S. Y. C.; Tuck, S. J.; Corey, J. M.; Chan, J. R., A rapid and reproducible assay for modeling myelination by oligodendrocytes using engineered nanofibers. *Nature Protocols* **2013,** *8* (4), 771-782.
32. Quraishe, S.; Forbes, L. H.; Andrews, M. R., The Extracellular Environment of the CNS: Influence on Plasticity, Sprouting, and Axonal Regeneration after Spinal Cord Injury. *Neural Plast* **2018,** *2018*, 2952386.
33. Benarroch, E. E., Extracellular matrix in the CNS. *Neurology* **2015,** *85* (16), 1417.
34. Pu, A.; Stephenson, E. L.; Yong, V. W., The extracellular matrix: Focus on oligodendrocyte biology and targeting CSPGs for remyelination therapies. *Glia* **2018,** *66* (9), 1809-1825.
35. O'Meara, R. W.; Michalski, J. P.; Kothary, R., Integrin signaling in oligodendrocytes and its importance in CNS myelination. *J Signal Transduct* **2011,** *2011*, 354091.

2 Engineering Biomaterials to Influence Oligodendroglial Growth, Maturation, and Myelin production

Published as: LN Russell, KJ Lampe, "Engineering biomaterials to influence oligodendroglial growth, maturation, and myelin production," *Journal of Cells, Tissues, and Organs*, 202: 85-101 (2016).

2.1 Abstract

Millions of people suffer from damage or disease to the nervous system resulting in a loss of myelin, such as through a spinal cord injury or multiple sclerosis. Diminished myelin levels lead to further cell death, in which unmyelinated neurons die. In the central nervous system, a loss of myelin is especially detrimental because of its poor ability to regenerate. Cell therapies such as stem or precursor cell injection have been investigated as stem cells are able to grow and differentiate into the damaged cells; however, stem cell injection alone has been unsuccessful in many areas of neural regeneration. Therefore, researchers have begun exploring combined therapies with biomaterials that promote cell growth and differentiation while localizing cells in the injured area. The regrowth of myelinating oligodendrocytes from neural stem cells through a biomaterials approach may prove to be a beneficial strategy following the onset of demyelination. This article reviews recent advancements in biomaterial strategies for differentiation of neural stem cells into oligodendrocytes, and presents new data indicating appropriate properties for oligodendrocyte precursor cell growth. In some cases, an increase in oligodendrocyte differentiation alongside of neurons is further highlighted for functional improvements where the biomaterial was then tested for increased myelination both *in vitro* and *in vivo*.

2.2 Introduction

Oligodendrocytes in the central nervous system (CNS) are responsible for generating myelin, which facilitates interneuronal communication while also providing structural and trophic support to axons [1]. The extreme toll of myelin diseases and injuries leading to demyelination requires new strategies that can support CNS regeneration via myelin production. In the context of spinal cord injury, for instance, while various experimental strategies have demonstrated an improvement in neuronal numbers, there has rarely been any evidence of myelin on spared or regenerated axons. Biomaterials can provide new insights to disease and regeneration via improved tissue models *in vitro*, as well as providing a potential therapeutic benefit via tissue engineering.

In development of the mammalian nervous system, oligodendrocytes form much later in CNS tissue maturation, following the establishment of neurons (Figure 2-1) [2]. A protective myelin sheath is formed when oligodendrocytes extend processes to many axons and concentrically wrap a segment of the axon in many layers [3]. Myelin is an electrically insulating layer that allows neurons to signal up to a hundred times faster than unmyelinated axons [4]. Without this myelin sheath, ion channels down the entire length of the axon open and require a larger charge to initiate an action potential [5]. This disrupts the functionality of neurons, stops trophic support, and leads to further cell death [6].

Figure 2-1 Human neurogenesis timeline. Myelination begins just before birth and continues until the age of 20 [Anderson, 2003]. Reprinted with permission from Elsevier.

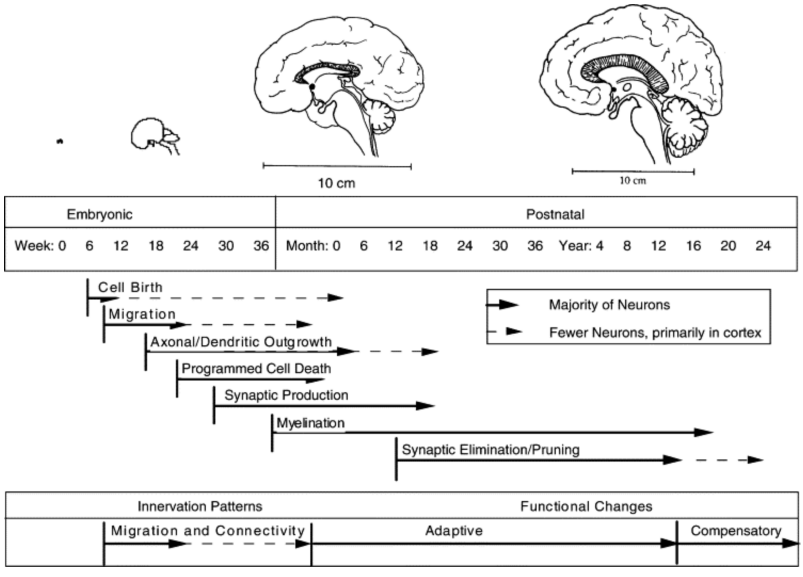

Diseases and injuries resulting in this loss of myelin and behavioral functionality affect over 5 million people worldwide [7]. In patients, demyelination occurs as a result of oligodendrocyte cell death often caused by injury, infections, or inflammation where the immune system targets oligodendrocytes. Multiple sclerosis (MS) is one of the most well-known inflammatory demyelinating diseases affecting 2.5 million people worldwide [7a]. Additionally, spinal cord injury induced paralysis affects over 2.5 million people, typically due in part to the demyelination of axons after an injury [7b]. Both spinal cord injuries and late stages of MS often leave patients dependent on permanent caregivers for everyday functions.

Following these demyelinating diseases or injuries, the body's own stem cells are often unable to migrate to the affected area and repair the damage due in part to the immune system (Figure 2-2). Following many injuries, astrocytes and microglia become activated and move to the injured area to clean up cell debris from the damaged cells [8]. In some cases, a large number of astrocytes and microglia become activated and wall off the damaged area by chemical or physical means, further preventing migration of neural stem cells (NSCs) into the injured area and preventing repair or regrowth from differentiating stem cells.

Figure 2-2 Oligodendrocytes myelinate neuronal axons within normal healthy tissue. Oligodendrocytes generate the myelin sheath in a pattern with defined unmyelinated areas, nodes of Ranvier. Axons form synapses via connections with dendrites of neighboring neurons. This all occurs in the tissue ECM, where both neuronal and oligodendroglial cells bind to the matrix via integrin-binding domains and remodel tissue under both healthy and diseased states. Following injury or disease, scavenger cells, such as T cells or astrocytes, migrate to the damaged area to clean up debris.

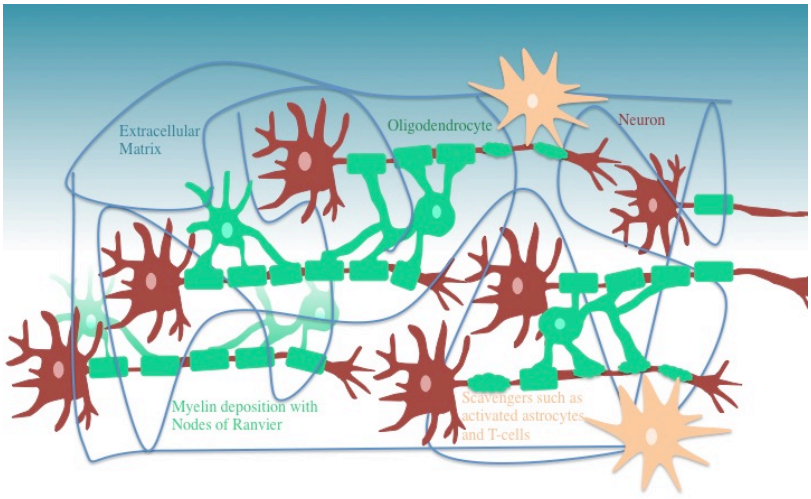

2.3 Biomaterials as vehicles for neural repair

Because of the impact demyelinating diseases have on so many people and the limited CNS repair that occurs without intervention, researchers are investigating many therapies for neural regeneration [9]. Drugs are being researched which prevent relapses (copaxone) [10], limit glial scarring (chondroitinase) [11], or induce myelination and axon growth (lovastin) [12]. One of the most promising areas of neural regeneration appears to be the use of stem cell therapies, where stem cells can be employed in the injured or damaged area to replace and regenerate damaged cells [13]. However, cell therapies themselves have shown limited success because injected cells often die [14] or differentiate largely into astrocytes [15], adding further to scar tissue. Several groups have demonstrated initial success of embryonic or NSC transplantation leading to oligodendroglial differentiation after injury, however this is not widely replicable or predictable [16] perhaps in part due to the poor retention and survival of cells at the injury site. This has caused researchers to begin investigating biomaterials, which can serve as an artificial extracellular matrix (ECM) to help guide cell fate and allow for stem cell proliferation, while limiting cell death(Figure 2-3). In this sense, biomaterials can act as a vessel for cell implantation supporting cell viability and localizing cells to the target site while also delivering necessary drugs or growth factors [17].

These biomaterials range from naturally derived polymers [18] to commercial or synthetic, manmade materials [19]. In either case, engineers and material scientists are able to tune many properties about the material to help guide cell fate. Often these materials are degradable to generate dynamic mechanical properties or desirable bioresorption properties to thereby prevent a permanent foreign body response, and to allow cells to integrate into native tissue over time. Material moduli are often designed to be within the range of native neural tissue, or have an elastic Young's modulus of about 0.5 kPa [20], and then can be further tuned to promote the desired differentiation. Bioactive peptide sequences, such as RGD or IKVAV, derived from natural ECM proteins such as collagen or laminin, can also be synthesized and linked to synthetic materials to endow them with integrin-binding functionality. These bioactive sequences at appropriately controlled concentrations can further guide differentiation or cell morphology, such as axon extension [21].

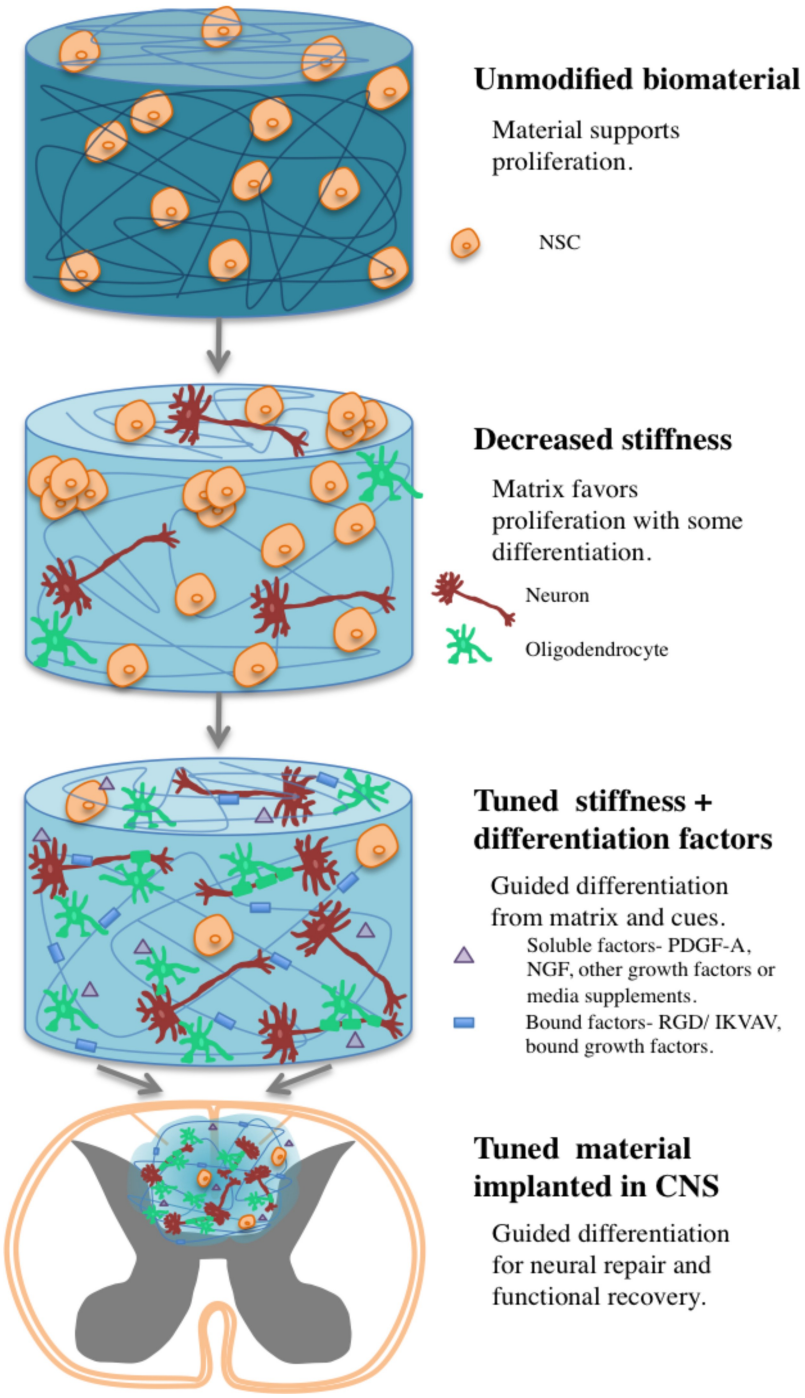

Figure 2-3 Transplanted stem cells respond to material properties for proliferation and differentiation. Transplanting cell scaffolds into host tissue keeps cells viable and in place while they respond to material properties. Materials can be unmodified or can incorporate inductive properties by varying stiffness, using bound or soluble growth factors, or incorporating bioactive sequences. Stem cells are then able to proliferate or differentiate in response to the modified materials.

Researchers have focused on many different matrices for neural applications, typically geared toward the regrowth of neurons [17a, 22]. Often for neural regeneration, hydrogels - polymer scaffolds made mostly of water - are utilized because of their broad range of flexibility and similarity to native tissue in transport and mechanical properties. However, traditional polymer scaffolds, such as those made of polylactic acid and not comprised mostly of water, have been used as well to facilitate regrowth of neurons. In addition to aliphatic polyesters, native proteins such as fibrin scaffolds, which can be modified to incorporate and release growth factors, allow for differentiation of NSCs into neurons [21a]. Neurogel™ is now a commercially available synthetic polymer hydrogel material, which has been shown to allow for axon extension and myelination by Schwann cells in cat spinal cords [23]. Poly(ethylene glycol) (PEG)-based materials have been used for numerous applications in the body due to their exquisitely tunable properties. In the nervous system PEG has been used to promote neurite growth by covalently binding bioactive sequences and taking advantage of its tunable mechanical and biochemical properties [24]. Throughout the literature there are substantial examples of hydrogel biomaterials used to influence differentiation into neurons, or neurite growth or branching.

Often when researching biomaterials for neural regeneration, researchers have focused primarily on the regrowth of neurons and the extension of axons. Little is known about how glial cell growth and development may be affected by biomaterial properties, and even less regarding oligodendrocyte-material interactions. For instance, it has been shown that NSCs prefer softer matrices in order to differentiate into neurons [24a, 25] and instead differentiate down astrocytic pathways forming scar-like tissue on stiff matrices [24a]. However, the effect of matrix stiffness on oligodendrocyte differentiation is unclear as are the effects of many other material properties.

While few articles have focused on biomaterial effects on oligodendrocyte growth and differentiation, some have characterized the relative amounts of neural cells in response to their hydrogels or media environments. Here, biomaterials that have promoted oligodendrocyte growth or permitted differentiation into oligodendrocytes will be discussed. In addition to engineering biomaterials to allow for growth and differentiation of stem cells into oligodendrocytes, research will be presented characterizing myelination *in vitro* and *in vivo* in or on biomaterials.

2.4 Biomaterials supporting oligodendroglial fate

2.4.1 Commercially available scaffolds

In recent years, commercially available scaffolds have become increasingly popular as advances in research have shown promising results. Of these, NeuroGel™ and Puramatrix™, in particular, have shown potential in use for regrowing glial cells or restoring function. Neurogel™ is composed of N-(2-hydroxypropyl)-methacrylamide and crosslinked using radical polymerization in phosphate buffered saline (PBS) [26]. This gel has been shown to promote CNS remyelination in a cat model, however migrating Schwann cells rather than resident oligodendrocytes were found to have deposited the new myelin [23]. Puramatrix™ on the other hand is derived from a series of self-assembled ionic peptides, which in aqueous solutions form hydrogels due to ionic interactions. These peptides include the arginine-alanine-aspartic acid-alanine repeat unit giving the material an alternative name "RADA" peptides [27]. Ylä-Outinen et al. showed that Puramatrix™ at concentrations from 5 to 25 weight percent in solution supported not only growth of neurons from human embryonic stem cells but some differentiation into glial cells as well [28]. Further investigation showed that while neuron growth was most favored at 10 weight percent, cells with oligodendrocyte precursor markers also remained viable and maintained typical morphology in that condition [28].

2.4.2 Native extracellular matrix proteins

Native ECM is composed of large structural proteins, such as laminin or fibrin, as well as glycosaminoglycan groups, like hyaluronic acid. Fibrin and collagen are both non-globular proteins that are often found in the ECM. Fibrin is found in scar tissue and generally serves to help blood clotting when fibrinogen is polymerized by thrombin, while collagen, and therefore its derivative-gelatin, is one of the main structural proteins found in many parts of the body from skin to muscle and bones. Despite their low concentration in native nervous tissue, both have been researched as a platform to study neural regeneration and specifically glial differentiation.

Fibrin based biomaterials have been shown to allow oligodendroglial maturation with varying success. Asmani et al. showed that in a 3mg/mL fibrin gel, endometrial stromal cell-derived oligodendrocyte precursor cells (OPCs) had improved viability and allowed a larger percentage of cells to retain a more differentiated Olig2+ oligodendrocyte state compared to traditional two dimensional polystyrene culture which remained high in A2B5+ cells[29]. Through

incorporating soluble growth factors or a heparin release system into a fibrin backbone, Willerth et al. was able to greatly increase the oligodendrocyte differentiation. Negatively charged heparin as an electrostatic drug release system was used to release growth factors for encapsulated NSCs and OPC growth. Varying the concentrations of the soluble growth factors neurotrophin-3 (NT-3), platelet derived growth factor (PDGF), basic fibroblast growth factor (bFGF), ciliary neurotropic factor (CNTF), and sonic hedgehog (SHH) influenced the differentiation into neurons, oligodendrocytes, and astrocytes[30]. The drug delivery system combinations of NT3 with PDGF and SHH further increased O4+ oligodendrocyte lineage differentiation to up to half of cells[31]. However, further exploration of *in vivo* studies showed mouse functionality improved after 4 weeks and declined after 8 weeks [32]. This decreased functionality by 8 weeks was due to the continued proliferation of undifferentiated precursor cells and the formation of tumors of neural progenitor cells (NPCs) in the animals with the drug release systems[32].

Collagen has shown promise as a potential matrix for neural regeneration[33], however only one study has presented information about oligodendrocytes in collagen scaffolds. Elias and Spector made collagen scaffolds at one weight percent per volume from type I and small amounts of type III collagen which formed gels at a stiffness comparable to rat brain. Scaffolds were then seeded with BrdU-labeled hippocampal NPCs and implanted in the rat brain where they were differentiated into a mix of neurons, oligodendrocytes, and astrocytes. Though this research did not examine the presence of myelin, oligodendrocyte differentiation after 4 weeks *in vivo* was consistent with both myelinating and perineuronal satellite phenotypes [34].

2.4.3 Plant and insect derived polymers

Plant and insect derived polymers, such as methylcellulose or spider silk, are readily available as biomaterials because of their easily accessible precursors. For instance, methylcellulose is synthetically derived from plant-based cellulose and has been investigated as a biomaterial supporting regeneration in tissues including nerve. Toward neural regeneration, methylcellulose and its derivatives have consistently been shown to support oligodendrocyte survival *in vitro* [25a, 35] as well as neuronal survival and axon extension(CITE).

In one instance, laminin type one (L1) was covalently attached to 40 kDa methylcellulose [35a]. A photocrosslinker N-sulfosuccinimidyl-6-[4'-azido-2'-nitrophenylamino] hexanoate was

incubated with L1 to bind laminin via the ester group on the photocrosslinker and can further be reacted with methylcellulose to form gels. Purified laminin-crosslinker product was then mixed on ice with methylcellulose in PBS and NSCs to form gels with covalently tethered laminin and encapsulated cells. NSC differentiation was induced by removal of bFGF. In this laminin-containing material, astrocytes and neurons were found to be present at higher levels compared to the methylcellulose control. OPCs were also found in higher levels in the material containing laminin than in the methylcellulose control, though mature oligodendrocytes were not found over the course of the experiment [35a].

Methylcellulose has also been combined with hyaluronic acid to create a material, termed HAMC, which showed that the presence of tethered PDGF-A promoted the differentiation of NSCs into oligodendrocytes [35b]. Biotinylated-PDGF-A was immobilized by functionalizing the methylcellulose with streptavidin and then combined with hyaluronic acid, NSCs, and heparin containing growth medium to form gels. 40% of the cells stained positive for RIP, a marker for mature and immature oligodendrocytes. The amino acid sequence GRGDS was additionally tethered to methylcellulose and these gels were shown to even further increase the amount of RIP+ cells up to around 50% of the total [35b].

In addition to cellulose polymers, chitosan has been highly investigated due in part to its availability in crustacean shells and arthropod exoskeletons [25a]. In one study, chitosan was functionalized with methacrylamide and crosslinking density was varied to control the Young's modulus of the substrate and influence NSC differentiation into neurons, oligodendrocytes, and astrocytes. Gels were photocrosslinked using the photoinitiator 2,2-dimethoxy-2-phenylacetophenone. By adjusting the photoinitator and macromer concentration, Young's modulus was modified from less than 1 kPa to greater than 30kPa. Neurons preferred the gel condition with the lowest Young's modulus while over a range of 1 kPa to 7 kPa the percentage of oligodendrocytes increased, showing that oligodendrocytes either prefer stiffer gels or fewer NSCs were directed towards neurons. In addition, the percentage of astrocytes decreased with increasing material stiffness. Despite the increase in oligodendrocytes in stiffer materials, myelin oligodendrocyte glycoprotein gene expression, and therefore mature oligodendrocytes and myelination, was best on 1kPa scaffolds [25a]. Methacrylamide chitosan was then used to test the affect of the bioactive sequence GRGDS and bound or soluble growth factor- pro-neural rat interferon-γ [35c]. In these studies, incorporating the growth factor into a 0.77 kPa hydrogel

increased both the neuron and oligodendrocyte cell differentiation. Soluble growth factor generated greater differentiation to oligodendrocytes than the immobilized case, however and the soluble growth factor showed more neural precursor cells as opposed to mature neurons. Large numbers of NSCs suggest that the biomaterial supports proliferation and could suggest a possible tumor formation *in vivo* if cells continue to remain undifferentiated and multiplying [35c].

Porous methacrylamide chitosan scaffolds have also been investigated for oligodendrocyte differentiation [36]. Laminin was bound to the methacrylamide chitosan by reacting equimolar amounts of N-hydroxysulfosuccinimide (NHS) with the laminin containing 1-ethyl-3-(3-dimethylamininopropyl)carbodiimide in a methacrylamide chitosan solution. 1-hydroxycyclohexyl phenyl ketone was used as a photoinitiator and D-mannitol was used at varying concentrations as a porogen to create large spaces for cell infiltration and expansion. It was found that media formulation was highly selective for differentiation where media containing PDGF-A favored over 50% oligodendrocyte differentiation in all material porosities [36].

More recent work has synthesized methacrylamide chitosan hydrogels to investigate cell differentiation on a 2D surface [37]. Here coverslips were first functionalized with methacrylates by allowing self-assembly of 3-(trimethoxysilyl)propyl on the surface. Then a thin layer of methacrylamide chitosan at 2wt% and the same photoinitiator as before was added to the coverslip and exposed to ultraviolet light. This gave a surface with a Young's modulus ranging from 0.5-0.7 kPa. Laminin or collagen type I was immobilized on the surfaces by reacting with 1-ethyl-(3-dimethylaminopropyl)carbodiimide hydrochloride and NHS for one hour. Collagen and laminin were immobilized either by themselves or together and at low to high concentrations. NSCs were found to remain as NSCs or differentiate into β-III-tubulin expressing neurons, mature neurons expressing synapsin, and glial precursor cells expressing NG2. In all conditions, at least 40% of cells were glial precursor cells potentially capable of differentiating into oligodendrocytes. They also found that in conditions that had a larger concentration of β-III-tubulin, NG2 positive cells were at a higher concentration. Imaging also found that NG2 positive cells were extending processes on the hydrogel[37].

2.4.4 Synthetic polymer hydrogels

Completely synthetic polymers provide users with innate control of structure and function of resultant materials. Like proteins, they are typically large molecules with repeated subunits, however synthetic polymers have an infinitely large selection of monomers from which to choose as opposed to the (relatively) limited 21 amino acids of protein polymers. While polymer hydrogels, such as those based on PEG have been utilized extensively for neural tissue engineering [24, 38], no existing research identifies any oligodendroglial cell interactions. Working with methylcellulose and chitosan, the Shoichet and Leipzig groups have shown the importance of material stiffness on oligodendrocyte development[25a, 37]. In our own lab with a purely synthetic methacrylated PEG hydrogel, we have similarly found that the material stiffness is important for OPC cell line[39] proliferation (Figure 2-4A-B).

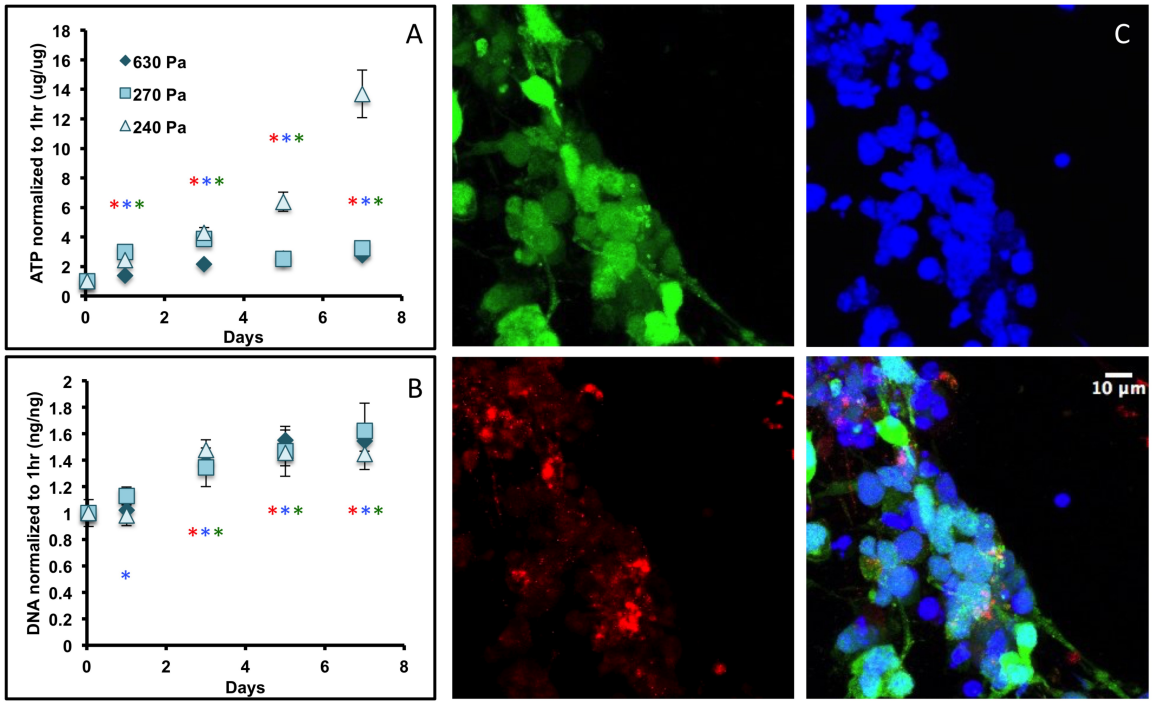

Figure 2-4 OPCs exhibit a stiffness-dependent trend. Both ATP (a) and DNA (b) exhibit a dependence on material stiffness with greater increases in more compliant hydrogels ($p < 0.05$, $n = 3$ experiments, red = 240 Pa compared to 1 h, blue = 270 Pa compared to 1 h, green = 630 Pa compared to 1 h; error bars indicate SD). Cells encapsulated in the gel express PDGFRα and cells on the surface extend processes (c). GFP+ cells are stained for nuclei (blue) and PDGFRα (red).

Similar to methacrylamide chitosan, crosslinking density and therefore material stiffness was varied by changing the concentration and molecular weight of dimethacrylated PEG. Methacrylate end groups were added to 4600 g/mol PEG by reacting methacrylic anhydride with PEG for 5 minutes in the microwave. Solutions of varying PEG concentrations formed hydrogels with storage moduli ranging from 191 to 634 Pa by exposing to UV light (365 nm, 4mW/cm^2) for 10 minutes in the presence of lithium phenyl-2,4,6-trimethylbenzoylphosphinate (LAP) photoinitiator. Glioma derived OPCs [39] were mixed in the pre-polymer solution and encapsulated in the PEG hydrogels at 1x10^7 cells per mL. Cell-loaded hydrogels were cultured for seven days in Dulbecco's modified eagle medium with N2 and B27 media supplements and 10ng/mL of PDGF and NT3. Viability and proliferation as determined by ATP and DNA concentration were dependent on the material storage moduli, or stiffness (Figure 2-4). DNA increased by at least 44% over 7 days in the least compliant material but increased even more in the most compliant material. ATP, an indicator of cell viability or metabolic state, suggests that cells in the most compliant material are 67% more metabolically active than those in the stiffer gels. Additionally, immunostaining indicates that many cells retain the OPC phenotype as they are PDGFR-α positive and display morphologies consistent with oligodendrocytes as they begin to extend processes (Figure 2-4C). These results suggest that PEG-based hydrogels are suitable for OPC proliferation and could be further tuned to guide differentiation and maturation into functional myelinating oligodendrocytes.

2.4.5 Polyesters

Polyesters are one heavily used class of synthetics, which contain ester groups as their major repeat unit. Their application as biomaterials is common because of their predictable degradation [19, 40]. Such behavior is desirable in biomaterials to limit the foreign body response, which would only be temporary until the structure degrades. Degradation can also confer advantages like beneficial degradation products or controlled release of encapsulated molecules [41]. Polylactic acid for instance, hydrolytically degrades releasing lactic acid, a normal metabolic product of glycolysis and which may be beneficial to radical scavenging and cell protection [42]. Controlled release, often through controlled degradation by combining polylactic acid with the faster degrading polyglycolic acid to form poly(lactic-co-glycolic acid) (PLGA), is also ideal because engineers can design materials which release molecules at a predetermined rate useful for cell survival or differentiation [41c, 43].

A potential limitation of polyesters is that they are typically less soluble in water and have less chain flexibility. This means rather than forming hydrogels, polycaprolactone or polylactic acid instead are typically spun or 3D printed into structures and cells are seed on top creating essentially 2D interactions. In one instance, polycaprolactone and starch structures were formed into tubular lattice conduits and cells were seeded in the center canal with gellan gum hydrogels. This gave unnaturally stiff compressive moduli from $4.42x10^6$ Pa to $2.74x10^7$ Pa, however in all cases oligodendrocyte-like cells remained viable, proliferated, and exhibited similar morphology [44]. These scaffolds were implanted in rat spinal cord injury models where they integrated with the native tissue [44]. Horne et al. created electrospun structures of polycaprolactone with either random or aligned fibers and additionally covalently bound brain-derived neurotrophic factor (BDNF) following functionalization of the scaffolds with ethylenediamine [45]. Embryonic cortical NSCs were seeded on the scaffolds and both the aligned and randomly orientated scaffolds showed a large growth of both NG2-positive oligodendrocyte precursor cells and TUJ1-positive neurons. However, the growth of glial fibrillary acidic protein (GFAP)-positive astrocytes was comparatively small when the BDNF was attached to the scaffolds. The number of OPCs increased over three fold in the scaffold compared to traditional poly-lysine coated coverslips while neurons had a two- to three-fold increase and astrocytes only increased ~30-40 percent [45].

2.5 Common themes

Throughout many of the material studies, a few recurring themes can be identified. Many of the articles incorporated growth factors for cellular differentiation by either tethering them to the matrix or loading them into the matrix for diffusional release. For instance, platelet derived growth factor, PDGF-A, was often incorporated in materials, which yielded high relative amounts of oligodendrocytes. This is in agreement with Aizawa et al. where incorporating PDGF-A either as a soluble factor or covalently bound increased the percentage of oligodendrocytes almost 100% when compared without the presence of PDGF-A [46]. Continued research from Li et al., similarly found that incorporation of PDGF-A immobilized on the methacrylamide chitosan conduits was preferential to the soluble form in order to maintain an effective concentration over a longer duration [47]. In traditional cellular culture, PDGF-A supports proliferation of OPCs and is often used in cellular media for OPCs and OPC-like cell

lines. However, in vivo tests show that there is a limit to the useful timespan or concentration as gliomas may form, perhaps caused by the high local drug concentration limited cell migration achieved by using biomaterials [32]. Najm et al. and Yang et al. both generated OPCs from fibroblasts using three transcription factors [48]. These cell lines were able to differentiate into mature oligodendrocytes while still in the presence of these transcription factors [48]. Here both found that Olig2 and Sox10 were necessary transcription factors for oligodendrocyte formation [49]. Thus, biomaterials may need to incorporate these transcription factors as well to support differentiation as well as OPC proliferation.

As is common with neuronal differentiation, NSCs prefer compliant matrices to follow an oligodendrocyte differentiation pathway. Mechanotransduction, or a cell's response to mechanical signals from the ECM, has been shown to have increasing importance in cell growth, in particular stem cell differentiation. A rapidly increasing number of publications have now shown that NSCs further differentiate into neurons when cultured on or in compliant materials, while slightly less compliant materials favor glial differentiation. This makes sense as the word "glia" is Greek for glue and stems from the idea that glial cells provide much of the structural support in the CNS. Shreiber et al. showed that the mechanical properties of natural tissue decreases significantly either from the death of oligodendrocytes and astrocytes or loss of myelin alone [50]. This suggests that OPCs, which may grow and differentiate in ECM and developing tissue more compliant than adult tissue, are also important contributors to the overall mechanics of neural tissues. This may provide additional insight to limited regeneration observed in regions of stiff glial scar tissue since glial scarring increases the tissue stiffness and prevents the normal mechanical differentiation response of NSCs and OPCs alike. However the field still lacks consistency as few papers have investigated oligodendroglial differentiation mechanics and a wide range of favorable material stiffnesses have been reported.

As a person ages, the body undergoes continuous changes in the properties of ECM, such as stiffening, that may correlate with age-related neurodegeneration. Neurodegeneration involves the loss of both neuronal cells and oligodendrocytes as well [51]. Sack et al. argues that as the total brain volume decreases with age, the white matter volume, though decreasing slightly, remains more stable than the total volume [52]. Furthermore, this decrease in volume correlated with a substantial decrease in brain-tissue mechanical elasticity [52]. Since, stiffening of tissue correlates with a decrease in oligodendrocytes one may hypothesize that glial cells give the

nervous system much of the structural support. OPCs mature primarily during early development when brain tissue is more compliant. Utilizing a matrix that replicates the "young" environmental conditions (ie, highly compliant) may bias OPCs to have the growth and myelination activity present during early development.

Table 1 Summary of biomaterials for oligodendroglial specification

Outcome	Material	Biological cues	Notes	Reference
OPC viability or proliferation	Fibrin gel		Endometrial stromal cells differentiated to OPCs	Asmani et al. [2013]
	Methylcellulose + laminin type I photocrosslinked to form a gel	bFGF was removed to induce differentiation into OPCs	NSCs differentiated to O4+ cells and proliferated with laminin present	Stabenfeldt et al. [2010]
	PCL starch tubular lattice structures loaded with gellan gum hydrogels		MO3-13 OPCs remained viable in the gellan gum + PCL scaffolds	Silva et al. [2010]
	Electrospun PCL with either aligned or unaligned fibers	BDNF either covalently bound or left soluble	Immobilized BDNF enhanced proliferation of OPCs	Horne et al. [2010]
OPC maturation	Puramatrix: RADA peptide self-assembling in aqueous solution		Cells maintained typical morphology	Ylä-Outinen et al. [2014]
	Fibrin gels	Soluble or heparin release system of PDGF, NT-3, SHH, CNTF, bFGF	Combinations of NT-3 with SHH or PDGF increased O4+ cell numbers	Willerth et al. [2007, 2008]
	HAMC: hyaluronan and methylcellulose	Tethered PDGF-A or the integrin-binding peptide GRGDS	PDGF greatly increased RIP+ cell numbers	Tam et al. [2012]
	Methacrylamide chitosan photocrosslinked	GRGDS or streptavidin functionalized to incorporate proneural rat interferon-γ	Young's moduli varied and a stiffer matrix yielded higher percentages of oligodendrocytes	Leipzig and Shoichet [2009]; Leipzig et al. [2011]
	Porous methacrylamide chitosan gels + laminin photoinitiated to form gels	PDGF-A in media	PDGF-A alone greatly favored differentiation	Li et al. [2012]
	Methacrylamide chitosan-coated coverslips + collagen or laminin immobilized		More NG2+ cells found where βIII-tubulin was also upregulated	Wilkinson et al. [2014]
	PLGA porous structures	NT-3 with silk fibroin	NSCs differentiated into neurons and glial cells. In vivo, Schwann cells rather than oligodendrocytes generated myelin	Xiong et al. [2012]
Myelination in vitro	Artificial axon structures from aligned polystyrene or polylactic acid structures	Coated poly(L-lysine), laminin	Cells have a threshold diameter for ensheathing myelin	Lee et al. [2012, 2013]
	PCL nanofibers	microRNA-219, -338	miR-219, -338 increased percentage of MBP+ cells	Diao et al. [2015]
OPC maturation in vivo	Collagen type 3		Neither functional recovery nor myelin were investigated	Elias and Spector [2012]
Functional recovery or myelination in vivo	Fibrin gel	Soluble or heparin release of PDGF-AA or NT-3	Tumors formed in release system and functionality decreased from 4–8 weeks	Johnson et al. [2010]
	Neurogel: N-(2-hydroxypropyl)-methacrylamide crosslinked through radical polymerization		Schwann cells responsible for myelination	Woerly et al. [2004]
	Heparin-modified PLGA bridges	Heparin release of SHH and NT-3 combinations	Oligodendrocytes generated myelin but did not wrap axons	Thomas et al. [2014]
	Hyaluronic acid and gelatin crosslinked by PEG diacrylate	Heparin release of PDGF, NT-3, bFGF, CNF, SHH	More compliant gels gave rise to more MBP	Li et al. [2013]

Few studies have focused on the use of biomaterials on OPCs or oligodendrocytes, with published outcomes ranging from simple survival of OPCs to maturation and myelination. Common themes include the delivery of growth factors and materials with similar Young's moduli.

2.6 Material-mediated induction of maturation and myelin production

Some materials have promoted myelination in vitro, although published studies to this effect remain rare or focus on Schwann cell myelination. This is true for a range of literature briefly discussed here, as it may inform myelination processes of oligodendrocytes as well. However, there are significant differences between oligodendrocyte and Schwann cell myelination, particularly that each oligodendrocyte myelinates multiple axons while each Schwann cell myelinates a single axon segment. Encapsulating dorsal root ganglion in a hydrogel and staining for classic myelin markers is the oldest method for quantifying myelination, performed extensively by Carenini [53]. While helpful in early efforts to show myelination in a matrix, the effects are exclusively due to Schwann cells as oligodendrocytes are not present in dorsal root ganglion.

Since then, Pittier et al. showed that myelination occurred in fibrin matrices using the Carenini technique. These matrices were made from fibrinogen and thrombin with more CNS-specific biomolecules: either L1 or modified cell adhesion molecules from L1. Here this cell adhesion molecule, the sixth Ig-like domain of L1, was modified to incorporate the sequence RGD as well as an n-terminal transglutaminase [54]. In some samples, neurite extension of encapsulated cells was recorded, while in other gels dorsal root ganglion from chickens were encapsulated in the matrices and examined for myelination. After 10 to 14 days, the transglutaminase modified matrices and L1 matrices all exhibited myelinating Schwann cells while the fibrin control matrices without either L1 transglutaminase or laminin did not. However, in these studies myelination still occurred by Schwann cells rather than oligodendrocytes [54]. Since then, numerous groups have observed myelination from Schwann cells in biomaterials [55].

Similarly, Xiong et al. showed that myelination occurred from Schwann cells in their PLGA matrix, which released NT3 from silk fibroin [55c]. They utilized a high molecular weight PLGA with a 3:1 (D,L-lactide:glycolide) block copolymer, but more importantly, utilized sodium chloride as a porogen to achieve a porous structure. Some PLGA rods were loaded with NT3 mixed with silk fibroin and soaked into the scaffold. NSCs seeded on top of the gel were found to differentiate into neurons, oligodendrocytes, and astrocytes. These neurons formed synaptic connections and exhibited myelinated axons, though infiltrating Schwann cells rather than oligodendrocytes generated the myelin [55c].

Li et al. was able to show that OPCs seeded in their hydrogel composed of hyaluronic acid and gelatin cross-linked by PEG were able to differentiate into myelinating oligodendrocytes both in vitro and in vivo [56]. Here, thiol-functionalized hyaluronic acid was mixed with thiol-functionalized gelatin and PEG diacrylate to generate materials with elastic moduli ranging from 1 to 1600 Pa. The greatest amount of adhesion of this OPC line, CG4, occurred on structures with the mid-range elastic modulus. Cells cultured on top of materials exhibiting an elastic modulus close to native rat moduli, 100 Pa, showed the most CG4-oligodendrocyte process extension while cells inside the materials exhibited more process extension on even more compliant materials with a stiffness of 13.8 Pa. When the material solution and cells were injected into rats, researchers found that this more compliant material elicited the most MBP, myelin basic protein, in the lesion site (Figure 2-5) [56].

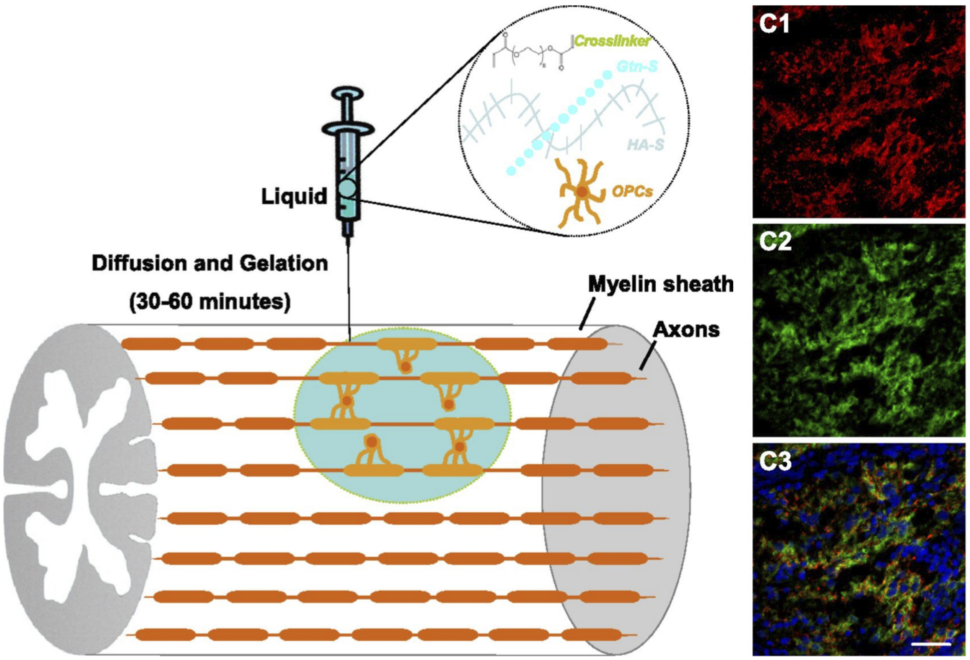

Figure 2-5 Experimental schematic representa- tion and results from Li et al. [2013]. Hyal- uronic acid and PEG are injected into spi- nal cords with OPCs where gelation occurs in under an hour. Immunocytochemistry shows axons in red, myelin in green, and cell nuclei in blue. Reproduced with per- mission of the Federation of American So- cieties for Experimental Biology.

Finally, oligodendrocyte maturation and myelin production can be induced through material properties themselves. This work followed initial studies of axon extension on poly-l-lactic acid fibers[57] and work with Schwann cells that showed they are able to extend along fibers and change gene expression in regards to topographical fiber cues [58]. Lee et al. generated a

system for oligodendrocyte precursor cells, which allowed OPCs to myelinate material fibers [59]. Here, polystyrene or poly(lactic acid) was electrospun to generate fibers ranging up to 4 μm in diameter. Fibers were then coated with combinations of ECM proteins and poly(l-lysine) and OPCs differentiated and extended processes throughout all diameter ranges of fibers (Figure 2-6). However, only on larger diameter fibers did oligodendrocyte processes actually wrap the fibers and generate myelin-like structures and there is a threshold diameter for myelination to occur in artificial axon structures (Figure 2-6). While myelin wrapping was found, compact myelin structures were still infrequent and it was concluded that axonal signals may play an important role in dictating the organization of myelin wraps[59a]. Following this work, groups have begun take this a step farther by generating fibers that release molecules of interest to further mimic the axons and axonal cues [60].

2.7 Conclusion and outlook

Demyelination is a major problem afflicting patients with neurological diseases or injuries. Without properly myelinated neurons, patients experience pain, loss of function, and often continuous degeneration from a cascade of events following the disruption of myelin segments. In addition to drug therapies or cell implantation alone, researchers are beginning to combat this through the use of biomaterials. Many materials, from synthetic matrices such as Neurogel™ to naturally based fibrin or methylcellulose matrices, have been shown to promote differentiation of stem cells into oligodendrocytes. The largest area of research with biomaterials for the CNS focuses on regrowth of neurons and thus very few groups have shown evidence of myelination in their material. As progress in neuronal growth and axon regeneration is made, researchers will need to look towards ways to increase remyelination and function of neurons. For these demyelinating diseases or injuries, it may be possible to use a combinatorial approach of biomaterials and stem cells, in order to provide cellular support and localization and facilitate the regrowth of oligodendrocytes. This work will undoubtedly build upon previous work with similar biomaterials that help stimulate differentiation and maturation of neurons as well as axon regeneration.

Figure 2-6 OPCs seeded on aligned fibers, used with permission from Lee et al., [2012]. a Cells prefer fibers with 2–4 μm diameter. MBP+ cells in the presence of large fibers (b) and small fibers (c). d Analysis of cel- lular morphology of OPCs and oligoden- drocytes on fibers. e Oligodendroglial cells were immunostained for PDGFR α (green), MBP (red), GFAP astrocytes (white), and DAPI nuclear stain (blue).

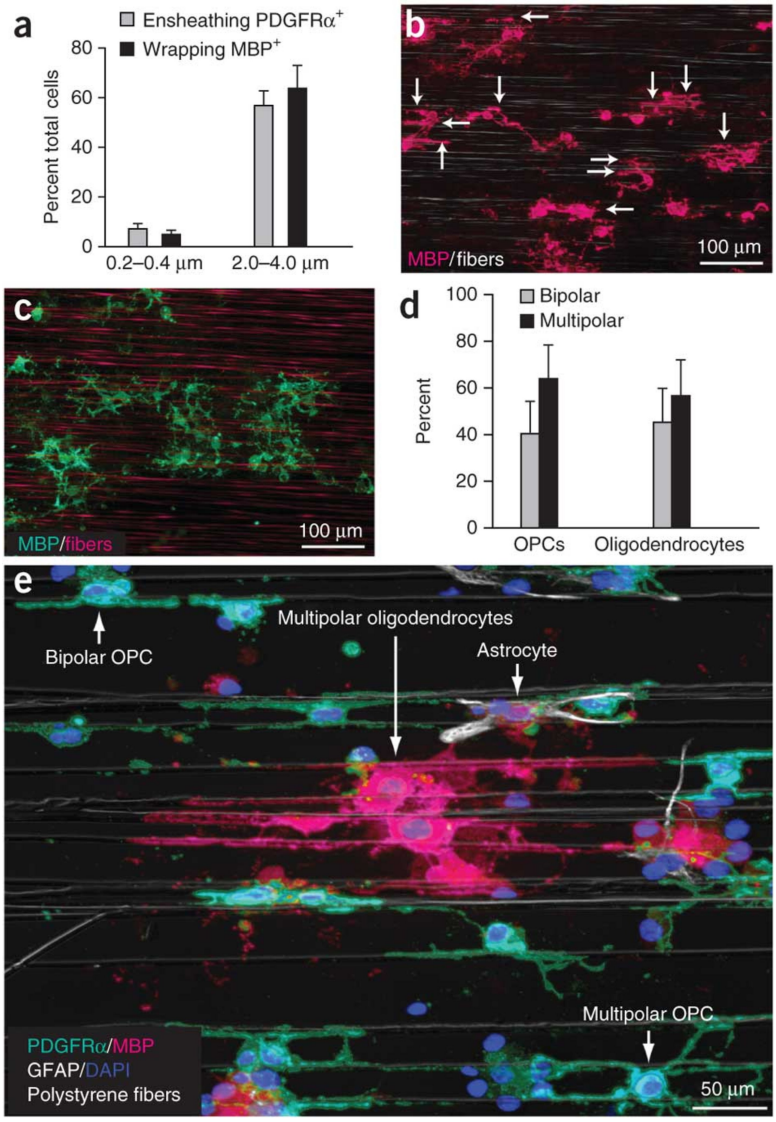

CNS tissue is a complex microenvironment where the cells ultimately depend on other cell types for both structural and trophic support. Biomaterials and cell therapies have each advanced neural regeneration research, however both of these strategies are limited without oligodendrocyte growth and maturation. Oligodendrocytes are the last cell type to mature in the CNS indicating their requirement for many of the structural and trophic cues provided from neurons and astrocytes. Oligodendrocytes help to restore normal function to the CNS through

formation of myelin around signal-transducing axons. Thus it is imperative in designing an effective OPC microenvironment to incorporate many of the diverse factors present in CNS tissue.

Because oligodendrocytes have been found to deposit myelin sheets in the absence of neurons *in vitro*, it has been suggested that trophic support from neurons is not necessary, but instead astrocytes provide many of the trophic factors necessary for differentiation and maturation. Electrospun fibers or other materials that mimic the structural and mechanical properties of a neuronal axon may be imperative to obtaining the necessary structural support by providing a high aspect ratio and desired curvature for myelin deposition. Further aligned fibrous materials may promote the development of mature oligodendrocytes, which could be transplanted into injured areas, allowing for further maturation into physiologically relevant myelinating oligodendrocytes. In addition, astrocytes have been shown to produce CNTF and NT3, trophic factors that are often used in oligodendrocyte differentiation media. Incorporating a release system of important chemical factors, such as PDGF or NT3 can further enhance the maturation. Taken together, this suggests that the structural aspects of neurons and chemical cues from astrocytes should both be incorporated into an engineered material.

Mechanotransduction has been shown to be highly important in many differentiation pathways as well and OPCs are no different. As shown in Figure 2-4, proliferation and metabolic activity are highly impacted simply by the material stiffness. Further incorporating bioactive sequences into the material for cells to bind may also prove favorable by triggering the chemical pathways that regulate motility and allow new OPCs to myelinate existing neuronal axons or integrate with the damaged tissue. Degradability of the material may be necessary as it helps to prevent an immune response as well as stiffening of the area as cells differentiate and build ECM. Degradability can be as simple as incorporating polyesters which degrade through hydrolysis or through adding cellular cleavage sites. Furthermore, mesh sizes are traditionally coupled with stiffness and regrowth of nervous tissue requires mesh sizes large enough for process extension, not only of neuronal axons but for potential myelinating oligodendrocyte processes as well.

There is a complex relationship between cell concentrations and cell signaling. Higher concentrations of neurons have been shown to further skew stem cell differentiation toward glial precursor cells, while oligodendrocytes and astrocytes have been found to produce neural

inhibitory proteins as well as factors guiding differentiation down the oligodendrocyte lineage. Though many things help to guide differentiation towards oligodendrocytes, it has also been shown that OPCs have discrete territories from one another and tend to migrate away from areas with other oligodendrocyte lineage cells [61]. This suggests that co-culturing of important cells may be a key strategy in determining forward research progress and could require engineered materials, which support migration and differentiation into both neurons and therapeutic glial cells in physiologic ratios and chronological order. Advances in oligodendrocyte growth and maturation, and most importantly, myelination, can proceed with a host of different strategies as describe above. These may continue to rely upon soluble factors, but recent work indicates that topographical cues [59b], physical properties of the ECM[25a], cell-cell communication[61-62], and chemical presentation[31] are just as vital to influencing oligodendrocyte fate. Pursuing such factors in the context of a relevant 3D environment will greatly advance the field, and provide unique insights to clinical regeneration strategies to spinal cord regeneration at the cellular and tissue level, ultimately resulting in better behavioral function. While we have concentrated here on the context of biomaterials, we wholeheartedly endorse the recent trend in neuroscience research that has shifted focus away from the exclusive focus on neurons to start examining glial, and specifically oligodendrocyte, fate as it relates to CNS regeneration strategies [59b, 63]

2.8 Acknowledgements

This work was supported by the UVA Biotechnology Training Program (LNR) and the University of Virginia. The authors thank the Gaultier lab at UVA for the generous gift of OPCs lines.

2.9 References

1. Bradl, M.; Lassmann, H., Oligodendrocytes: biology and pathology. *Acta neuropathologica* **2010,** *119* (1), 37-53.
2. Andersen, S. L., Trajectories of brain development: point of vulnerability or window of opportunity? *Neuroscience & Biobehavioral Reviews* **2003,** *27* (1-2), 3-18.
3. Pfeiffer, S. E.; Warrington, A. E.; Bansal, R., The oligodendrocyte and its many cellular processes. *Trends in cell biology* **1993,** *3* (6), 191-7.
4. Lodish, H.; Berk, A.; Zipursky, S. L.; Matsudaira, P.; Balitimore, D.; Darnell, J., *Molecular Cell Biology*. 4 ed.; New York, 2000.
5. Morell, P.; Quarles, R. H., *Basic Neurochemistry: Molecular, Cellular and Medical Aspects*. 6 ed.; Lippincott-Raven: Philadelphia, 1999.

6. Pohl, H. B.; Porcheri, C.; Mueggler, T.; Bachmann, L. C.; Martino, G.; Riethmacher, D.; Franklin, R. J.; Rudin, M.; Suter, U., Genetically induced adult oligodendrocyte cell death is associated with poor myelin clearance, reduced remyelination, and axonal damage. *The Journal of neuroscience : the official journal of the Society for Neuroscience* **2011,** *31* (3), 1069-80.
7. (a) Trapp, B. D.; Nave, K. A., Multiple sclerosis: an immune or neurodegenerative disorder? *Annual review of neuroscience* **2008,** *31*, 247-69; (b) Mekhail, M.; Almazan, G.; Tabrizian, M., Oligodendrocyte-protection and remyelination post-spinal cord injuries: a review. *Progress in neurobiology* **2012,** *96* (3), 322-39.
8. Fawcett, J. W.; Asher, R. A., The glial scar and central nervous system repair. *Brain Research Bulletin* **1999,** *49* (6), 337-391.
9. (a) Stabenfeldt, S. E.; Irons, H. R.; LaPlaca, M. C., Stem Cells and Bioactive Scaffolds as a Treatment for Traumatic Brain Injury. *Current Stem Cell Research & Therapy* **2011,** *6* (3), 208-220; (b) Pathan, S. A.; Iqbal, Z.; Zaidi, S. M. A.; Talegaonkar, S.; Vohra, D.; Jain, G. K.; Azeem, A.; Jain, N.; Lalani, J. R.; Khar, R. K.; Ahmad, F. J., CNS Drug Delivery Systems: Novel Approaches. *Recent Patents on Drug Delivery & Formulation* **2009,** *3* (1), 71-89; (c) Schmidt, C. E.; Leach, J. B., Neural tissue engineering: strategies for repair and regeneration. *Annual review of biomedical engineering* **2003,** *5*, 293-347; (d) Sindou, M. P.; Mertens, P.; Garcia-Larrea, L., Surgical Procedures for Neuropathic Pain. *Neurosurgery Quarterly* **2001,** *11* (1), 45-65; (e) Cao, Q.; Benton, R. L.; Whittemore, S. R., Stem cell repair of central nervous system injury. *Journal of neuroscience research* **2002,** *68* (5), 501-10.
10. Karandikar, N. J.; Crawford, M. P.; Yan, X.; Ratts, R. B.; Brenchley, J. M.; Ambrozak, D. R.; Lovett-Racke, A. E.; Frohman, E. M.; Stastny, P.; Douek, D. C.; Koup, R. A.; Racke, M. K., Glatiramer acetate (Copaxone) therapy induces CD8(+) T cell responses in patients with multiple sclerosis. *The Journal of clinical investigation* **2002,** *109* (5), 641-9.
11. Bradbury, E. J.; Moon, L. D. F.; Popat, R. J.; King, V. R.; Bennet, G. S.; Patel, P. N.; Fawcett, J. W.; McMahon, S. B., Chondroitinase ABC promotes functional recovery after spinal cord injury. *Letters to Nature* **2002,** *416*, 636-640.
12. Paintlia, A. S.; Paintlia, M. K.; Singh, A. K.; Singh, I., Inhibition of rho family functions by lovastatin promotes myelin repair in ameliorating experimental autoimmune encephalomyelitis. *Molecular pharmacology* **2008,** *73* (5), 1381-93.
13. (a) Yu, D.; Silva, G. A., Stem cell sources and therapeutic approaches for central nervous system and neural retinal disorders. *Neurosurgical focus* **2008,** *24* (3-4), E11; (b) Burns, A. J.; Thapar, N., Neural stem cell therapies for enteric nervous system disorders. *Nature reviews. Gastroenterology & hepatology* **2014,** *11* (5), 317-28; (c) Aboody, K.; Capela, A.; Niazi, N.; Stern, J. H.; Temple, S., Translating stem cell studies to the clinic for CNS repair: current state of the art and the need for a Rosetta stone. *Neuron* **2011,** *70* (4), 597-613; (d) Schouten, J. W.; Fulp, C. T.; Royo, N. C.; Saatman, K. E.; DWatson, D. J.; Snyder, E. Y.; Trojanowski, J. Q.; Prockop, D. J.; Maas, A. I. R.; McIntosh, T. K., A Review and Rationale for the Use of Cellular Transplantation as a Therapeutic Strategy for Traumatic Brain Injury. *Journal of Neurotrauma* **2004,** *21* (11), 1501-1538.
14. (a) Zhang, M.; Methot, D.; Poppa, V.; Fujio, Y.; Walsh, K.; Murry, C. E., Cardiomyocyte grafting for cardiac repair: graft cell death and anti-death strategies. *Journal of molecular and cellular cardiology* **2001,** *33* (5), 907-21; (b) Riess, P.; Zhang, C.; Saatman, K. E.; Laurer, H. L.; Longhi, L. G.; Raghupathi, R.; Lenzlinger, P. M.; Lifshitz, J.; Boockvar, J.; Neugebauer, E.; Snyder, E. Y.; McIntosh, T. K., Transplanted Neural Stem Cells Survive, Differentiate, and Improve Neurological Motor Function After Experimental Traumatic Brain Injury. *Neurosurgery*

2002, *51* (4), 1043-1052; (c) Cooke, M. J.; Vulic, K.; Shoichet, M. S., Design of biomaterials to enhance stem cell survival when transplanted into the damaged central nervous system. *Soft matter* **2010,** *6* (20), 4988; (d) Bakshi, A.; Keck, C. A.; Koshkin, V. S.; LeBold, D. G.; Siman, R.; Snyder, E. Y.; McIntosh, T. K., Caspase-mediated cell death predominates following engraftment of neural progenitor cells into traumatically injured rat brain. *Brain research* **2005,** *1065* (1-2), 8-19.

15. (a) Blurton-Jones, M.; Kitazawa, M.; Martinez-Coria, H.; Castello, N. A.; Muller, F. J.; Loring, J. F.; Yamasaki, T. R.; Poon, W. W.; Green, K. N.; LaFerla, F. M., Neural stem cells improve cognition via BDNF in a transgenic model of Alzheimer disease. *Proceedings of the National Academy of Sciences of the United States of America* **2009,** *106* (32), 13594-9; (b) Jeong, S. W.; Chu, K.; Jung, K. H.; Kim, S. U.; Kim, M.; Roh, J. K., Human neural stem cell transplantation promotes functional recovery in rats with experimental intracerebral hemorrhage. *Stroke; a journal of cerebral circulation* **2003,** *34* (9), 2258-63.

16. (a) McDonald, J. W.; Howard, M. J., Repairing the damaged spinal cord: a summary of our early success with embryonic stem cell transplantation and remyelination. *Progress in Brain Research* **2002,** *137*, 299-309; (b) Nakamura, M.; Okano, H., Cell transplantation therapies for spinal cord injury focusing on induced pluripotent stem cells. *Cell research* **2013,** *23* (1), 70-80; (c) Goddaard, D. R.; Berry, M.; Butt, A. M., In Vivo Actions of Fibroblast Growth Factor-2 and Insulin-LIke Growth Factor-I on Oligodendrocyte Development and Myelination in the Central Nervous System. *Journal of neuroscience research* **1999,** (57), 74-85; (d) Hammang, J. P.; Archer, D. R.; Duncan, I. D., Myelination Following Transplantation of EGF-Responsive Neural Stem Cells into a Melin-Dificient Environment. *Experimental Neurology* **1997,** (147), 84-95.

17. (a) Zhong, Y.; Bellamkonda, R. V., Biomaterials for the central nervous system. *Journal of the Royal Society, Interface / the Royal Society* **2008,** *5* (26), 957-75; (b) Subramanian, A.; Krishnan, U. M.; Sethuraman, S., Development of biomaterial scaffold for nerve tissue engineering: Biomaterial mediated neural regeneration. *Journal of biomedical science* **2009,** *16*, 108.

18. Sakiyama-Elbert, S. E.; Hubbell, J. A., Functional Biomaterials: Design of Novel Biomaterials. *Annual Review of Materials Research* **2001,** *31*, 183-201.

19. Aurand, E. R.; Lampe, K. J.; Bjugstad, K. B., Defining and designing polymers and hydrogels for neural tissue engineering. *Neuroscience research* **2012,** *72* (3), 199-213.

20. Taylor, Z.; Miller, K., Reassessment of brain elasticity for analysis of biomechanisms of hydrocephalus. *Journal of biomechanics* **2004,** *37* (8), 1263-9.

21. (a) Lampe, K. J.; Heilshorn, S. C., Building stem cell niches from the molecule up through engineered peptide materials. *Neuroscience letters* **2012,** *519* (2), 138-46; (b) Silva, G. A.; Czeisler, C.; Niece, K. L.; Beniash, E.; Harrington, D. A.; Kessler, J. A.; Stupp, S. I., Selective Differentiation of Neural Progenitor Cells by High-Epitope Density Nanofibers. *Science* **2004,** *303* (5662), 1352-1355; (c) Lampe, K. J.; Antaris, A. L.; Heilshorn, S. C., Design of three-dimensional engineered protein hydrogels for tailored control of neurite growth. *Acta biomaterialia* **2013,** *9* (3), 5590-9.

22. Nisbet, D. R.; Crompton, K. E.; Horne, M. K.; Finkelstein, D. I.; Forsythe, J. S., Neural Tissue Engineering of the CNS Using Hydrogels. *Journal of Biomedical Materials Research Part B- Applied Biomaterials* **2008,** *87*, 251-263.

23. Woerly, S.; Doan, V. D.; Sosa, N.; de Vellis, J.; Espinosa-Jeffrey, A., Prevention of gliotic scar formation by NeuroGel allows partial endogenous repair of transected cat spinal cord. *Journal of neuroscience research* **2004,** *75* (2), 262-72.

24. (a) Lampe, K. J.; Mooney, R. G.; Bjugstad, K. B.; Mahoney, M. J., Effect of macromer weight percent on neural cell growth in 2D and 3D nondegradable PEG hydrogel culture. *Journal of biomedical materials research. Part A* **2010,** *94* (4), 1162-71; (b) Zustiak, S. P.; Pubill, S.; Ribeiro, A.; Leach, J. B., Hydrolytically degradable poly(ethylene glycol) hydrogel scaffolds as a cell delivery vehicle: Characterization of PC12 cell response. *Biotechnology Progress* **2013,** *29* (5), 1255-1264.
25. (a) Leipzig, N. D.; Shoichet, M. S., The effect of substrate stiffness on adult neural stem cell behavior. *Biomaterials* **2009,** *30* (36), 6867-78; (b) Saha, K.; Keung, A. J.; Irwin, E. F.; Li, Y.; Little, L.; Schaffer, D. V.; Healy, K. E., Substrate modulus directs neural stem cell behavior. *Biophysical journal* **2008,** *95* (9), 4426-38.
26. (a) Woerly, S.; Pinet, E.; De Robertis, L.; Bousmina, M.; Laroche, G.; Roitback, T.; Vargova, L.; Sykova, E., Heterogeneous PHPMA hydrogels for tissue repair and axonal regeneration in the injured spinal cord. *Journal of Biomaterials Science, Polymer Edition* **1998,** *9* (7), 681-711; (b) Woerly, S.; Petrov, P.; Sykova, E.; Roitbak, T.; Simonova, Z.; Harvey, A. R., Neural Tissue Formation Within Porous Hydrogels Implanted in Brain and Spinal Cord Lesions: Ultrastructural, Immunohistochemical, and Diffusion Studies. *Tissue Engineering* **1999,** *5* (5), 467-488.
27. Gelain, F.; Lomander, A.; Vescovi, A. L.; Zhang, S., Systematic studies of a self-assembling peptide nanofiber scaffold with other scaffolds. *Journal of Nanoscience and Nanotechnology* **2007,** *7* (2), 424-434.
28. Yla-Outinen, L.; Joki, T.; Varjola, M.; Skottman, H.; Narkilahti, S., Three-dimensional growth matrix for human embryonic stem cell-derived neuronal cells. *Journal of tissue engineering and regenerative medicine* **2014,** *8* (3), 186-94.
29. Asmani, M. N.; Ai, J.; Amoabediny, G.; Noroozi, A.; Azami, M.; Ebrahimi-Barough, S.; Navaei-Nigjeh, M.; Ai, A.; Jafarabadi, M., Three-dimensional culture of differentiated endometrial stromal cells to oligodendrocyte progenitor cells (OPCs) in fibrin hydrogel. *Cell biology international* **2013,** *37* (12), 1340-9.
30. Willerth, S. M.; Faxel, T. E.; Gottlieb, D. I.; Sakiyama-Elbert, S. E., The effects of soluble growth factors on embryonic stem cell differentiation inside of fibrin scaffolds. *Stem cells* **2007,** *25* (9), 2235-44.
31. Willerth, S. M.; Rader, A.; Sakiyama-Elbert, S. E., The effect of controlled growth factor delivery on embryonic stem cell differentiation inside fibrin scaffolds. *Stem Cell Res* **2008,** *1* (3), 205-18.
32. Johnson, P. J.; Tatara, A.; McCreedy, D. A.; Shiu, A.; Sakiyama-Elbert, S. E., Tissue-engineered fibrin scaffolds containing neural progenitors enhance functional recovery in a subacute model of SCI. *Soft matter* **2010,** *6* (20), 5127-5137.
33. Cholas, R. H.; Hsu, H. P.; Spector, M., The reparative response to cross-linked collagen-based scaffolds in a rat spinal cord gap model. *Biomaterials* **2012,** *33* (7), 2050-9.
34. Elias, P. Z.; Spector, M., Implantation of a collagen scaffold seeded with adult rat hippocampal progenitors in a rat model of penetrating brain injury. *Journal of neuroscience methods* **2012,** *209* (1), 199-211.
35. (a) Stabenfeldt, S. E.; Munglani, G.; Garcia, A. J.; LaPlaca, M. C., Biomimetic microenvironment modulates neural stem cell survival, migration, and differentiation. *Tissue engineering. Part A* **2010,** *16* (12), 3747-58; (b) Tam, R. Y.; Cooke, M. J.; Shoichet, M. S., A covalently modified hydrogel blend of hyaluronan–methyl cellulose with peptides and growth factors influences neural stem/progenitor cell fate. *Journal of Materials Chemistry* **2012,** *22* (37),

19402; (c) Leipzig, N. D.; Wylie, R. G.; Kim, H.; Shoichet, M. S., Differentiation of neural stem cells in three-dimensional growth factor-immobilized chitosan hydrogel scaffolds. *Biomaterials* **2011,** *32* (1), 57-64; (d) Martin, B. C.; Minner, E. J.; Wiseman, S. L.; Klank, R. L.; Gilbert, R. J., Agarose and methylcellulose hydrogel blends for nerve regeneration applications. *J Neural Eng* **2008,** *5* (2), 221-31; (e) Hsieh, A.; Zahir, T.; Lapitsky, Y.; Amsden, B.; Wan, W.; Shoichet, M. S., Hydrogel/electrospun fiber composites influence neural stem/progenitor cell fate. *Soft matter* **2010,** *6* (10), 2227.
36. Li, H.; Wijekoon, A.; Leipzig, N. D., 3D differentiation of neural stem cells in macroporous photopolymerizable hydrogel scaffolds. *PloS one* **2012,** *7* (11), e48824.
37. Wilkinson, A. E.; Kobelt, L. J.; Leipzig, N. D., Immobilized ECM molecules and the effects of concentration and surface type on the control of NSC differentiation. *Journal of Biomedical Materials Research Part A* **2014,** *102* (10), 3419-3428.
38. (a) Gunn, J. W.; Turner, S. D.; Mann, B. K., Adhesive and mechanical properties of hydrogels influence neurite extension. *Journal of biomedical materials research. Part A* **2005,** *72* (1), 91-7; (b) Burdick, J. A.; Ward, M.; Liang, E.; Young, M. J.; Langer, R., Stimulation of neurite outgrowth by neurotrophins delivered from degradable hydrogels. *Biomaterials* **2006,** *27* (3), 452-9.
39. Liu, C.; Sage, J. C.; Miller, M. R.; Verhaak, R. G.; Hippenmeyer, S.; Vogel, H.; Foreman, O.; Bronson, R. T.; Nishiyama, A.; Luo, L.; Zong, H., Mosaic analysis with double markers reveals tumor cell of origin in glioma. *Cell* **2011,** *146* (2), 209-21.
40. Martens, P. J.; Bryant, S. J.; Anseth, K. S., Tailoring the degradation of hydrogels formed from multivinyl poly(ethylene glycol) and poly(vinyl alcohol) macromers for cartilage tissue engineering. *Biomacromolecules* **2003,** *4* (2), 283-92.
41. (a) Lampe, K. J.; Bjugstad, K. B.; Mahoney, M. J., Impact of degradable macromer content in a PEG hydrogel on neural cell metabolic activity, redox state, proliferation, and differentiation. *Tissue engineering. Part A* **2010,** *16* (6), 1857-1866; (b) van Lith, R.; Gregory, E. K.; Yang, J.; Kibbe, M. R.; Ameer, G. A., Engineering biodegradable polyester elastomers with antioxidant properties to attenuate oxidative stress in tissues. *Biomaterials* **2014,** *35* (28), 8113-22; (c) Murphy, W. L.; McDevitt, T. C.; Engler, A. J., Materials as stem cell regulators. *Nature materials* **2014,** *13* (6), 547-57.
42. Lampe, K.; Namba, R.; Silverman, T.; Bjugstad, K.; Mahoney, M., Impact of Lactic Acid on Cell Proliferation and Free Radical-Induced Cell Death in Monolayer Cultures of Neural Precursor Cells. *Biotechnology and bioengineering* **2009,** *103* (6), 1214-1223.
43. (a) Soderquist, R. G.; Milligan, E. D.; Sloane, E. M.; Harrison, J. A.; Douvas, K. K.; Potter, J. M.; Hughes, T. S.; Chavez, R. A.; Johnson, K.; Watkins, L. R.; Mahoney, M. J., PEGylation of brain-derived neurotrophic factor for preserved biological activity and enhanced spinal cord distribution. *Journal of biomedical materials research. Part A* **2009,** *91* (3), 719-29; (b) Bible, E.; Chau, D. Y.; Alexander, M. R.; Price, J.; Shakesheff, K. M.; Modo, M., The support of neural stem cells transplanted into stroke-induced brain cavities by PLGA particles. *Biomaterials* **2009,** *30* (16), 2985-94.
44. Silva, N. A.; Salgado, A. J.; Sousa, R. A.; Joliveira, J. T.; Pedro, A. J.; Leite-Almeida, H.; Cerqueira, R.; Almeida, A.; Mastronardi, F.; Mano, J. F.; Neves, N. M.; Sousa, N.; Reis, R. L., Development and Characterization of a Novel Hybrid Tissue Engineering-Based Scaffold for Spinal Cord Injury Repair. *Tissue engineering. Part A* **2010,** *16* (1), 45-54.

45. Horne, M. K.; Nisbet, D. R.; Forsythe, J. S.; Parish, C. L., Three-dimensional nanofibrous scaffolds incorporating immobilized BDNF promote proliferation and differentiation of cortical neural stem cells. *Stem cells and development* **2010,** *19* (6), 843-52.
46. Aizawaa, Y.; Leipzig, N. D.; Zahira, T.; Shoichet, M. S., The effect of immobilized platelet derived growth factor AA on neural stem/ progenitor cell differentiation on cell-adhesive hydrogels. *Biomaterials* **2008,** *29*, 4676–4683.
47. Li, H.; Koenig, A. M.; Sloan, P.; Leipzig, N. D., In vivo assessment of guided neural stem cell differentiation in growth factor immobilized chitosan-based hydrogel scaffolds. *Biomaterials* **2014,** *35* (33), 9049-57.
48. (a) Yang, N.; Zuchero, J. B.; Ahlenius, H.; Marro, S.; Ng, Y. H.; Vierbuchen, T.; Hawkins, J. S.; Geissler, R.; Barres, B. A.; Wernig, M., Generation of oligodendroglial cells by direct lineage conversion. *Nat Biotechnol* **2013,** *31* (5), 434-9; (b) Najm, F. J.; Lager, A. M.; Zaremba, A.; Wyatt, K.; Caprariello, A. V.; Factor, D. C.; Karl, R. T.; Maeda, T.; Miller, R. H.; Tesar, P. J., Transcription factor-mediated reprogramming of fibroblasts to expandable, myelinogenic oligodendrocyte progenitor cells. *Nat Biotechnol* **2013,** *31* (5), 426-33.
49. Noble, M.; Mayer-Proschel, M.; Proschel, C., iOPs: a new tool for studying myelin pathologies? *Cell stem cell* **2013,** *12* (5), 503-4.
50. Shreiber, D. I.; Hao, H.; Elias, R. A., Probing the influence of myelin and glia on the tensile properties of the spinal cord. *Biomechanics and modeling in mechanobiology* **2009,** *8* (4), 311-21.
51. Kandel, E. R.; Schwartz, J. H.; Jessell, T. M., *Principles of Neural Science, Fourth Edition*. Fourth Edition ed.; McGraw-Hill: New York, 2000.
52. Sack, I.; Streitberger, K. J.; Krefting, D.; Paul, F.; Braun, J., The influence of physiological aging and atrophy on brain viscoelastic properties in humans. *PloS one* **2011,** *6* (9), e23451.
53. Carenini, S.; Montag, D.; Schachner, M.; Martini, R., MAG-deficient Schwann cells myelinate dorsal root ganglion neurons in culture. *Glia* **1998,** *22* (3), 213-20.
54. Pittier, R.; Sauthier, F.; Hubbell, J. A.; Hall, H., Neurite extension and in vitro myelination within three-dimensional modified fibrin matrices. *Journal of neurobiology* **2005,** *63* (1), 1-14.
55. (a) Gingras, M.; Beaulieu, M. M.; Gagnon, V.; Durham, H. D.; Berthod, F., In vitro study of axonal migration and myelination of motor neurons in a three-dimensional tissue-engineered model. *Glia* **2008,** *56* (3), 354-64; (b) Thomas, A. M.; Seidlits, S. K.; Goodman, A. G.; Kukushliev, T. V.; Hassani, D. M.; Cummings, B. J.; Anderson, A. J.; Shea, L. D., Sonic hedgehog and neurotrophin-3 increase oligodendrocyte numbers and myelination after spinal cord injury. *Integrative biology : quantitative biosciences from nano to macro* **2014,** *6* (7), 694-705; (c) Xiong, Y.; Zhu, J. X.; Fang, Z. Y.; Zeng, C. G.; Zhang, C.; Qi, G. L.; Li, M. H.; Zhang, W.; Quan, D. P.; Wan, J., Coseeded Schwann cells myelinate neurites from differentiated neural stem cells in neurotrophin-3-loaded PLGA carriers. *International journal of nanomedicine* **2012,** *7*, 1977-89.
56. Li, X.; Liu, X.; Cui, L.; Brunson, C.; Zhao, W.; Bhat, N. R.; Zhang, N.; Wen, X., Engineering an in situ crosslinkable hydrogel for enhanced remyelination. *FASEB journal : official publication of the Federation of American Societies for Experimental Biology* **2013,** *27* (3), 1127-36.

57. Wang, H. B.; Mullins, M. E.; Cregg, J. M.; Hurtado, A.; Oudega, M.; Trombley, M. T.; Gilbert, R. J., Creation of highly aligned electrospun poly-L-lactic acid fibers for nerve regeneration applications. *J Neural Eng* **2009,** *6* (1), 016001.
58. (a) Schnell, E.; Klinkhammer, K.; Balzer, S.; Brook, G.; Klee, D.; Dalton, P.; Mey, J., Guidance of glial cell migration and axonal growth on electrospun nanofibers of poly-epsilon-caprolactone and a collagen/poly-epsilon-caprolactone blend. *Biomaterials* **2007,** *28* (19), 3012-25; (b) Chew, S. Y.; Mi, R.; Hoke, A.; Leong, K. W., The effect of the alignment of electrospun fibrous scaffolds on Schwann cell maturation. *Biomaterials* **2008,** *29* (6), 653-61.
59. (a) Lee, S.; Leach, M. K.; Redmond, S. A.; Chong, S. Y.; Mellon, S. H.; Tuck, S. J.; Feng, Z. Q.; Corey, J. M.; Chan, J. R., A culture system to study oligodendrocyte myelination processes using engineered nanofibers. *Nature methods* **2012,** *9* (9), 917-22; (b) Lee, S.; Chong, S. Y. C.; Tuck, S. J.; Corey, J. M.; Chan, J. R., A rapid and reproducible assay for modeling myelination by oligodendrocytes using engineered nanofibers. *Nature Protocols* **2013,** *8* (4), 771-782.
60. Diao, H. J.; Low, W. C.; Milbreta, U.; Lu, Q. R.; Chew, S. Y., Nanofiber-mediated microRNA delivery to enhance differentiation and maturation of oligodendroglial precursor cells. *Journal of controlled release : official journal of the Controlled Release Society* **2015,** *208*, 85-92.
61. Kirby, B. B.; Takada, N.; Latimer, A. J.; Shin, J.; Carney, T. J.; Kelsh, R. N.; Appel, B., In vivo time-lapse imaging shows dynamic oligodendrocyte progenitor behavior during zebrafish development. *Nat Neurosci* **2006,** *9* (12), 1506-11.
62. Syed, Y. A.; Baer, A. S.; Lubec, G.; Hoeger, H.; Widhalm, G.; Kotter, M. R., Inhibition of oligodendrocyte precursor cell differentiation by myelin-associated proteins. *Neurosurgical focus* **2008,** *24* (3-4), E5.
63. (a) Rafalski, V. A.; Ho, P. P.; Brett, J. O.; Ucar, D.; Dugas, J. C.; Pollina, E. A.; Chow, L. M.; Ibrahim, A.; Baker, S. J.; Barres, B. A.; Steinman, L.; Brunet, A., Expansion of oligodendrocyte progenitor cells following SIRT1 inactivation in the adult brain. *Nature cell biology* **2013,** *15* (6), 614-24; (b) Zuchero, J. B.; Barres, B. A., Glia in mammalian development and disease. *Development* **2015,** *142* (22), 3805-9.

3 Oligodendrocyte Precursor Cell Viability, Proliferation, and Morphology is Dependent on Mesh Size and Storage Modulus in 3D Poly(ethylene glycol) Based Hydrogels

Published as: LN Russell, KJ Lampe, "Oligodendrocyte Precursor Cell Viability, Proliferation, and Morphology is Dependent on Mesh Size and Storage Modulus in 3D Poly(ethylene glycol) Based Hydrogels," *ACS Biomater. Sci. Eng.* (2017).

3.1 Abstract

Oligodendrocytes in the central nervous system (CNS) are responsible for generating myelin, an electrically insulating layer around neuronal axons. When myelin is damaged, neurons are incapable of sustaining normal communications which can manifest in patients as pain and loss of mobility and vision. A plethora of research has used biomaterials to promote neuronal regeneration, but despite the wide implications of a disrupted myelin sheath, very little is known about how biomaterial environments impact proliferation of oligodendrocyte precursor cells (OPCs) or their differentiation into myelinating oligodendrocytes. This work investigates how the storage modulus and mesh size of a polyethylene glycol (PEG)-based hydrogel, varied via two different mechanisms, directly affect the proliferation of two OPC lines encapsulated and cultured in 3D. Viability and proliferation of both OPC lines was dependent on hydrogel swelling and stiffness, where the concentration of ATP increased more in the more compliant

gels. OPCs multiplied in the 3D hydrogels, creating significantly larger spheroids in the less crosslinked conditions. Stiffer, more highly crosslinked materials lead to greater expression of PDGFRα, an OPC receptor, indicating that fewer cells were committed to the oligodendrocyte lineage or had de-differentiated. Laminin incorporation in the 3D matrix was found to have little affect on viability or proliferation. These findings provide valuable information on how mesh size and stiffness affect OPCs, where more compliant materials favor proliferation of OPCs and less commitment to a mature oligodendrocyte lineage. Such information will be useful in the development of translational biomaterials to stimulate oligodendrocyte maturation for neural regeneration.

3.2 Introduction

The electrically insulating myelin sheath around neuronal axons, produced by oligodendrocytes in the central nervous system (CNS), enables neurons to communicate efficiently with each other[1]. However, in demyelinating diseases such as multiple sclerosis (MS) oligodendrocytes and their myelin are damaged and degraded, and the CNS is intrinsically limited in its regeneration capability. Current MS treatments address secondary damage, but do not directly target oligodendrocytes or their precursors[2]. A mechanism to better understand and study oligodendrocytes and oligodendrocyte precursor cells (OPCs), the glial-restricted neural precursor cells (NPCs) that give rise to myelinating oligodendrocytes, may present new therapeutic targets.

Following demyelinating diseases, the injury and disease microenvironment pose significant challenges for regeneration by stem or precursor cells. OPCs have been found to migrate effectively to the damaged tissue[3], but they often fail to survive, differentiate, or regenerate the damaged myelin[4]. Stem cell transplantation may help circumvent these

limitations, however transplantation strategies are variable and irreproducible[5] as cells do not survive transplantation[6] or do not differentiate into functional cell types[7].

Biomaterials can act as a matrix for cell delivery, improving transplanted cell localization, survival, and differentiation[8]. Tunable biomaterial properties such as stiffness, integrin binding domains, and topography have been widely investigated for their effects on neuronal differentiation[9]. Despite the wide use of biomaterials in neural regeneration applications and their biophysical impacts on stem cells, few studies have investigated the effect of biomaterial properties on differentiation into oligodendrocyte lineages[10]. Most studies that did focus on the delivery of growth factors to regenerate oligodendrocytes rather than the biophysical material properties[11]. In limited studies OPCs respond to mechanical stimuli in 2D[9f, 12] and fewer still show the effect of 3D matrix stiffness on OPCs differentiation into oligodendrocytes[13]. Left unanswered is how the stiffness of a material directly affects OPC proliferation, particularly in 3D.

Poly(ethyelene gycol) (PEG)-based biomaterials are widely used for applications in neural regeneration as they readily mimic the highly hydrated, compliant CNS tissue[14]. PEG can be chemically functionalized to incorporate degradable sites, bioactive sequences, and growth factor or drug release systems[8, 15]. PEG-based hydrogels have been used to investigate material effects on NPCs and/or their differentiation into neurons[16]. In particular, NPCs in low concentration PEG-dimethacrylate (PEG-DM) gels, and therefore lower stiffness gels, exhibit higher metabolic activity, greater neuronal differentiation, and lower apoptotic activity[17].

Here we use PEG-DM hydrogels of varying mesh sizes and storage moduli to determine the effect(s) of hydrogel properties on viability and proliferation of two different OPC lines encapsulated in 3D. We varied the stiffness and mesh size via two different molecular

mechanisms; changing macromer molecular weight, and changing the concentration of polymer in solution. We encapsulated two different OPC lines, N20.1[18] and MADM[19], to verify observed trends, as large differences have been observed in OPC development and differentiation potential based on the cell source[20]. DNA and ATP were measured from cell lysates within the hydrogel as a measure of viability and proliferation. In addition, ATP has been found to be an important regulator in cellular migration, proliferation, and differentiation or remyelination[21]. With both cell lines, we found that cells remained viable and proliferated in all hydrogel conditions, although in a stiffness and mesh size dependent trend. Larger increases in ATP and greater amounts of proliferation were observed in hydrogels of 1) lower macromer concentrations and 2) higher macromer molecular weights. These materials had higher mesh sizes, lower stiffnesses, and therefore a lower crosslinking density. Our PEG-based system alone is sufficient for OPC growth, as incorporating laminin did not affect morphology or viability. This is to our knowledge the first study demonstrating hydrogel-mediated effects on glial-restricted precursor cell proliferation in a 3D environment. These results indicate the potential PEG-based hydrogels may have in expanding OPCs and directing cell fate in CNS regeneration applications.

3.3 Materials and Methods

3.3.1 Macromer Synthesis

PEG-DM macromer was synthesized from PEG (Sigma-Aldrich, USA) at varying molecular weights: 4600, 6000 and 8000 g/mol according to established protocols[22]. Up to 5 grams PEG were massed out in a glass scintillation vial and mixed with 10X molar ratio of methacrylic anhydride (Alfa-Aesar, USA). Vials were microwaved (Rival, 900 watts) for 5 minutes, vortexing every 30 seconds. PEG-DM was purified by dissolving in dichloromethane and precipitating into ice cold ethyl ether. The precipitate was recovered through vacuum

filtration and remaining solvent was removed under vacuum. PEG-DM was dialyzed against diH_20 for 3 days and subsequently lyophilized to obtain a high purity dry macromer. Methacrylation efficiency of the macromer was determined using proton nuclear magnetic resonance spectroscopy and determined to be 82-86% for all molecular weights. Lyophilized macromer was stored at 4°C and protected from light until use.

3.3.2 Photoinitiator Synthesis

PEG-DM was gelled using the photoinitiator lithium phenyl-2,4,6-trimethylbenzoylphosphonate (LAP) synthesized using previously published protocols [23]. Briefly, 3.0 g of dimethyl phenylphosphonate (Acros Organics, USA) was reacted under argon at room temperature with 3.2 grams of 2,4,6-trimethylbenzoyl chloride (Sigma-Aldrich). The reaction was stirred for 18 hours at which time 6.1 grams of lithium bromide (Sigma-Aldrich) and 100 mL of methyl ethyl ketone were added. The temperature was increased to 50 ºC and after ten minutes a white precipitate formed. The mixture was then cooled to room temperature for four hours before filtering and washing with methyl ethyl ketone.

3.3.3 Cell Culture

N20.1 and GFP^+ MADM OPC lines were expanded in vitro on tissue culture treated plates. N20.1 cells are a cell line from mice with a temperature dependent differentiation vector[18], while MADM cells are mouse glioma-derived cells that express many OPC markers[19]. MADM cell culture plates were coated with polyornithine before seeding cells, while N20.1 cells were grown on plates without modification. N20.1 OPCs were maintained in their undifferentiated state by culturing at 34 ºC in proliferation media consisting of Dulbecco's modified eagle media with high glucose and F12 media (1:1) (Corning, USA), 10% fetal bovine

serum (Corning, USA), 3.38 mg/mL HEPES, 2.4 mg/mL sodium bicarbonate, 100 μg/mL G418 (Life Technologies, USA), 20 μg/mL gentamicin (Life Technologies), and 1% penicillin-streptomycin (Life Technologies). GFP^+ MADM OPCs were cultured in Dulbecco's modified eagle medium with high glucose, 4mM L-glutamine, 1mM sodium pyruvate (Life Technologies) with N2 supplement (Life Technologies), B27 supplement (Life Technologies), 1% penicillin/streptomycin (Life Technologies), 10 ng/mL mouse PDGF-AA (eBioscience, USA) and 50 ng/mL human NT3 (Peprotech, USA). Cell media was changed every two to three days and cells were grown to 90% confluency and passaged using 0.25% trypsin in Dulbecco's phosphate buffered saline (PBS) without divalent cations.

3.3.4 Hydrogel Gelation and Material Characterization

For mesh size calculations and rheological measurements, hydrogels were made in PBS. Gels were made at varying concentrations from 6 to 20 % (wt/v) of macromer, and LAP was maintained at 0.05 mole ratio to PEG-DM. Macromer solutions were exposed to light at 365 nm with an intensity of 4 mW/cm^2 for 10 minutes.

Gel masses were obtained immediately after gel formation and then placed in PBS for one day to swell. Swollen gels were again massed, then frozen at -80 ^oC overnight and lyophilized. Mass swelling ratios were calculated as the wet mass over dry mass, and mesh sizes were subsequently calculated using the Canal and Peppas equation[24]. The critical ratio, C_n, average bond length, l, and Flory interaction parameter, χ, were assumed to be 4, 1.46 Å, and 0.426, respectively, according to previous literature[24].

Gels used to determine storage and loss modulus were made in an 8 mm diameter mold and allowed to swell for 24 hours in PBS before running a strain sweep on an Anton Paar MCR

rheometer using an 8mm parallel plate. Strain sweeps were preformed over strains from 0.001% to 100% strain with a fixed frequency of 10 s^{-1} to obtain the storage moduli in the linear viscoelastic region. The rheometer plates were fixed at 20°C.

3.3.5 Cell Encapsulation and Analysis

Hydrogels for cell encapsulation were made with macromer and cell media absent serum, growth factors, or media supplements. 40 μL hydrogels with 1 x 10^7 cells/mL were made by mixing the cells and macromer to a desired concentration, 6-10% macromer (wt/v), and polymerizing for 10 minutes at ~4 mW/cm^2. For laminin studies, type one laminin (Invitrogen, Carlsbad, CA) was mixed in prior to polymerization to achieve a final concentration in the gel of 25 μg/mL. Following polymerization, gels were rinsed 3X in PBS and cultured in complete growth media. Media was changed 24 hrs after encapsulation and every two days thereafter. Gels were collected at discrete time points and either imaged with the live/dead assay (ThermoFisher, USA) or stored at -80 °C in lysis buffer before running ATP or DNA quantification assays. For quantification, gels were homogenized in lysis buffer using a hand grinder until only small gel particulates were observed (particulates with diameters of approximately 0.5 mm). Following homogenization, samples were sonicated for 30 seconds in an attempt to further break up the samples release biomolecules into solution. ATP and DNA of cell lysates were measured using the CellTiter-Glo luminescent Cell Viability Assay (Promega, USA) and the Quant-iT PicoGreen dsDNA assay (ThermoFisher) according to manufacturer protocols. Briefly, equal volumes of homogenized gel/cell samples were added with reagent in 384 well plates in triplicate and compared with standards of known concentration.

3.3.6 Live/dead Image Collection and Analysis

Gels were rinsed for 15 minutes in PBS plus glucose (PBSG), stained with 2 μM calcien and 4 μM ethidium homodimer for 30 minutes in PBSG, and rinsed in PBSG prior to imaging. Live/dead images were collected using a Zeiss LSM 510 confocal microscope. 200 μm z-stack images were collected with a frame distance of 1 μm. Representative images shown in figures are 100 μm thick z-stacks. Analysis for cluster sizing was performed in ImageJ on non-overlapping 20 μm thick sections. To prevent counting clusters twice, 20 μm image sections were alternatively included and excluded in analysis from the 100 μm thick z-stacks. For cluster analysis, 3 gels were imaged in 3 different locations for a total of 15 quantified sections per gel condition.

3.3.7 EdU staining

At four or seven days after encapsulation, EdU was added to cell culture media at a concentration of 50 μg/mL for four hours. EdU media was aspirated and gels were rinsed with PBS 3 times, for five minutes. Cells were then fixed in 4% paraformaldehyde for 1 hour at 4 ºC and permeablized overnight at 4 ºC in PBS with 0.3 % triton X. The Click-iT reaction solution was added to each gel for 35 minutes. The Click-iT reaction solution consists of 0.1 M Tris-HCl (Fisher), 0.001M $CuSO_4$ (Fisher), Alexa Fluor 555 azide (1:1000) (ThermoFisher), and 0.1 M ascorbic acid (Sigma). Click-iT solutions were made immediately before use to ensure proper oxidation states of the copper ions. The Click-iT reaction solution was then removed from the gels and replaced with DAPI staining solution (1:1000 in PBS) for 20 minutes. Gels were subsequently washed three times in PBS with 0.3% triton for five minutes before imaging on a Zeiss 780 confocal microscope.

3.3.8 Immunostaining

After 7 days of culture, gels were fixed in 4% paraformaldehyde for 20 minutes at 4 ºC and permeablized overnight at 4 ºC in PBS with 5 % normal donkey serum and 0.3 % triton X. Gels were incubated at room temperature for 6 hours with goat platelet derived growth factor receptor-α (PDGFRα) primary antibody (1:250, R&D Systems, Minneapolis, MN). After washing four times in PBS with 0.3% triton X for 20 minutes each, gels were incubated overnight at 4 ºC with donkey anti-goat Alexa 555 secondary antibody (1:250, Invitrogen). In the last 20 minutes, 4',6-diamidino-2-phenylindole (DAPI) was added to stain cell nuclei. Gels were then washed 4 x 20 minutes in PBS and imaged with a Zeiss LSM 780 confocal microscope.

3.3.9 Statistical Analysis

Values for material characterization data were presented as the average plus or minus standard deviation (n = 4). A two tailed t-test was used to determine significance ($\alpha < 0.05$) between hydrogels of different macromer molecular weights. In cell studies, three gels were collected for each time point of an experiment and the experiment was repeated 3 times for a total of n = 9. Initial ATP and DNA values were compared to verify that the encapsulation process was not artificially biasing results before normalizing to the 1 hr experimental time point. ATP and DNA data shown are the average fold change from 1 hr plus or minus standard deviation. The average for each time point was then compared to 1hr or the other conditions at that time using a students' two tailed t-test to determine significance ($\alpha < 0.05$). For both cell types, all ATP values at later time points were statistically significant and greater than the initial, one hour time point ATP value. DNA values for both cell types at seven days were all statistically significant and greater than the initial time points, except where indicated in Figure 5. Figures indicate significance between macromer molecular weights, using the students' two tailed t-test ($\alpha < 0.05$).

3.4 Results and Discussion

3.4.1 Hydrogel properties can be changed by tuning macromer molecular weight and concentration in solution

Consistent with previous reports[17], tuning the crosslinking density by changing the macromer molecular weight or the concentration in solution during polymerization resulted in predictable differences in mass swelling ratio, mesh size, and storage moduli (Figure 3-1). Crosslinking density, while not directly determined, is inversely related to the mesh size and mass swelling ratios. In addition, an increase in storage moduli indicates an increase in crosslinking density. Changing the concentration of macromer in solution yielded the largest differences in stiffnesses and mesh sizes compared to changing the range of molecular weights, 4600 to 8000 Da. Mass swelling ratios were large due to PEG hydrophilicity, and range from 31.5 ± 3.1 to 7.0 ± 0.1 (Figure 3-1A). This mass swelling ratio corresponded with a large percent swelling, 60 %, in the most compliant 6 % (w/v) 8000 MW PEG. A higher swelling ratio and a large percent swelling after gelation are indicative of an increase in mesh size, and with cell studies can correlate to a decrease in cell concentration as the gel expands. Mesh sizes sufficient to enable protein diffusion ranged from 120 to 66 Å in gels where the macromer concentration changed from 6 % to 10 % (wt/v), respectively (Figure 3-1B). It is important to note that these mesh sizes were still smaller than average process diameters and therefore only limited process extension can occur inside the hydrogel. Additionally, mesh sizes on the order of 120 to 66 Å would hinder the diffusion of larger proteins with hydrodynamic radii greater than 6 nm, such as extracellular matrix proteins like laminin. Swelling and mesh characterizations were similar to previous literature, differing slightly due to increases in methacrylation efficiency[16-17].

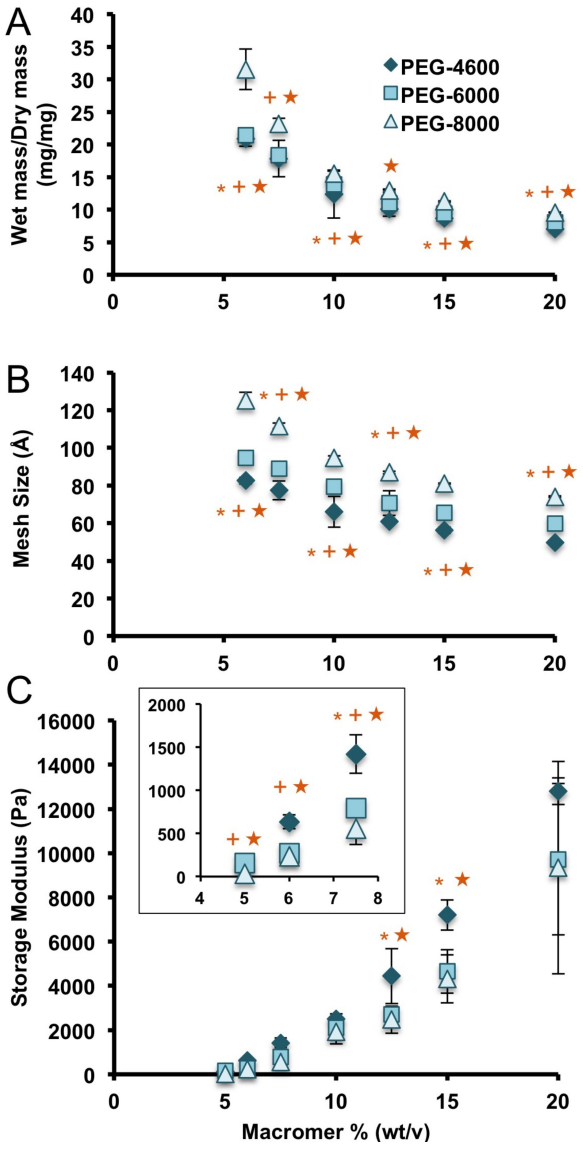

*Figure 3-1 Material properties of PEG-DM hydrogels can be tuned by changing the molecular weight or concentration in solution during crosslinking. Mass swelling ratio (A) and mesh size (B) decreased with increasing concentration and decreasing molecular weight. Storage moduli were obtained from oscillatory shear rheology and showed an increase in moduli with increasing concentrations (C). The stiffnesses of lower concentration hydrogels were similar to native brain tissue (C, inset). * indicates that data for the 4600 MW PEG gel is statistically different ($\alpha < .05$) from the 6000 MW PEG gel, + for 6000 MW PEG gel vs. 8000 MW PEG, and ★ for 4600 MW PEG gel vs. 8000 MW PEG. Changing the concentration in solution always resulted in changes in swelling ratios, mesh size, and storage moduli that were statistically different for PEG 8000 ($\alpha < .05$).*

Gels of different compositions exhibited a large range of storage moduli after a 24 hour hydrogel equilibration in PBS (Figure 3-1C). 6% gels yielded the most compliant storage moduli and those most similar to native brain tissue[14a] with values of 240 ± 84, 270 ± 87, and 630 ± 79 Pa for the 8000, 6000, and 4600 g/mol PEG macromers, respectively. Gels made at 7.5% (wt/v) yielded moderate stiffnesses of 1420, 790, 560 for 4600, 6000, and 8000 g/mol PEG. 8000 g/mol PEG hydrogels at 10% wt/v were the stiffest, most crosslinked hydrogels used in cell studies and had a storage modulus of 1910 ± 500 Pa. These storage moduli were comparable to moduli reported from other PEG hydrogel systems[25]. Native neural tissue is typically reported with a storage moduli around 1 kPa[26]. Recently, CNS tissue storage moduli have been shown to decrease following injury to around 300 Pa[27], compared to previous findings in other tissues that stiffen in response to injury[26]. Materials used here for cell studies cover a range from 230 Pa to 1910 Pa to mimic native neural tissue from different brain regions as well as injury microenvironments.

3.4.2 Cells respond to changes in crosslinking density with differences in viability and proliferation

Changing the molecular weight

As previously discussed, the stiffness and mesh size of PEG-DM hydrogels can be tuned by changing both the molecular weight as well as the concentration (Figure 3-2A). Photoinitated crosslinking enabled fully 3D encapsulation of cells within the hydrogel (Figure 3-2A). First we examined how smaller changes in stiffness and swelling, obtained by adjusting the molecular weight could affect the proliferation and viability of OPCs. Two OPC cell lines, the N20.1 line and MADM line, were used to further validate the translation of stiffness and swelling trends to primary cells.

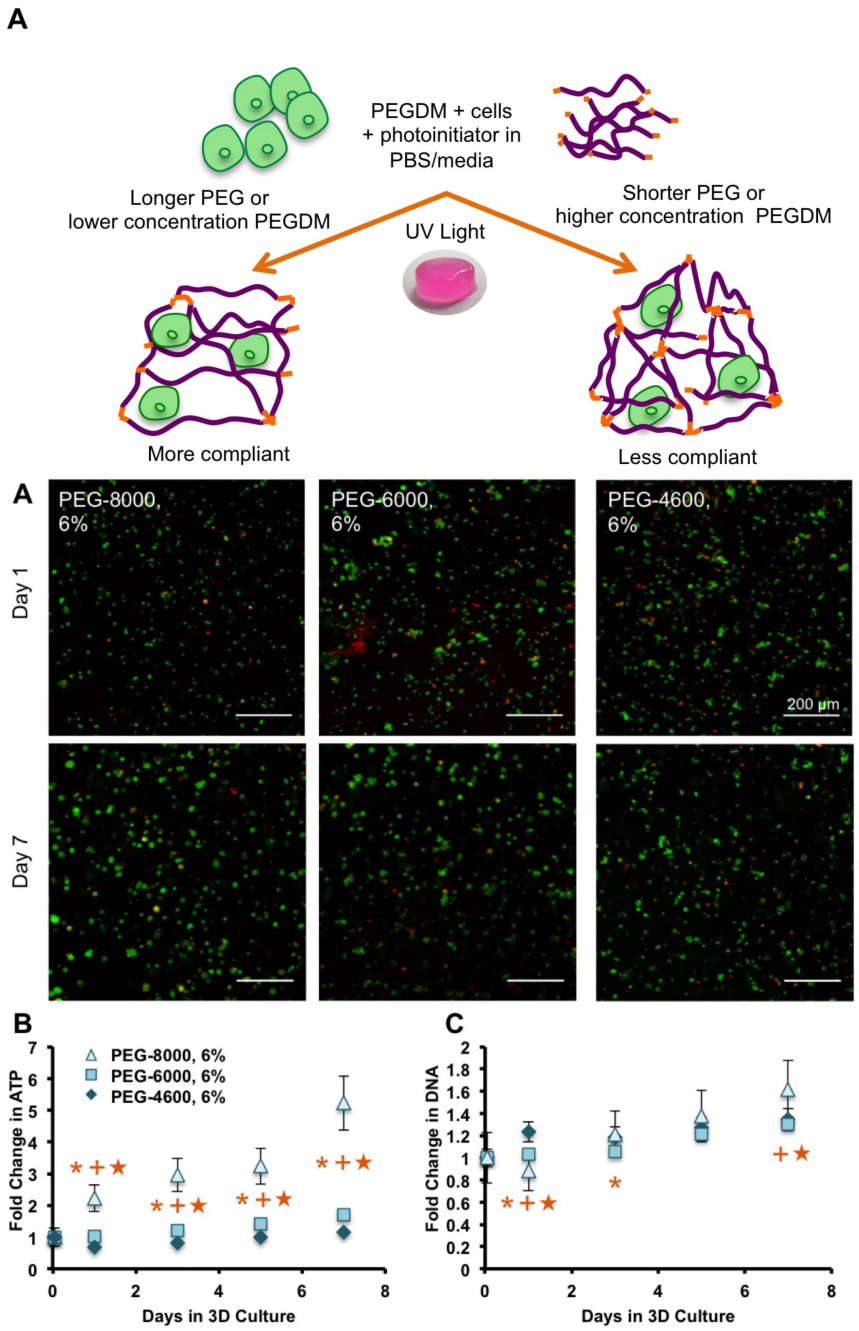

*Figure 3-2 Cell encapsulation scheme and N20.1 oligodendrocyte precursor cell line encapsulated in 6 wt% gels of varying molecular weights. Cells were encapsulated in the PEG hydrogels by mixing with macromer solutions of varying molecular weight or concentration in solution and exposing to UV light for 10 minutes (A). N20.1 cells remained viable after encapsulation and for at least 7 days as shown by live/dead (green/red) staining and confocal microscopy (B). * indicates that data for the 4600 MW PEG gel is statistically different ($\alpha < .05$) from the 6000 MW PEG gel, + for 6000 MW PEG gel vs. 8000 MW PEG, and ★ for 4600 MW*

PEG gel vs. 8000 MW PEG gel. ATP (C) and DNA (D) both increased over seven days in 3D culture ($\alpha < .05$).

Both cell types remain viable and proliferated in all hydrogel conditions. 6 % (wt/v) gels resulted in similar swelling and stiffness-dependent trends for both the N20.1 line (Figure 3-2) and MADM line[10]. The live/dead assay indicated a high percentage of viable cells with minimal differences in the three conditions for N20.1 cells (Figure 3-2B). Live/dead viability trends were consistent with previous results with Schwann cells, the peripheral nervous system equivalent cell type[28]. Previously, Schwann cells encapsulated in PEG-diacrylate microgels of similar stiffnesses remained viable and exhibited elongated morphologies[28]. Here, over the course of the culture period, OPC cellular areas appeared to increase in size, indicative of clonal expansion (Figure 3-2B). However, despite the increase in cellular area, cells remained in spherical clusters (Figure 3-2B). This is distinctly different from previous data with Schwann cells, where cell elongation and process extension was possible. These differences in observed morphologies were likely due to differences in hydrogel mesh size and the incorporation of collagen in the Schwann cell studies[28]. The mesh size of the PEG microgels used with Schwann cells was not quantified, however the architecture of the gels suggest macroporous regimes that would enable cell process extension. In addition, OPCs both in vivo and in in vitro co-cultures with neurons extend processes and migrate toward unoccupied areas to create uniform OPC distribution[29]; our PEG-DM hydrogel formulations will likely need to be modified, to obtain greater mesh sizes, higher porosity or increased degradability, to allow migration of cells through the dense hydrogel mesh.

With both OPC lines, fold increases in ATP were greatest in the most compliant hydrogels with the larger mesh sizes. Alternatively, ATP values, while still increasing over time, were lower in the hydrogels that were stiffer and had smaller mesh sizes. Here, ATP can not only be used as an indicator of viability, but also functionality as it has been shown that myelinating

oligodendrocytes are able to produce and deliver ATP to neuronal axons[30]. In addition, ATP has been found to be an important regulator in OPC migration, proliferation, and differentiation or remyelination[21]. For N20.1 cells, the most compliant, 240 Pa, hydrogel made from 6%, 8000 g/mol PEG resulted in a fold change in ATP of 5.2, which is significantly greater than both 270 and 630 Pa hydrogels (Figure 3-2C). This was comparable to results with NSCs and other neural cells which showed stiffness impacts proliferation, morphology, and differentiation[17, 31]. Slight changes in stiffness from 240 to 630 Pa and mesh sizes from 94.7 to 66.1 Å, by changing the molecular weight of 6% (wt/v) gels from 8000 to 4600 g/mol, resulted in significant increases in ATP from one hour ($\alpha < 0.05$) as well as from one another with N20.1 cells (Figure 3-2C).

DNA increased in all conditions over time for N20.1 cells (Figure 3-2D), however smaller differences between conditions were observed than with ATP (Figure 3-2C). After seven days the DNA fold change observed in the 8000 g/mol PEG condition was statistically greater than fold changes in the 6000 and 4600 g/mol PEG at 6% (wt/v) (Figure 3-2D). In addition, DNA concentrations after seven days were statistically greater than at one hour, however the fold changes observed are much lower than ATP changes. Disagreement in fold changes with ATP and DNA was likely due to the difficulty of extracting large DNA molecules from the hydrogel particulate following homogenization (Figure 3-2C).

These growth and viability results were consistent with previous results where neural stem cells encapsulated in PEG hydrogels proliferated differentially as a function of hydrogel stiffness[17]. However, it had previously been found that on stiffer surfaces neural stem cells tend to differentiate down a glial lineage including oligodendrocytes or astrocytes[13b], suggesting that OPCs might prefer a stiffer matrix for differentiation.

We made gels at 7.5 % to slightly increase the stiffness and decrease swelling and investigated again for ATP and DNA increases (Figure 3-3, S1). Similar trends were found to that of 6% gels, where more compliant gels led to larger increases of ATP and less compliant led to smaller increases in ATP, although still supported increasing values over time (Figure 3-3A,C). DNA also exhibited similar trends with fewer statistical differences between gel mechanics in the range of molecular weights from 4600 to 8000 g/mol (Figure 3-3B,D). While low fold changes occured in DNA concentrations, the values obtained after seven days in 3D culture were all statistically greater than the one hour time point. Relatively small increases in DNA compared to ATP were again likely due to the difficulty of extracting DNA from the hydrogel mesh, although the comparatively large increases in ATP may be due to the importance of ATP in OPC migration, proliferation, and differentiation[21]. ATP increases were consistent with live/dead staining showing large clonal cell clusters of MADM OPCs after seven days (Figure 3-3E). Quantitative measurements indicated larger cluster sizes of MADM OPCs in the most compliant materials (Table 2) and therefore a greater number of cells. Similar live/dead images were observed for N20.1 OPCs, but had limited formation of large spheroids (Figure 3-S1), likely due to the overall lower rate of proliferation for this cell type compared to MADM OPCs.

Table 2 Average cell cluster diameter in 7.5% PEGDM hydrogels of varying macromer molecular weight. Cluster diameter increases as macromer molecular weight increases.

7.5% (wt/v)	**Average cluster diameter (μm)**	**Error (S.D.)**	**Total # of clusters measured**
PEG-4600	13.6	±2.49	2645
PEG-6000	15.5	±1.67	1968

PEG-8000	21.1	±1.43	1047

EdU staining confirmed that proliferation was occurring leading to larger clusters over time in 7.5% (wt/v) hydrogels (Figure 3-4). As the macromer molecular weight increased resulting in more compliant hydrogels, a higher ratio of EdU+ nuclei were observed indicating more proliferating cells (Figure 3-4). Images display a single z-slice for clarity, while the ratio of EdU to DAPI presented are from max projections of 50 μm z-stacks. These qualitative and quantitative increases in proliferation follow the cell cluster analysis and ATP trends. The highest proliferation rate was observed in the most compliant 8000 g/mol hydrogel, with 49.2% of cells labeling for EdU at 4 days after encapsulation, compared to 41.2% for 4600 g/mol hydrogels. EdU staining from 4 to 7 days indicated a decreasing proliferation rate over that timespan. This is consistent with BrdU staining of MADM cells *in vivo,* which have been shown to decrease in proliferation rate from 5 to 10 days[19].

Changing the macromer concentration

Similar to results obtained from tuning molecular weight, MADM cells demonstrated a stiffness and swelling ratio dependent trend in ATP concentration (Figure 3-5A) and DNA concentration (Figure 3-5B) when the macromer concentration in solution was tuned. Here, cells

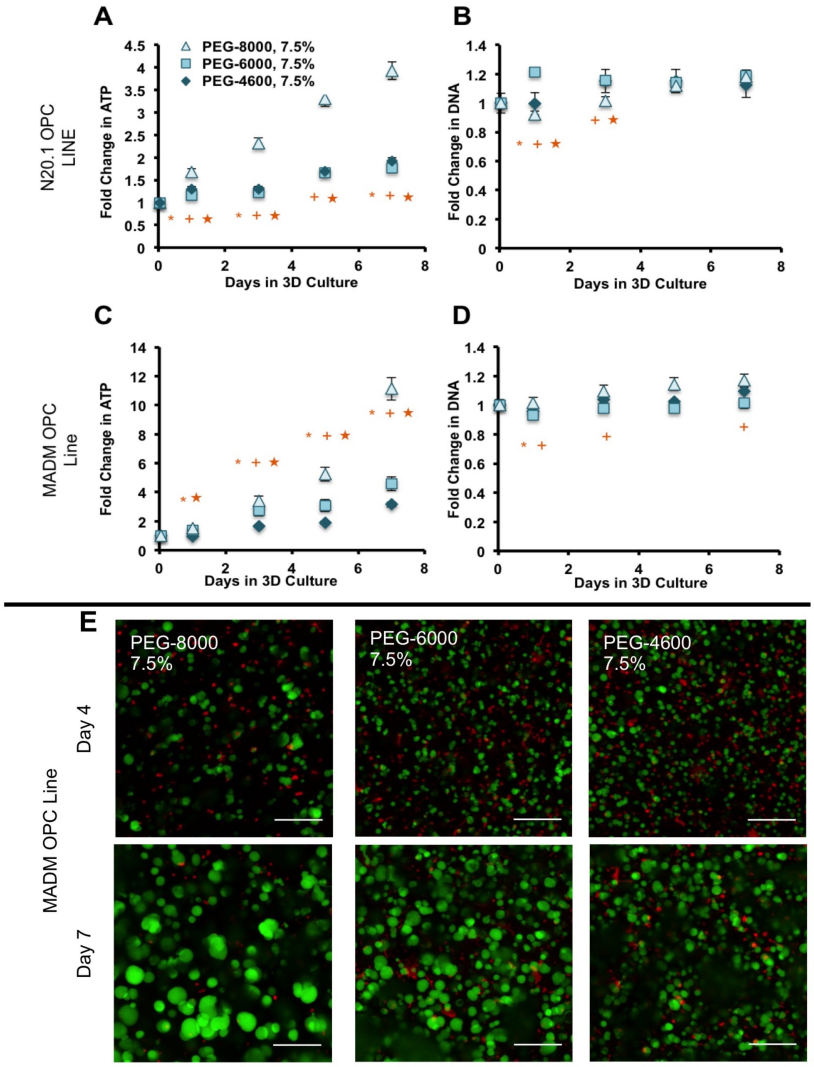

*Figure 3-3 N20.1 OPC line and MADM OPC line encapsulated in 7.5% (wt/v) gels of varying molecular weights. N20.1 cells showed an increase in ATP (A) over time and an increase in DNA (B) dependent on macromer molecular weight. MADM cells showed similar ATP (C) and DNA (D) trends. * indicates that data for the 4600 MW PEG gel is statistically different ($\alpha < .05$) from the 6000 MW PEG gel, + for 6000 MW PEG gel vs. 8000 MW PEG, and ★ for 4600 MW PEG gel vs. 8000 MW PEG gel. At 7 days, all conditions were statistically greater than the initial, 1hr time point. MADM OPCs remained viable after encapsulation and proliferated over 7 days in 7.5 wt% gels of varying molecular weight as demonstrated by live/dead (green/red) staining and confocal microscopy (E). Over the course of 7 days, large clusters formed as individual cells proliferated to form spheroids, with the largest clusters in the hydrogels of highest macromer molecular weight.*

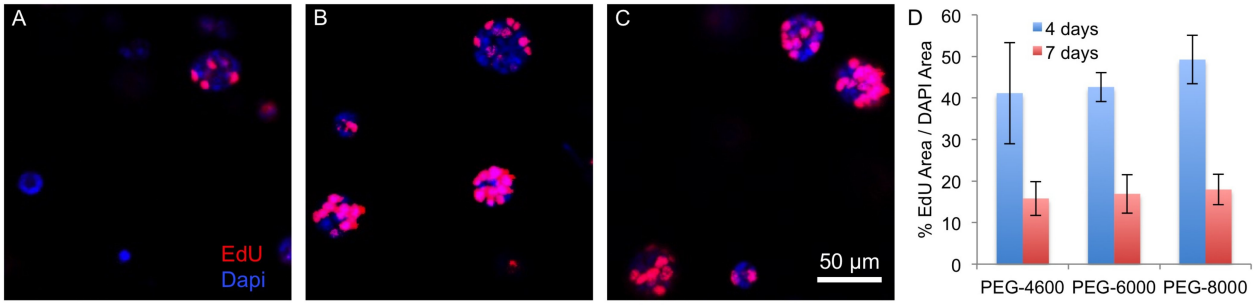

Figure 3-4 Cells proliferate in 7.5% (wt/v) hydrogels. After 4 days cell nuclei were stained with DAPI (blue) and EdU (red) in 7.5% hydrogels made with PEG-4600 (A), PEG 6000 (B), PEG-8000 (C) macromers. Higher ratios of EdU+ nuclei to DAPI nuclei are observed in PEG-8000, 7.5% hydrogels at 4 days and 7 days compared to the PEG-4600 and PEG-6000 hydrogels.

were encapsulated in gels from 6 to 10 % (w/v) with a fixed macromer molecular weight of 8000 g/mol. MADM OPCs in 10 % gels remained viable after encapsulation, however appeared to proliferate less than those in more compliant conditions (Figure 3-5E). N20.1 cells showed similar mesh size and stiffness dependent trends (Figure 3-5C, D). Again, most compliant hydrogels with the greatest swelling led to larger increases in ATP than stiffer hydrogels with less swelling. These results, along with those obtained from changing the macromer molecular weight, were consistent with prior biomaterials work, which found that NSCs proliferated less or had a higher death rate on less compliant materials[13b, 17]. While paracrine signaling could play a role in differences in ATP and DNA across gel types, the mesh size (66.1-125.3 Å) in all conditions were greater than necessary for intercellular chemical signal diffusion. For example, most model proteins, with determined structures, have hydrodynamic radii on the order of 1 to 6 nm[32].

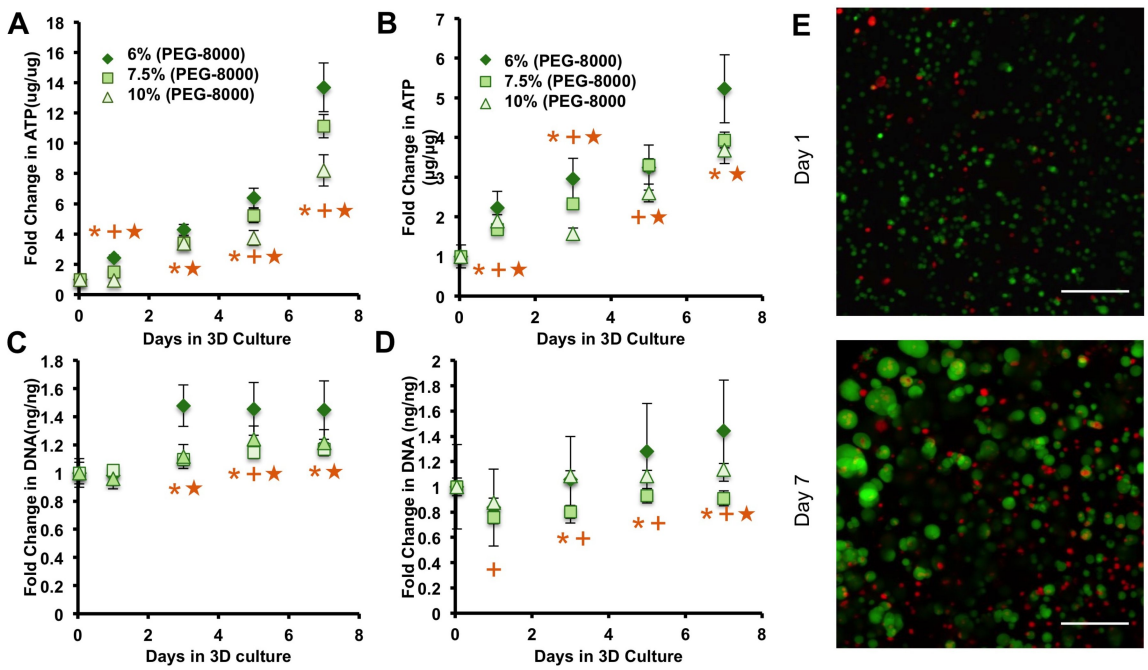

*Figure 3-5 OPCs in PEG-DM of varying concentrations at a fixed macromer molecular weight of 8000 g/mol. ATP increases in a macromer concentration dependent trend for MADM cells (A) and N20.1 cells (B). DNA shows the greatest increase in the hydrogels of lower macromer concentration for MADM cells (C) and N20.1 cells (D). * indicates that data at 6% (wt/v) is statistically different (α <0.05) from 7.5%, + for 7.5% vs. 10%, and ★ for 6% vs. 10% (wt/v). MADM OPCs remain viable even in the 10% condition following encapsulation and proliferate over 7 days as demonstrated by live/dead (green/red) staining and confocal microscopy (E).*

3.4.3 Incorporating laminin has little effect on viability or morphology

Bioactive peptide sequences from native extracellular matrix proteins such as IKVAV, RGD, and YIGSR from laminin are well known to promote cellular adhesion and neurite extension in 3D biomaterials[33]. Here, laminin type 1 was incorporated at 25 μg/mL, a concentration sufficient for cellular interaction without significantly affecting stiffness. Laminin was not covalently bound in the hydrogels, however likely remained encapsulated in the material as the hydrodynamic radius, about 21 nm, is greater than the mesh size for all gel conditions[34].

Incorporating laminin does not change cell viability as determined by live/dead staining (Figure 3-6). Cells on the surface of the hydrogels extend processes both on gels with and without laminin (Figure 3-6A), however inside the gels small process extension and less rounded clusters are only found with laminin (Figure 3-S2). Differences in process extension are not observed between conditions of different stiffnesses and mesh size. This suggests that MADM OPCs are able to generate their own extracellular matrix over seven days enabling process extension on the surface of all PEG hydrogels, while in 3D, mesh size potentially restricts process extension. This is consistent with Li et al. and Lampe et al. who observed that stiffer matrices prohibited CG4 OPCs from extending processes or dorsal root ganglia from extending neurites, respectively[9d, 13a]. Cell clusters were analyzed from the live/dead images with laminin and no significant differences are found in clonal sizes (Figure 3-6B, Figure 3-S2, Video S1), suggesting that the PEG hydrogel environment itself is sufficient enough to promote viability and proliferation (Table 2, Figure 3-3 & 5B).

3.4.4 PDGFR+ cells are more abundant in less compliant hydrogels

OPCs are capable of differentiating not only into oligodendrocytes but type two astrocytes as well[1]. PDGFRα is a surface receptor that is found on OPCs committed to generating myelinating oligodendrocytes in the CNS[35]. MADM OPCs in gels of varying stiffnesses expressed differences in PDGFRα (Figure 3-7). A larger percentage of cells encapsulated in the stiffer PEG hydrogel, 1910 Pa, express PDGFRα compared to the most compliant gel, with a storage modulus of 240 Pa, where staining is nearly completely absent, and clearly not found organized on cell surfaces. These results are interesting since almost all MADM cells plated on coverslips express PDGFRα[19], suggesting that the cells are in fact responding to the material stiffness and swelling alone and changing their phenotype and expression level. These results suggest a different trend than that of NPCs which tended to

differentiate towards neurons on more compliant materials[17], but consistent with the findings where NSCs differentiated towards glial lineages on stiffer matrices[13b]. It is possible that compliant hydrogels may be promoting de-differentiation of OPCs, which thus lose their PDGFRα expression.

Figure 3-6 MADM OPC line encapsulated with laminin in 3D PEGDM gels. Cells on the surface of the laminin-doped gels extend processes (A). Live/dead (green/red) confocal imaging shows good viability at 4 days (B) and 7 days (C). Large spheroids form over time in the PEG-8000 hydrogels (B,C).

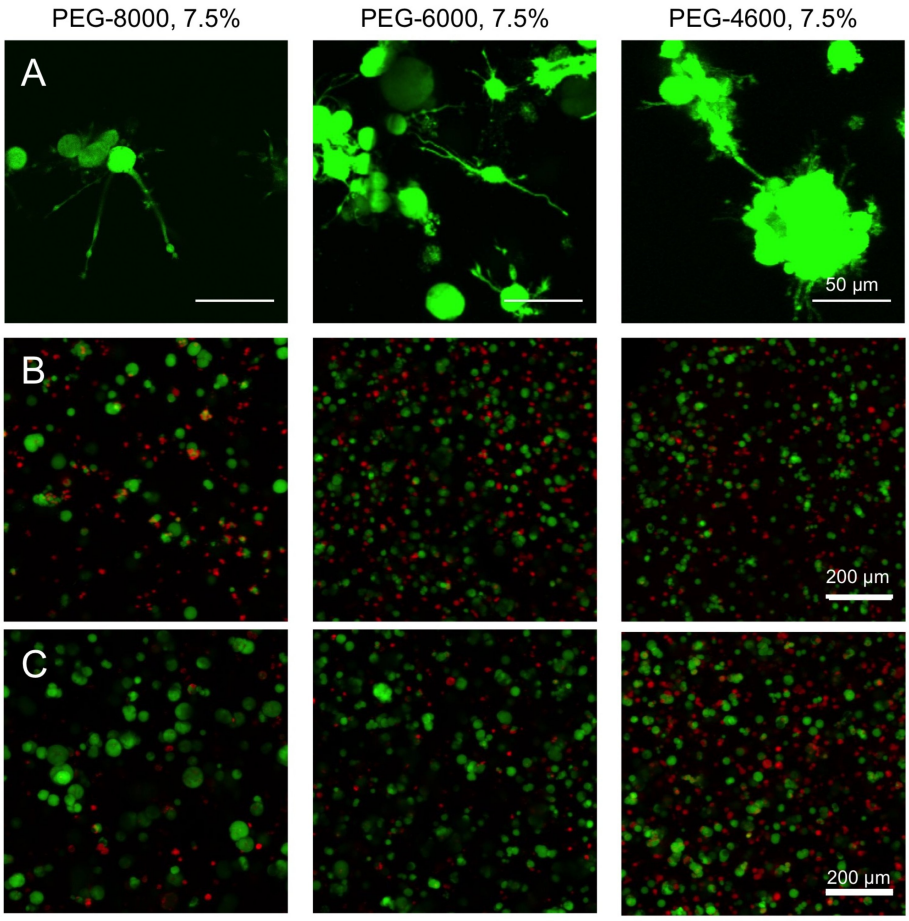

Myelinating oligodendrocytes develop later in neurogenesis[1], after many cells have generated extracellular matrix proteins or built and maintained morphological structures, which stiffen native tissue. Previous biomaterials papers in the neural field have also found that stiffer

matrices lead to more oligodendrocytes or glial cells[13b], though incorporation of PDGF or sonic hedgehog as soluble or immobilized factors alone have a large influence on oligodendrocyte lineage differentiation[9b, 11a]. Cell-cell signaling may be an important variable, but our hydrogels maintained sufficient mesh size, high cell concentration, and homogeneity of PDGFR expression throughout an individual experimental condition. Similar PDGFR expression was observed in clusters throughout the depth of individual hydrogels (Figure 3-7). This observation would indicate that accessibility of growth factors diffusing through the hydrogels is not a limited feature toward OPC proliferation.

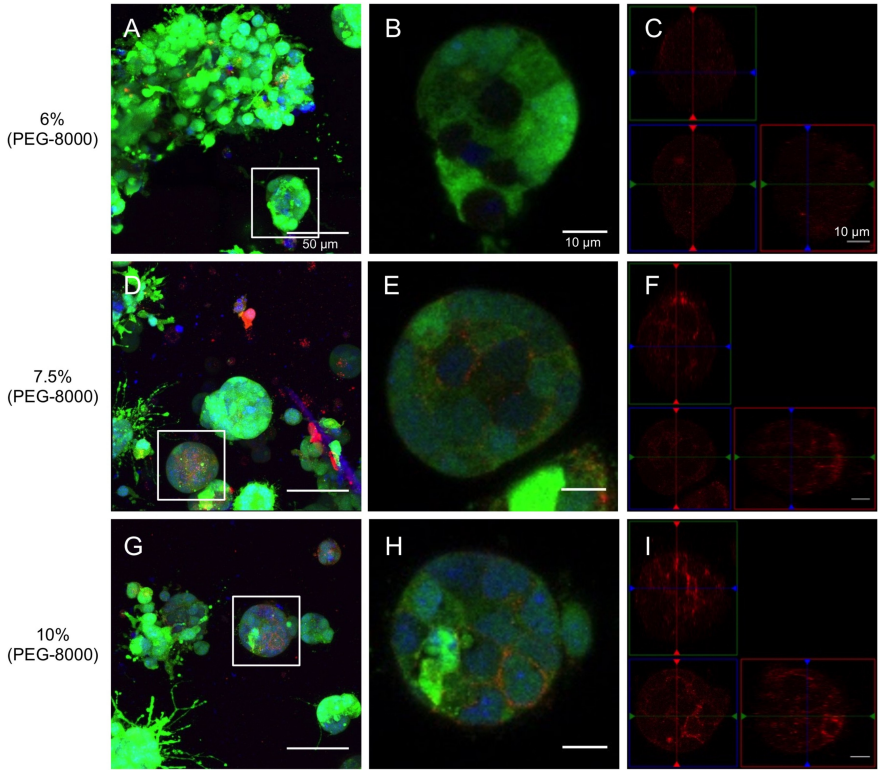

Figure 3-7 MADM OPCs formed clusters of cells positive for PDGFR α on cell surfaces. MADM cells were encapsulated in 6% (A,B,C), 7.5% (D,E,F), and 10% (wt/v) (G, H, I) 3D PEG-8000 hydrogels and cultured for 7 days. Cells were immunostained for PDGFR α (red) and DAPI nuclear stain (blue), and express cytosolic GFP (green). A,D,G are 100 μm thick max projections to show a large portion of the hydrogels, including the surface. B, E, H are zoomed images of individual cell clusters. PDGFR

α expression in the clusters decreased as the concentration of macromer increased (C, F, I).

3.5 Conclusions

In multiple sclerosis, oligodendrocytes are the primary cell that is damaged. Biomaterials may be a potential method of repair because they can localize OPCs to the injured area promote repair of damaged tissue. However biomaterial effects on oligodendrocytes have been rarely studied and thus are poorly understood. In this study, we specifically investigated the use of PEG-based hydrogels for influencing the growth of two OPC lines. Nonfunctionalized PEG hydrogels alone were sufficient and permitted OPCs to survive and grow in spheroid-like clusters. Simply tuning the hydrogel crosslinking through changes in polymer concentration or molecular weight resulted in gels of different material mechanics, and varying levels of proliferation and PDGFRα gene expression. The most compliant hydrogels permitted greater proliferation, while staining revealed that fewer cells were either committed to the OPC lineage or de-differentiated, shown by a decrease in PDGFRα expression. Despite the potential benefits of laminin and its integrin-binding domains, laminin incorporation had little affect on proliferation and viability. Though marginal differences in morphology were observed with laminin incorporation in our 3D PEG hydrogels or on 2D tissue culture plastic, it is likely that additional tuning of hydrogel degradation or incorporation of topographical cues will make a large impact on cell morphology, as the hydrogel mesh sizes are smaller than cell process diameters. Taken together, these results solidify the hypothesis that self-renewal and differentiation capabilities of OPCs are dependent on hydrogel mechanics, while further optimization will be critical to future success for regeneration of myelinating oligodendrocytes in damaged CNS tissue. Though oligodendrocytes and their precursors are poorly studied in 3D

hydrogel systems, gels could promote their regeneration and have dramatic implications in multiple sclerosis and demyelinating disease progression or prevention.

3.6 Acknowledgements

This work was supported by the UVA Biotechnology Training Program (5T32 GM008715) to LNR and the University of Virginia (KJL). The authors thank the Zong and Gaultier labs at UVA for the generous gift of OPC lines and antibody aliquots. The authors also thank the W.M. Keck Center for Cellular Imaging at the University of Virginia for use of confocal microscopes and expert advice.

3.7 References

1. Baumann, N.; Pham-Dinh, D., Biology of Oligodendrocyte and Myelin in the Mammalian Central Nervous System. *Physiological Reviews* **2001,** *81* (2), 871-927.
2. Levy, M.; Boulis, N.; Rao, M.; Svendsen, C. N., Regenerative cellular therapies for neurologic diseases. *Brain research* **2016,** *1638* (Pt A), 88-96.
3. Kuhlmann, T.; Miron, V.; Cui, Q.; Wegner, C.; Antel, J.; Bruck, W., Differentiation block of oligodendroglial progenitor cells as a cause for remyelination failure in chronic multiple sclerosis. *Brain* **2008,** *131* (Pt 7), 1749-58.
4. Harlow, D. E.; Honce, J. M.; Miravalle, A. A., Remyelination Therapy in Multiple Sclerosis. *Front Neurol* **2015,** *6*, 257.
5. McDonald, J. W.; Howard, M. J., Repairing the damaged spinal cord: a summary of our early success with embryonic stem cell transplantation and remyelination. *Progress in Brain Research* **2002,** *137*, 299-309.
6. Cooke, M. J.; Vulic, K.; Shoichet, M. S., Design of biomaterials to enhance stem cell survival when transplanted into the damaged central nervous system. *Soft matter* **2010,** *6* (20), 4988.
7. Willerth, S. M.; Sakiyama-Elbert, S. E., Cell therapy for spinal cord regeneration. *Advanced drug delivery reviews* **2008,** *60* (2), 263-76.
8. Murphy, W. L.; McDevitt, T. C.; Engler, A. J., Materials as stem cell regulators. *Nature materials* **2014,** *13* (6), 547-57.
9. (a) McCreedy, D. A.; Sakiyama-Elbert, S. E., Combination therapies in the CNS: engineering the environment. *Neuroscience letters* **2012,** *519* (2), 115-21; (b) Willerth, S. M.; Rader, A.; Sakiyama-Elbert, S. E., The effect of controlled growth factor delivery on embryonic stem cell differentiation inside fibrin scaffolds. *Stem Cell Res* **2008,** *1* (3), 205-18; (c) Hsieh, A.; Zahir, T.; Lapitsky, Y.; Amsden, B.; Wan, W.; Shoichet, M. S., Hydrogel/electrospun fiber composites influence neural stem/progenitor cell fate. *Soft matter* **2010,** *6* (10), 2227; (d) Lampe, K. J.; Antaris, A. L.; Heilshorn, S. C., Design of three-dimensional engineered protein hydrogels for tailored control of neurite growth. *Acta biomaterialia* **2013,** *9* (3), 5590-9; (e) Wang, H. B.;

Mullins, M. E.; Cregg, J. M.; Hurtado, A.; Oudega, M.; Trombley, M. T.; Gilbert, R. J., Creation of highly aligned electrospun poly-L-lactic acid fibers for nerve regeneration applications. *J Neural Eng* **2009,** *6* (1), 016001; (f) Ribeiro, A.; Vargo, S.; Powell, E. M.; Leach, J. B., Substrate three-dimensionality induces elemental morphological transformation of sensory neurons on a physiologic timescale. *Tissue engineering. Part A* **2012,** *18* (1-2), 93-102.
10. Russell, L. N.; Lampe, K. J., Engineering biomaterials to influence oligodendroglial growth, maturation, and myelin production. *Journal of Cells, Tissues, and Organs* **2016,** *202*, 85-101.
11. (a) Aizawaa, Y.; Leipzig, N. D.; Zahira, T.; Shoichet, M. S., The effect of immobilized platelet derived growth factor AA on neural stem/ progenitor cell differentiation on cell-adhesive hydrogels. *Biomaterials* **2008,** *29*, 4676–4683; (b) Thomas, A. M.; Seidlits, S. K.; Goodman, A. G.; Kukushliev, T. V.; Hassani, D. M.; Cummings, B. J.; Anderson, A. J.; Shea, L. D., Sonic hedgehog and neurotrophin-3 increase oligodendrocyte numbers and myelination after spinal cord injury. *Integrative biology : quantitative biosciences from nano to macro* **2014,** *6* (7), 694-705.
12. (a) Jagielska, A.; Norman, A. L.; Whyte, G.; Vliet, K. J.; Guck, J.; Franklin, R. J., Mechanical environment modulates biological properties of oligodendrocyte progenitor cells. *Stem cells and development* **2012,** *21* (16), 2905-14; (b) Hernandez, M.; Patzig, J.; Mayoral, S. R.; Costa, K. D.; Chan, J. R.; Casaccia, P., Mechanostimulation Promotes Nuclear and Epigenetic Changes in Oligodendrocytes. *The Journal of neuroscience : the official journal of the Society for Neuroscience* **2016,** *36* (3), 806-13.
13. (a) Li, X.; Liu, X.; Cui, L.; Brunson, C.; Zhao, W.; Bhat, N. R.; Zhang, N.; Wen, X., Engineering an in situ crosslinkable hydrogel for enhanced remyelination. *FASEB journal : official publication of the Federation of American Societies for Experimental Biology* **2013,** *27* (3), 1127-36; (b) Leipzig, N. D.; Shoichet, M. S., The effect of substrate stiffness on adult neural stem cell behavior. *Biomaterials* **2009,** *30* (36), 6867-78.
14. (a) Prevost, T. P.; Balakrishnan, A.; Suresh, S.; Socrate, S., Biomechanics of brain tissue. *Acta biomaterialia* **2011,** *7* (1), 83-95; (b) Aurand, E. R.; Lampe, K. J.; Bjugstad, K. B., Defining and designing polymers and hydrogels for neural tissue engineering. *Neuroscience research* **2012,** *72* (3), 199-213.
15. Sawhney, A. S.; Pathak, C. P.; Hubbell, J. A., Bioerodible Hydrogels Based on Phoopolymerized Poly(ethylene glycol)-co-poly(a-hydroxy acid) Diacrylate Macromers. *Macromolecules* **1993,** *26*, 581-587.
16. Lampe, K. J.; Bjugstad, K. B.; Mahoney, M. J., Impact of degradable macromer content in a PEG hydrogel on neural cell metabolic activity, redox state, proliferation, and differentiation. *Tissue engineering. Part A* **2010,** *16* (6), 1857-1866.
17. Lampe, K. J.; Mooney, R. G.; Bjugstad, K. B.; Mahoney, M. J., Effect of macromer weight percent on neural cell growth in 2D and 3D nondegradable PEG hydrogel culture. *Journal of biomedical materials research. Part A* **2010,** *94* (4), 1162-71.
18. Verity, A.; Bredesen, D.; Vonderscher, C.; Handley, V.; Campagnoni, A., Expression of Myelin Protein Genes and Other Myelin Components in an Oligodendrocytic Cell Line Conditionally Immortalized with a Temperature-Sensitive Retrovirus. *Journal of neurochemistry* **1993,** *60* (2), 577-587.
19. Liu, C.; Sage, J. C.; Miller, M. R.; Verhaak, R. G.; Hippenmeyer, S.; Vogel, H.; Foreman, O.; Bronson, R. T.; Nishiyama, A.; Luo, L.; Zong, H., Mosaic analysis with double markers reveals tumor cell of origin in glioma. *Cell* **2011,** *146* (2), 209-21.

20. Kaur, G.; Dufour, J. M., Cell Lines: Valuable tools or useless artifacts. *Spermatogenesis* **2012,** *2* (1), 1-5.
21. Agresti, C.; Meomartini, M. E.; Amadio, S.; Ambrosini, E.; Volonte, C.; Aloisi, F.; Visentin, S., ATP regulates oligodendrocyte progenitor migration, proliferation, and differentiation: involvement of metabotropic P2 receptors. *Brain Res Brain Res Rev* **2005,** *48* (2), 157-65.
22. Van Hove, A. H.; Wilson, B. D.; Benoit, D. S. W., Microwave-assisted Functionalization of Poly(ethylene glycol) and On-resin Peptides for Use in Chain Polymerizations and Hydrogel Formation. **2013,** (80), e50890.
23. Fairbanks, B. D.; Schwartz, M. P.; Bowman, C. N.; Anseth, K. S., Photoinitiated polymerization of PEG-diacrylate with lithium phenyl-2,4,6-trimethylbenzoylphosphinate: polymerization rate and cytocompatibility. *Biomaterials* **2009,** *30* (35), 6702-7.
24. Bryant, S. J.; Anseth, K. S., Hydrogel Properties Influence ECM Production by Chondrocytes Photoencapsulated in Poly(ethylene Glycol) Hydrogels. *Journal of Biomedical Materials Research* **2002,** *59*, 63-72.
25. Zustiak, S. P.; Durbal, R.; Leach, J. B., Influence of cell-adhesive peptide ligands on poly(ethylene glycol) hydrogel physical, mechanical and transport properties. *Acta biomaterialia* **2010,** *6* (9), 3404-14.
26. Taylor, Z.; Miller, K., Reassessment of brain elasticity for analysis of biomechanisms of hydrocephalus. *Journal of biomechanics* **2004,** *37* (8), 1263-9.
27. Moeendarbary, E.; Weber, I. P.; Sheridan, G. K.; Koser, D. E.; Soleman, S.; Haenzi, B.; Bradbury, E. J.; Fawcett, J.; Franze, K., The soft mechanical signature of glial scars in the central nervous system. *Nat Commun* **2017,** *8*, 14787.
28. Zhou, W.; Stukel, J. M.; Cebull, H. L.; Willits, R. K., Tuning the Mechanical Properties of Poly(Ethylene Glycol) Microgel-Based Scaffolds to Increase 3D Schwann Cell Proliferation. *Macromol Biosci* **2016,** *16* (4), 535-44.
29. Hughes, E. G.; Kang, S. H.; Fukaya, M.; Bergles, D. E., Oligodendrocyte progenitors balance growth with self-repulsion to achieve homeostasis in the adult brain. *Nat Neurosci* **2013,** *16* (6), 668-76.
30. Adriano, E.; Perasso, L.; Panfoli, I.; Ravera, S.; Gandolfo, C.; Mancardi, G.; Morelli, A.; Balestrino, M., A novel hypothesis about mechanisms affecting conduction velocity of central myelinated fibers. *Neurochem Res* **2011,** *36* (10), 1732-9.
31. Saha, K.; Keung, A. J.; Irwin, E. F.; Li, Y.; Little, L.; Schaffer, D. V.; Healy, K. E., Substrate modulus directs neural stem cell behavior. *Biophysical journal* **2008,** *95* (9), 4426-38.
32. Erickson, H. P., Size and shape of protein molecules at the nanometer level determined by sedimentation, gel filtration, and electron microscopy. *Biol Proced Online* **2009,** *11*, 32-51.
33. Cunha, C.; Panseri, S.; Villa, O.; Silva, D.; Gelain, F., 3D culture of adult mouse neural stem cells within functionalized self-assembling peptide scaffolds. *International journal of nanomedicine* **2011,** *6*, 943-55.
34. Onuma, K.; Kanzaki, N., Size Distribution and Intermolecular Interaction of Laminin-1 in Physiological Solutions. *J. Phys. Chem. B* **2003,** *107* (42
), 11799-11804.
35. Rivers, L. E.; Young, K. M.; Rizzi, M.; Jamen, F.; Psachoulia, K.; Wade, A.; Kessaris, N.; Richardson, W. D., PDGFRA/NG2 glia generate myelinating oligodendrocytes and piriform projection neurons in adult mice. *Nat Neurosci* **2008,** *11* (12), 1392-401.

4 Engineering the PEG Hydrogel to Release Lactic Acid Degradable Motifs

4.1 Abstract

Remodeling of the extracellular matrix (ECM) is crucial for cell migration and process extension. This is more easily accomplished in materials designed with degradable components. Recent studies have found that matrix degradability plays an important role in cell migration as well as maturation and proliferation. Neural stem cells, in particular, require a degradable matrix to maintain their stemness within the brain. The extracellular environmental cues that affect proliferation or differentiation of oligodendrocyte precursor cells (OPCs), the cells that give rise to myelinating oligodendrocytes, are less well known. This work investigates the importance of incorporating hydrolytically degradable polylactic acid (PLA) in polyethylene glycol (PEG) hydrogels on intracellular redox state and viability of encapsulated OPC-like cells. Here, the concentration of the degradable PLA portion in the PEG hydrogel was tuned to create hydrogels with different degradation rates. As they degrade, the hydrogel mesh size increases and the polymer backbone releases lactic acid, a mild antioxidant capable of scavenging reactive oxygen species (ROS). Despite the added benefit lactic acid release may provide in this hydrogel system, we found that while OPC-like cells did extend processes in degradable PEG hydrogels, the degradable conditions produced minimal differences in encapsulated OPC-like intracellular redox state, metabolic activity, and viability. In addition to studying cancer derived OPC-like cells, which preferentially undergo anaerobic respiration to produce lactic acid in cell metabolism, primary rat OPCs were also encapsulated. However, no differences in primary OPC redox state or metabolic activity were found as a function of degradable gel conditions, likely due to poor OPC viability. While results were inconclusive, more work remains to further elucidate the impact matrix degradability and lactic acid have on primary OPCs and the potential impact they may have to create a suitable *in vitro* tissue model.

4.2 Introduction

Native ECM consists of structural proteins and glycoproteins that cells interact with by binding, physically rearranging, or degrading[1]. This degradability and rearrangement of the ECM

is crucial for many cell functions, such as migration, process extension, and cell fate determination[2]. During neurogenesis, neural cells actively degrade and deposit the extracellular matrix as they extend processes and migrate to their ultimate spatial domain[3]. Recent studies have found that the degradable character of biomaterials is also critical for cell migration and process extension *in vitro*[4]. Degradability enables neural stem cells to maintain their stemness and ability to proliferate in 3D biomaterials *in vitro*[5]. However, the knowledge of matrix interactions of oligodendrocytes or their precursors, OPCs, is currently poorly understood[6]. OPCs are considerably more migratory than mature oligodendrocytes and other neural cell types[7]. It is well known that oligodendrocytes can extend many processes towards numerous axons and therefore also require matrix degradation and remodeling[8]. Furthermore, OPCs deposit small amounts of the extracellular matrix proteins, laminin and fibronectin, however oligodendrocytes have not been found to synthesize these proteins[9].

In order to understand cell-ECM interactions, biomaterials have been engineered with many degradable motifs[10]. Cell-responsive biomaterials have been engineered that degrade in response to cell-secreted proteases[4]. These biomaterials are typically made from engineered or native proteins. Synthetic materials have been engineered to degrade through the incorporation of enzymatically degradable peptide crosslinks as well[11]. Synthetic polymer hydrogels have been designed to degrade via natural cell interactions or through simple chemistries[12]. One such material is a degradable PEG hydrogel that incorporates polylactic acid domains[12a]. Ester groups in the PLA portion of a PEG-PLA-DM macromer enable degradation through hydrolysis. This enables simple, tunable degradation of the hydrogel over time by controlling the amount of PLA in the bulk hydrogel. As water breaks ester bonds, the PEG hydrogel mesh size opens up and the biomaterial becomes more compliant[13]. Additionally, as the PLA degrades it releases its monomer unit, lactic acid[13]. Lactic acid has been shown to act as a mild antioxidant with the potential to scavenge ROS[14]. Furthermore, lactic acid can be utilized in many aspects of cellular processes. Cells are capable of glycolysis via anaerobic or aerobic respiration, where a biproduct of anaerobic respiration is lactic acid. Oligodendrocytes and OPCs in particular are known to utilize lactic acid as a precursor to lipid formation in the creation of the myelin sheath[15]. They also readily supply neurons with lactic acid for ATP synthesis[16]. In addition, lactic acid is a prevalent redox pair within cells utilized in maintaining the intracellular redox state[17].

The intracellular redox state gives a measure of the oxidation or reduction potential of a cell[18]. This intracellular redox state provides insight on the cell's proliferation or differentiation potential. In particular, OPCs with a more reduced intracellular redox state remain more proliferative while a more reduced intracellular redox state generally indicates the cell is less proliferative and, instead maturing[19]. Both OPCs and oligodendrocytes are highly susceptible to oxidative stress. OPCs exposed to high levels of oxidative stress, often found in injury or disease microenvironments, are less likely to fully mature[20] while oxidized oligodendrocytes have less myelination potential and poor viability[21]. Together these added benefits of a PEG-PLA-DM hydrogel may be ideal for the generation of an *in vitro* myelination model. Here, the effects of lactic acid and the degradable PEG-PLA-DM hydrogel were investigated for potential impacts of the intracellular redox state of an OPC-like cell line and primary OPCs.

4.3 Materials and Methods

4.3.1 Macromer synthesis and gel formulations

The PEG-DM, non-degradable macromer, was synthesized as outlined in chapter 3. Nondegradable gels for soluble lactic acid studies were made from PEG-DM with 8000 g/mol PEG at 6, 7.5, and 10% (wt/v) in solution [22]. Degradable hydrogel studies were all 7.5% (wt/v) macromer with the indicated percentages (0-50%) of degradable PEG-PLA-DM macromer and remaining nondegradable PEG-DM macromer. PEG-PLA-DM macromer was synthesized first through creating PLA-PEG-PLA through a ring opening polymer melt reaction[13]. PEG (8000 g/mol) was mixed with d-l-lactide at 140 ºC under vacuum for 5 hours. D-l-lactide was added stoichiometrically with a 60% reaction efficiency to create the desired 2.5 lactic acid units per side. PLA-PEG-PLA was purified by dissolving in dichloromethane followed by dropwise precipitation in diethyl ether. This purification was preformed three times and the product dried under vacuum before functionalizing the macromer with methacrylate end groups. PEG-PLA-DM was synthesized by adding 10 molar excess methacrylate anhydride to PLA-PEG-PLA. The mixture was then microwaved for 5 minutes in a Rival 900 watt microwave at full power, and vortexed every 30 seconds [23]. Then, PEG-PLA-DM was purified using the same dropwise precipitation as before then stored under vacuum.

Hydrogels were made by mixing the desired ratios of PEG-DM and PEG-PLA-DM in media with cells and the photoinitiator, lithium phenyl-2,4,6, trimethylbenzoylphosphinate

(LAP). LAP was added at a 0.05:1 mole ratio with the PEG macromer and enabled the PEG macromer to crosslink via a 10 minute exposure to ultraviolet light (~4mW/cm^2, 365 nm). Cells were encapsulated at 1x10^7 cell/mL for the soluble lactic acid studies and 2x10^6 cells/mL for the subsequent hydrogen peroxide and released lactic acid studies.

4.3.2 Cell culture

Two cell types were utilized in these experiments, the GFP$^+$ MADM OPC-like cells and primary rat OPCs. GFP$^+$ MADM OPC-like cells were cultured according to the protocols outlined in chapter 3. Primary rat OPCs were isolated immediately prior to use from 6-8 day old rat pups[24]. The isolation protocol is explained in more detail in chapter 5. Briefly, a single cell suspension was obtained from rat cortices that had been treated with Accutase. The single cell suspension was then purified through immunopanning with lectin and O4 coated plates to deselect and select OPCs, respectively. OPCs collected from the O4 coated plates were resuspended in the same OPC media as before and encapsulated in the PEG hydrogels. Cell containing hydrogels were cultured in 500 μL of media in individual wells of 24 well plates. Media was changed every other day for the first 4 days and then each day after for the GFP$^+$ MADM OPC-like cells. Primary OPC gel media was changed every other day for the duration of the experiment.

4.3.3 Exposing cells to hydrogen peroxide as a model of oxidative stress

GFP$^+$ MADM cells were oxidatively challenged with hydrogen peroxide. These studies were performed on cells cultured in 2D 24 well plates or cells encapsulated in 3D nondegradable PEG-DM hydrogels. 1mM H_2O_2 was added to the cell media of half the gels in a given experiment. Cells were maintained in 1mM hydrogen peroxide for the duration of the experiment [25]. At discrete time points, 3 samples of each condition, cultured with and without hydrogen peroxide, were collected in 500 μL of passive lysis buffer (Promega). Gel samples were mechanically homogenized and the glutathione concentrations of 2D and 3D samples were measured with the GSH-Glo assay (Promega)[13]. Briefly, 2D and 3D cell lysates and glutathione standards were pipetted in triplicate into 384 well plates. One plate was loaded with samples useing the normal assay buffers while a duplicate second plate used samples with an assay buffer containing 1mM tris(2-carboxyethyl)phosphine (TCEP) (Thermo Scientific) [13]. TCEP is a

reducing agent, that serves to reduce the oxidized disulfide form of glutathione (GSSG) into the reduced form, GSH[13]. This assay measured the total amount of glutathione as well as the reduced GSH to determine the intracellular redox state. Samples and standards were measured using a ClarioStar plate reader.

In addition to measuring the intracellular redox state via glutathione concentrations, 2D cells or 3D gel encapsulated cells cultured with and without 1mM hydrogen peroxide were stained with Mitotracker Orange CM-H_2TMRos dye (Life Technologies) and imaged. Briefly, 500 μL of 1mM Mitracker Orange dye in media was added to each sample well and cultured for 45 minutes. After 45 minutes, the media was removed and cells were fixed with 4% paraformaldehyde (PFA) at room temperature for 5 minutes. Cells or gels were rinsed 3 times with PBS and transferred on coverslips for imaging. The green (GFP) channel and red (mitotracker orange) channels of gel conditions were then imaged on the Zeiss 510 microscope in the Keck Center for Cellular Imaging. Widefield images were collected from the labs Zeiss AxioObserver Z1 microscope. The red and green channels were changed to binary and the pixel area of red area over green area was calculated using ImageJ image analysis. Each experiment was repeated 3 times, with 3 samples collected per condition.

4.3.4 Soluble lactic acid studies

Soluble lactic acid studies were performed on nondegradable gels of varying stiffness as described in Chapter 3. Gels were cultured in individual wells of a 24 well plate where half the gels of each condition were cultured in media with 5 mM lactic acid (Millipore Sigma)[14, 17]. Samples were taken at discrete time points and homogenized in passive lysis buffer. Gel lysates were analyzed with the glutathione assay as described before. Additionally, some gels of each condition were analyzed with the alamarBlue assay (Thermo Fisher). Gels were cultured in media or media with lactic acid until incubating with alamarBlue. AlamarBlue was added to media and cultured for 4 hours with the gels. At the end of the time, 100 μL of cell media was transferred in triplicate to individual wells of a 96 well plate. Fluorescence and absorbance values were collected according to the manufacturers protocol. Experiments were repeated 3 times with 3 samples per condition.

4.3.5 Degradable hydrogel studies

Degradable PEG-PLA-DM hydrogels release the lactic acid monomer as the macromer degrades hydrolytically. To tune the amount of lactic acid that has been released, the ratio of degradable macromer was changed relative to nondegradable PEG-DM macromer. In these studies, GFP^+ MADM cells or primary rat OPCs were utilized. Cells were cultured in degradable hydrogels and measured via AlamarBlue and, glutathione concentrations as described previously. Experiments were repeated 3 times with 3 samples per condition.

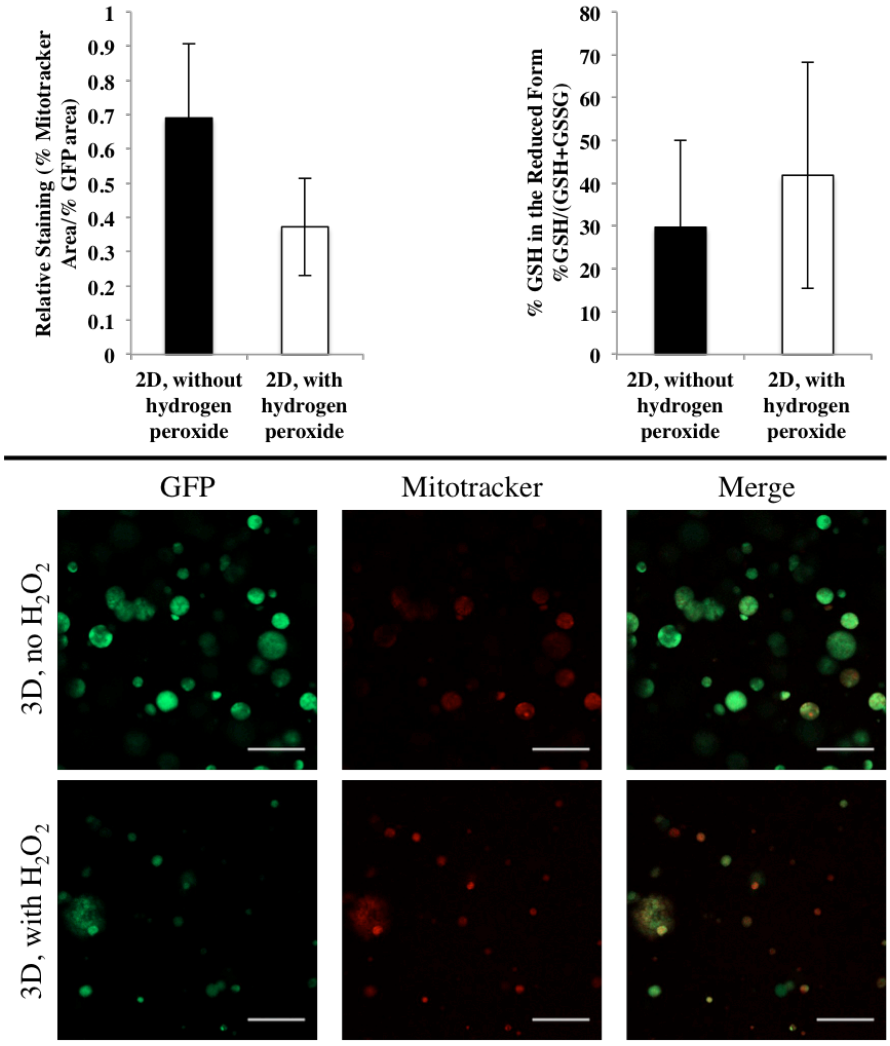

Figure 4-1 OPC like cells exposed to 1mM H_2O_2 respond differently in 2D and 3D. In 2D intracellular redox state is reduced measured through Mitotracker staining (top left) and GSH assay (top right), while in 3D the intracellular redox state is oxidized with H_2O_2 (bottom).

4.4 Results and Discussion

4.4.1 Hydrogen Peroxide reduces intracellular redox state in 2D and 3D

Hydrogen peroxide was used to simulate a mild oxidative injury environment that could then be rescued by either released or soluble lactic acid[14, 25]. 1mM hydrogen peroxide was added to GFP^+ MADM OPC-like cells in both 2D and in a 3D nondegradable PEG-DM hydrogel. Intracellular redox state of cells with and without H_2O_2 were measured through the Mitotracker Orange stain and glutathione assay in 2D (Figure 4-1). As H_2O_2 causes oxidative stress it is expected that exposure to hydrogen peroxide would create a more oxidized redox state. However, when quantifying the percentage of glutathione in the reduced form of 2D cultured cells, the intracellular redox state became more reduced upon exposure to hydrogen peroxide (Figure 4-1). This decreased ratio of reduced to total glutathione when hydrogen peroxide was added indicates a more reduced intracellular redox state rather than oxidized. 2D cultures without hydrogen peroxide compared to 2D cultures with hydrogen peroxide confirms this reduction as cultures with hydrogen peroxide had a lower staining for Mitotracker Orange, a molecule that fluoresces when oxidized. These results are unexpected, as hydrogen peroxide is well known to act as an oxidizer and regulate protein function through the oxidation of cysteine thiols[26].

However, this shift in the intracellular redox state measured through glutathione can potentially be explained from the cell origin. The GFP^+MADM cells are glioma-derived cells with a high proliferation rate[27]. Cancer cells generate a significant amount of reactive oxygen species while maintaining their high proliferation rate[28], and cancer cells with a high concentration of glutathione are more prone to survival against these oxidative stresses[10]. Furthermore, cancer cells undergo unique cellular pathways that help prevent the accumulation of reactive oxygen species, such as a higher propensity of anaerobic respiration that generates lactic acid, rather than aerobic respiration[29]. Together, these ideas suggest that high amounts of ROS are possible while the cell maintains a more reduced intracellular redox state. Therefore, cells exposed to hydrogen peroxide may be capable of compensating for the oxidative stress by generating more glutathione and utilizing more lactate[29], causing a shift in the intracellular redox state.

When cells in the 3D nondegradable PEG-DM hydrogel were cultured in a condition with and without hydrogen peroxide the opposite trends were observed through the mitotracker staining (Figure 4-1). These trends aligned with the hypothesis that hydrogen peroxide would cause an oxidative intracellular redox state. Cells in the gels with hydrogen peroxide experienced

a more oxidized intracellular redox state compared to the cells without hydrogen peroxide measured by an increased fluorescence in mitotracker compared to the gels without hydrogen peroxide (Figure 4-1). Additionally, while no morphological changes were shown in 2D cultures with and without hydrogen peroxide, cells exposed to hydrogen peroxide in the 3D PEG-DM hydrogel appear to have proliferated less as smaller cluster sizes were observed.

These results are confounding and further experiments are required to explain the differences between 2D and 3D trends. Hydrogen peroxide has been shown to act as an oxidizer in both 2D and 3D[25]. Cells in 2D and 3D gels are both cultured in 500 μL of media with 1 mM hydrogen peroxide, however the dosage of hydrogen peroxide per cell is significantly less in 3D as more cells are cultured in the 3D hydrogel. Additionally, mass transfer into and out of the hydrogel would be slightly different than in 2D[30]. In 2D, all cells are in direct contact with hydrogen peroxide media directly upon seeding the well plates. However, gels in 3D are made in regular media and then cultured in hydrogen peroxide loaded media. While diffusion of hydrogen peroxide would be very quick in the hydrogels, it is likely that the cells closer to the surface of the hydrogel would be subjected to more oxidative stress each time media is refreshed. This would be observed through a location dependent staining for mitotracker, however in 500 μM z-stack images, no location depending staining was observed. Together, these results suggest that the glioma derived OPC-like cells respond differently to reactive oxygen species in 2D and 3D.

4.4.2 OPC-like cellular redox state is not affected by soluble lactic acid

Figure 4-2 Glutathione in the reduce form is not significantly different for OPC-like cells in hydrogels of different stiffnesses. 6% corresponds to a storage moduli of 240 Pa, 7.5% to 560 Pa, and 10% to 1910 Pa.

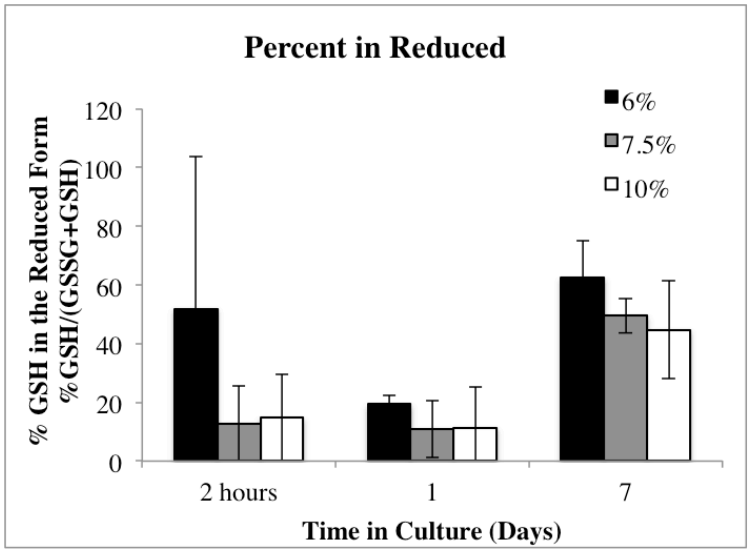

Lactic acid is known to act as a mild antioxidant that can help protect cells from reactive oxygen species[17]. OPC intracellular redox state has been shown to greatly impact cell proliferation. Cells with a more reduced state are more proliferative where cells with a more oxidized state are more mature[31]. However, that redox state is tightly regulated as both oligodendrocytes and OPCs are highly susceptible to oxidative stress[21a]. When OPCs are subjected to oxidative stress they often are unable to mature[20], while oligodendrocytes often have a reduction in myelination capabilities upon exposure to oxidative stress[21b].. Additionally in OPCs and oligodendrocytes, lactic acid is used in the myelin synthesis processes[15]. Here, we wanted to investigate soluble lactic acid on intracellular redox state in hydrogels of varying stiffness to determine if lactic acid would protect cells from reactive oxygen species and or perhaps guide maturation processes. First, we sought to determine the effect of hydrogel mechanics on intracellular redox state alone. The glutathione assay shows that over 7 days of 3D cell culture, intracellular redox state of the GFP^+ MADM cells is not statistically different across conditions (Figure 4-2). These gel conditions (6, 7.5 and 10%, 8000 g/mol PEG-DM) are discussed in Chapter 3 and have storage moduli of 240 Pa, 560 Pa, and 1910 Pa, respectively. Previously the hydrogels lead to different amounts of proliferation, however these rates of proliferation were not measured with different intracellular redox states.

Furthermore, when lactic acid was added at 5 mM in media to cells in the 7.5% and 10% gels, the intracellular redox state was again not statistically different from the other conditions (Figure 4-3). 5mM lactic acid was used in these studies as they were within the range studied by other literature. These results are not surprising as it was discussed previously that cancer cells preferentially undergo anaerobic respiration resulting in high quantities of intracellular lactic acid[29]. Therefore, concentrations of lactic acid doped into the media may not be able to alter intracellular redox state. Additionally, 5 mM lactic acid in media may not be high enough considering the amounts of intracellular lactic acid, measured between 10 and 40 mM in tumors[32]. Lactic acid was added into media with B27 and N2 media supplements. B27 has tocopherols, another class of antioxidants. In addition to lactic acid intracellularly, this supplement of tocopherol may already reduce intracellular redox state. However, when these studies were performed without B27 in the media, again minimal differences were found (data not shown).

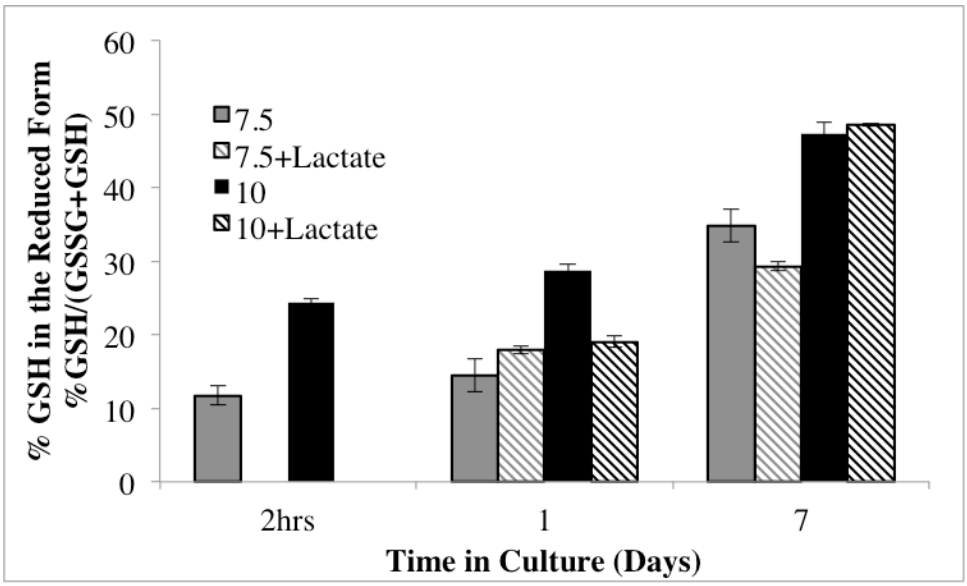

Figure 4-3 Lactic acid added into media alongside of cells in 7.5 and 10% 8000 g/mol PEG-DM hydrogels has little effect on the percentage of glutathione in the reduced form.

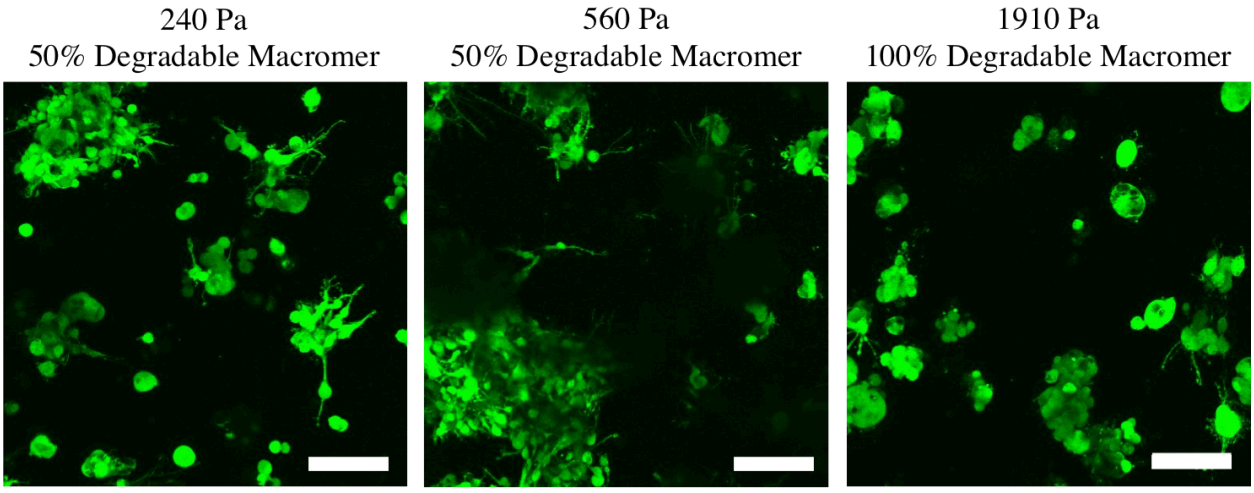

Figure 4-4 OPC-like cells encapsulated in degradable hydrogels extend processes. Longer processes are observed on gels with the lowest initial stiffness, largest mesh size, and degradable macromer concentration. Images shown were collected after 7 days of culture. Scale bar represents 100 μm.

4.4.3 Lactic acid released from degradable hydrogels minimally impacts OPC intracellular redox state

While lactic acid as a soluble factor did not show significant differences in the percentage of glutathione in the reduced form, we further investigated the effect of lactic acid released from the PEG hydrogel. PEG-PLA-DM hydrogels can slowly release lactic acid through hydrolysis. Again we tested the effects of lactic acid release on OPCs. OPC-like cells were able to extend processes in the hydrogel relative to the starting hydrogel mesh size and the degradability content (Figure 4-4). As the hydrogels degrade, crosslinks are broken opening up the hydrogel mesh size[4, 12b]. Therefore, the hydrogels with a lower starting stiffness and larger mesh sizes had significantly more process extension than hydrogels with the same degradability content and initially higher stiffness or lower mesh size. This process extension is more like native OPCs than the circular clusters that are observed in nondegradable hydrogels.

Next, we investigated the release of lactic acid on cell metabolism of OPC-like cells and primary rat OPCs. GFP^+ MADM cells cultured in the hydrogel were not affected by the release of lactic acid. This has been explained previously, but cancer cells readily undergo anaerobic respiration, which results in a high concentration of lactic acid in the cell[29]. Likely this low release of lactic acid is not enough to impact the intracellular redox state. Additionally, primary OPCs were encapsulated and measured with alamarBlue to determine if difference exhist in the metabolic rate. However, these primary OPCs all had a low viability and were encapsulated at a low concentration so minimal differences were found. Despite the lack of significant differences, a trend is seen with the primary OPCs at later time points. That is, when hydrogen peroxide was dosed in to the media, a higher degradable macromer content resulted in a higher reduction of alamarBlue. This increased reduction of alamarBlue suggests that cells are more metabolically active in the degradable hydrogels, as a direct result of the release of lactic acid.

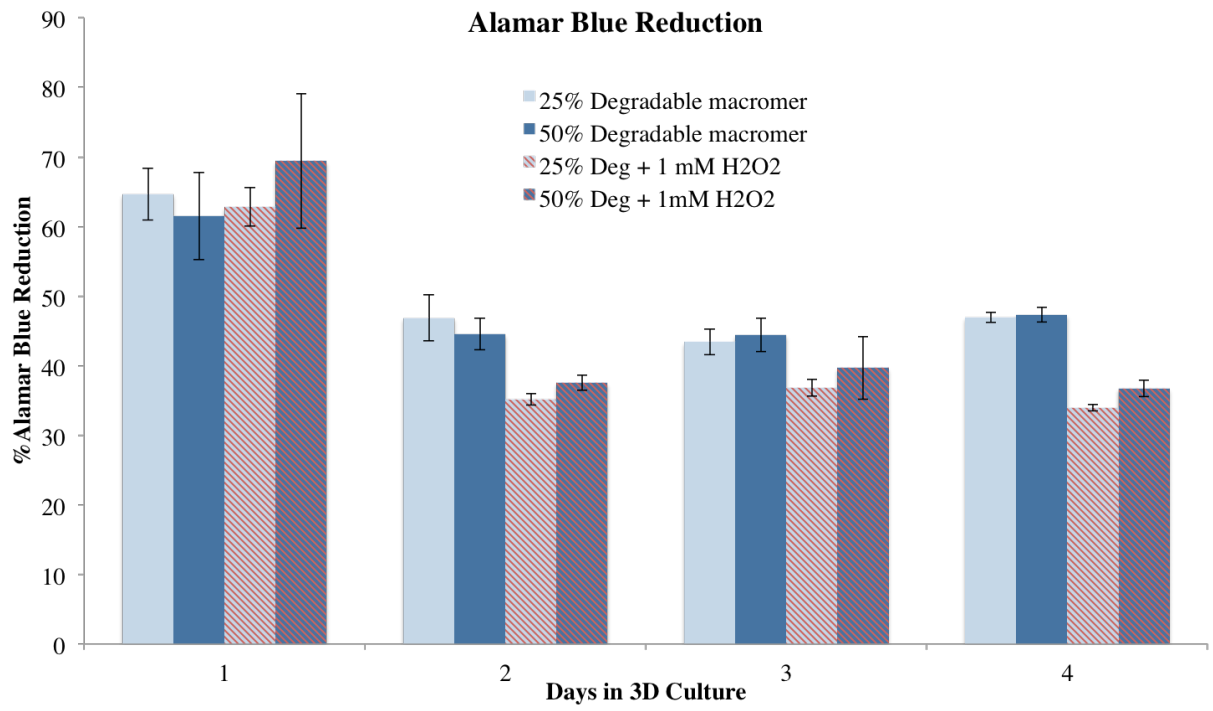

Figure 4-5 Reduction of alamarBlue is not significantly different across degradable types in the control or hydrogen peroxide injury. 50% degradable macromer might have a slight protective effect against oxidative stress compared to the 25% degradable macromer.

4.5 Conclusions

These results highlight the significant differences between OPCs and cancer cells of OPC origin. While soluble lactic acid or lactic acid released from the hydrogel backbone was not found to cause a significant difference in redox state or metabolism of OPC-like cells, this is likely due to the high concentration of lactic acid in cancer cells[32]. Limited numbers of primary OPCs and low yields were investigated, though in one study found that the increase in degradability content resulted in a slight increase in the reduction of alamarBlue in primary OPCs. These results were found in both gels cultured without hydrogen peroxide and gels with hydrogen peroxide. Further studies remain to further elucidate these results and further determine if the release of lactic acid can play a role on the differentiation and maturation of OPCs into oligodendrocytes.

4.6 References

1. Murphy, W. L.; McDevitt, T. C.; Engler, A. J., Materials as stem cell regulators. *Nature materials* **2014,** *13* (6), 547-57.
2. Lu, P.; Takai, K.; Weaver, V. M.; Werb, Z., Extracellular matrix degradation and remodeling in development and disease. *Cold Spring Harb Perspect Biol* **2011,** *3* (12).
3. (a) Franco, S. J.; Muller, U., Extracellular matrix functions during neuronal migration and lamination in the mammalian central nervous system. *Dev Neurobiol* **2011,** *71* (11), 889-900; (b) Lourenco, T.; Paes de Faria, J.; Bippes, C. A.; Maia, J.; Lopes-da-Silva, J. A.; Relvas, J. B.; Graos, M., Modulation of oligodendrocyte differentiation and maturation by combined biochemical and mechanical cues. *Scientific reports* **2016,** *6*, 21563.
4. Pittier, R.; Sauthier, F.; Hubbell, J. A.; Hall, H., Neurite extension and in vitro myelination within three-dimensional modified fibrin matrices. *Journal of neurobiology* **2005,** *63* (1), 1-14.
5. Madl, C. M.; LeSavage, B. L.; Dewi, R. E.; Dinh, C. B.; Stowers, R. S.; Khariton, M.; Lampe, K. J.; Nguyen, D.; Chaudhuri, O.; Enejder, A.; Heilshorn, S. C., Maintenance of neural progenitor cell stemness in 3D hydrogels requires matrix remodelling. *Nature materials* **2017,** *16* (12), 1233-1242.
6. Russell, L. N.; Lampe, K. J., Engineering biomaterials to influence oligodendroglial growth, maturation, and myelin production. *Journal of Cells, Tissues, and Organs* **2016,** *202*, 85-101.
7. Kessaris, N.; Fogarty, M.; Iannarelli, P.; Grist, M.; Wegner, M.; Richardson, W. D., Competing waves of oligodendrocytes in the forebrain and postnatal elimination of an embryonic lineage. *Nat Neurosci* **2006,** *9* (2), 173-9.
8. Colognato, H.; Tzvetanova, I. D., Glia unglued: how signals from the extracellular matrix regulate the development of myelinating glia. *Dev Neurobiol* **2011,** *71* (11), 924-55.
9. Yang, Z.; Suzuki, R.; Daniels, S. B.; Brunquell, C. B.; Sala, C. J.; Nishiyama, A., NG2 glial cells provide a favorable substrate for growing axons. *The Journal of neuroscience : the official journal of the Society for Neuroscience* **2006,** *26* (14), 3829-39.
10. Piskin, E., Biodegradable polymers as biomaterials. *Journal of Biomaterials Science, Polymer Edition* **1995,** *6* (9), 775-795.
11. DeForest, C. A.; Polizzotti, B. D.; Anseth, K. S., Sequential click reactions for synthesizing and patterning three-dimensional cell microenvironments. *Nature materials* **2009,** *8* (8), 659-64.
12. (a) Sawhney, A. S.; Pathak, C. P.; Hubbell, J. A., Bioerodible Hydrogels Based on Phoopolymerized Poly(ethylene glycol)-co-poly(a-hydroxy acid) Diacrylate Macromers. *Macromolecules* **1993,** *26*, 581-587; (b) Zustiak, S. P.; Pubill, S.; Ribeiro, A.; Leach, J. B., Hydrolytically degradable poly(ethylene glycol) hydrogel scaffolds as a cell delivery vehicle: Characterization of PC12 cell response. *Biotechnology Progress* **2013,** *29* (5), 1255-1264.
13. Lampe, K. J.; Bjugstad, K. B.; Mahoney, M. J., Impact of degradable macromer content in a PEG hydrogel on neural cell metabolic activity, redox state, proliferation, and differentiation. *Tissue engineering. Part A* **2010,** *16* (6), 1857-1866.
14. Lampe, K.; Namba, R.; Silverman, T.; Bjugstad, K.; Mahoney, M., Impact of Lactic Acid on Cell Proliferation and Free Radical-Induced Cell Death in Monolayer Cultures of Neural Precursor Cells. *Biotechnology and bioengineering* **2009,** *103* (6), 1214-1223.
15. Rinholm, J. E.; Hamilton, N. B.; Kessaris, N.; Richardson, W. D.; Bergersen, L. H.; Attwell, D., Regulation of oligodendrocyte development and myelination by glucose and lactate.

The Journal of neuroscience : the official journal of the Society for Neuroscience **2011,** *31* (2), 538-48.
16. Marinelli, C.; Bertalot, T.; Zusso, M.; Skaper, S. D.; Giusti, P., Systematic Review of Pharmacological Properties of the Oligodendrocyte Lineage. *Front Cell Neurosci* **2016,** *10*, 27.
17. Groussard, C.; Morel, I.; Chevanne, M.; Monnier, M.; Cillard, J.; Delamarche, A., Free radical scavenging and antioxidant effects of lactate ion: an in vitro study. *Journal of Applied Physiology* **2000,** *89* (1), 169-175.
18. Martinovich, G. G.; Cherenkevich, S. N.; Sauer, H., Intracellular redox state: towards quantitative description. *Eur Biophys J* **2005,** *34* (7), 937-42.
19. Smith, J.; Ladi, E.; Mayer-Proschel, M.; Noble, M., Redox state is a central modulator of the balance between self-renewal and differentiation in a dividing glial precursor cell. *Proceedings of the National Academy of Sciences of the United States of America* **2000,** *97* (18), 10032-7.
20. French, H. M.; Reid, M.; Mamontov, P.; Simmons, R. A.; Grinspan, J. B., Oxidative stress disrupts oligodendrocyte maturation. *Journal of neuroscience research* **2009,** *87* (14), 3076-87.
21. (a) Giacci, M. K.; Bartlett, C. A.; Smith, N. M.; Iyer, K. S.; Toomey, L. M.; Jiang, H.; Guagliardo, P.; Kilburn, M. R.; Fitzgerald, M., Oligodendroglia Are Particularly Vulnerable to Oxidative Damage after Neurotrauma In Vivo. *The Journal of neuroscience : the official journal of the Society for Neuroscience* **2018,** *38* (29), 6491-6504; (b) Jana, A.; Pahan, K., Oxidative stress kills human primary oligodendrocytes via neutral sphingoyelinase: implications for multiple sclerosis. *J Neuroimmune Pharmacol* **2007,** *2* (2), 184-193.
22. Russell, L. N.; Lampe, K. J., Oligodendrocyte Precursor Cell Viability, Proliferation, and Morphology is Dependent on Mesh Size and Storage Modulus in 3D Poly(ethylene glycol)-Based Hydrogels. *ACS Biomaterials Science & Engineering* **2017**.
23. Van Hove, A. H.; Wilson, B. D.; Benoit, D. S. W., Microwave-assisted Functionalization of Poly(ethylene glycol) and On-resin Peptides for Use in Chain Polymerizations and Hydrogel Formation. **2013,** (80), e50890.
24. Dugas, J. C.; Emery, B., Purification of oligodendrocyte precursor cells from rat cortices by immunopanning. *Cold Spring Harb Protoc* **2013,** *2013* (8), 745-58.
25. Halliwell, B.; Clement, M. V.; Ramalingam, J.; Long, L. H., Hydrogen Peroxide. Ubiquitous in Cell Culture and In vivo? *IUBMB Life* **2000,** *50* (4 - 5), 251-257.
26. Poole, L. B., The basics of thiols and cysteines in redox biology and chemistry. *Free Radic Biol Med* **2015,** *80*, 148-57.
27. Liu, C.; Sage, J. C.; Miller, M. R.; Verhaak, R. G.; Hippenmeyer, S.; Vogel, H.; Foreman, O.; Bronson, R. T.; Nishiyama, A.; Luo, L.; Zong, H., Mosaic analysis with double markers reveals tumor cell of origin in glioma. *Cell* **2011,** *146* (2), 209-21.
28. Liou, G. Y.; Storz, P., Reactive oxygen species in cancer. *Free Radic Res* **2010,** *44* (5), 479-96.
29. Strickland, M.; Stoll, E. A., Metabolic Reprogramming in Glioma. *Front Cell Dev Biol* **2017,** *5*, 43.
30. Amsden, B., Solute Diffusion within Hydrogels. Mechanisms and Models. *Macromolecules* **1998,** *31*, 8382-8395.
31. Noble, M.; Smith, J.; Power, J.; Mayer-Proschel, M., Redox State as a Central Modulator of Precursor Cell Function. *Ann. N.Y. Acad. Sci.* **2003,** *991*, 251-271.

32. Romero-Garcia, S.; Moreno-Altamirano, M. M.; Prado-Garcia, H.; Sanchez-Garcia, F. J., Lactate Contribution to the Tumor Microenvironment: Mechanisms, Effects on Immune Cells and Therapeutic Relevance. *Front Immunol* **2016,** *7*, 52.

5 Incorporating Axon Mimic Topography into the Amorphous PEG hydrogel

5.1 Abstract

In the central nervous system (CNS), oligodendrocyte precursor cells (OPCs) extend processes toward and around neuronal axons as they differentiate into oligodendrocytes and generate the electrically insulating myelin sheath. While it is well understood that OPCs and oligodendrocytes utilize the biophysical cue of high aspect ratio axons to create myelin, there are few *in vitro* myelination models. One promising myelination model uses electrospun fibers as artificial axons to allow OPCs to make myelin, however this 2D model had small amount of differentiation likely because it fails to recapitulate the 3D geometry of native tissue. Here, an amorphous polyethylene glycol (PEG) based hydrogel was designed to incorporate electrospun fibers thereby creating a 3D *in vitro* tissue model toward the ultimate goal of engineering an environment suitable for OPC maturation and myelination. Fibers were incorporated into the hydrogel through two methods to simulate different brain regions, one where long fibers were electrospun directly into gel molds and a second where shorter fibers were cryosectioned and mixed with the hydrogel macromer solution prior to gelation. OPC-like cells were encapsulated with fibers in the hydrogels. OPC-like cells remained more viable in gels with fibers and extended processes toward and along fibers, more like mature oligodendrocytes. Finally, primary OPCs were encapsulated and qPCR was used to determine if maturation occurred in response to fibers. Despite promising preliminary results, qPCR did not show a down regulation in OPC genes or an up regulation in mature oligodendrocyte genes. While more optimization needs to be performed on the hydrogel-fiber system, fibers in amorphous hydrogels can be used to guide cells to exhibit more native like OPC morphology.

5.2 Introduction

In the CNS, oligodendrocytes are responsible for creating the electrically insulating myelin sheath around neurons. This insulating layer enables neurons to send quick and efficient signals to downstream neurons enabling functionality throughout the body[1]. In diseases such as multiple sclerosis, the myelin sheath is damaged and destroyed, resulting in a patient's blurred

vision, problems with mobility, and shaking[2]. Most treatments for multiple sclerosis focus on preventing the prominent immune response that occurs simultaneously, rather than focusing on regenerating the myelin sheath. The reason for the lack of myelin regeneration treatments is at least in part due to the absence of promising myelination models to aid development of novel therapeutics. Current *in vitro* myelination models are based on traditional 2D cell culture where oligodendrocytes or OPCs are seeded on neurons[3]. More recently, a myelination model was developed where OPCs are seeded on electrospun fibers that are engineered to mimic artificial axons in terms of diameter and aspect ratio[4]. While this advancement is a promising way to decouple neuronal-oligodendroglial communication and focus on topography, this model resulted in a low percentage of myelinating OPCs and failed to recapitulate the 3D geometry or mechanical properties of the native extracellular matrix[4].

Biomaterials are an attractive alternative to traditional 2D cell culture as they are able to more adequately mimic the geometry and mechanical properties of native tissue. For instance, neurons cultured on 2D were found to be more multipolar in shape compared to neurons grown in 3D[5]. Neurons cultured in 3D became more bipolar and more closely mimic native neurons in the brain[5]. In addition to the simple geometry aspects, biomaterials are able to recapitulate the stiffness of native neural tissue. The storage modulus of traditional tissue culture plastic is on the order of 10^5 to 10^6 kPa whereas novel biomaterials for neural tissue engineering readily mimic native neural tissue, on the order of 1 kPa[6]. Additionally, biomaterials can be designed to mimic disease or injury morphology where the extracellular matrix has been found to decrease following injury and in certain diseases[7]. For instance in multiple sclerosis, the viscoelasticity of brain tissue decreases by 13%[7b].

To date, most attractive biomaterials for native neural tissues are amorphous hydrogel systems without clearly defined topography[8]. While these materials adequately mimic the compliancy and hydrophilicity, and enable some cell maturation, amorphous hydrogel biomaterials fail to mimic many of the topographical cues present during development. For instance, neurons are well known to migrate along radial glia in the developing brain, while OPCs are known to migrate along the brain vasculature[9]. Additionally, OPCs extend processes toward neuronal axons where it is believed that a critical diameter plays a large role in facilitating myelination[1, 4]. Some promising systems have employed fibrous biomaterials[10], however to date few materials have designed a hydrogel material with fibrous axon mimics.

Here, electrospun polystyrene fibers were incorporated into an amorphous PEG based hydrogel to provide topographical cues as axon mimics to guide OPC maturation. Electrospun polystyrene fibers were engineered to mimic axonal geometry, with a high aspect ratio and diameter similar to neuronal axons. PEG-dimethacrylate (PEG-DM) macromer was mixed with PEG-PLA-DM macromer to create a hydrolytically degradable hydrogel. Additionally, this hydrogel recapitulates the stiffness and high-water content of native neural tissue. Two types of OPCs, an OPC-like cell type and primary rat OPCs, were encapsulated in fiber containing hydrogels to investigate maturation of the OPCs.

5.3 Materials & Methods

5.3.1 Electrospinning:

Polystyrene (PS) fibers were produced similarly to previously reported protocols[11] from a 15% (wt/v) 250,000 MW (g/mol) PS (Acros Organics) solution in 70% (v/v) dichloromethane (DCM) (Fisher, USA), 20% (v/v) *N,N*-dimethylformamide (DMF) (Fisher, USA), and 10% (v/v) tetrahydrofuran (THF) (Fisher, USA). Briefly, PS was completely dissolved in DCM and vortexed before adding THF and DMF and vortexing again. Finally, a small amount (<1mg) of sulforhodamine 101 (Sigma-Aldrich, USA) was added to the solution to enable visualization of the fibers with fluorescence microscopy. Fibers were spun in two different ways to incorporate fibers through two methods. Both fiber conditions were stored at room temperature and protected from light until use.

In the first method, fiber webs were electrospun using a SprayBase electrospinning setup with a climate control chamber, syringe pump, and high voltage power supply. Temperature and relative humidity were maintained near 35ºC and 36% in the climate control chamber, respectively. The solution was loaded into a 10 cc Hamilton glass syringe with a 24-gauge blunt-tip needle (emitter). The span between the emitter and collecting plate within the SprayBase system was 151.5 mm. Electrospinning was induced by flowing the polymer solution at 0.75 mL/h with 12 kV applied to the emitter by the power supply. Fibers were collected on either silicone molds or silicon wafers placed on the SprayBase collector plate. Molds were made from a 1 mm thick silicone sheet with three circular holes cut in it using an 8mm diameter biopsy punch. Fibers were allowed to spin and collect on the mold until a web of fibers was clearly

visible in the mold, typically about three minutes. Molds were then transferred to cover slips to create gel molds for the fiber web condition before preparing for encapsulation.

For cryosectioned fibers, fibers were spun directly onto a flat sheet of aluminum foil under ambient conditions using a 24-gauge emitter at 151.5mm height. The solution was pumped through the syringe with a flow rate of 1.3 mL/h as 10kV was supplied by the power supply. Fibers were collected directly on to aluminum foil for about 30 minutes for each fiber mat. Fiber mats were then collected and prepared as described below.

5.3.2 Fiber Preparation:

Fibers in both the cyrosectioned and fiber web condition were first coated in polyornithine to increase the hydrophilicity and enable cell-fiber interactions similar to the coating of polystyrene tissue culture plates. For the fiber web condition, the day prior to use, 120 μL of 10 μg/mL polyornithine solution (30-70 kDa, Sigma-Aldrich) in phosphate buffered saline (PBS) was pipetted into each well of a mold containing fibers to coat the fiber surface and increase their hydrophilicity The following day, the silicone molds were removed from their coverslips, dabbed dry with a KimWipe and placed onto clean coverslips. Fiber containing molds were sterilized under germicidal UV light in the tissue culture hood for at least 2 hours. In this format, macromer solution can be added directly to the fiber webs to create fiber web containing hydrogels.

Cryosectioned fibers were prepared from fibers collected on a sheet of aluminum foil. Electrospun fibers were gathered from numerous sheets of aluminum foil, loosely placed inside a cubic cryosection mold, and frozen in optimal cutting temperature compound (Tissue Tek, USA). Frozen fibers were then cryosectioned on a Lyca cryostat, with a section thickness of 250μm. Sections were collected in PBS at room temperature to dissolve the OCT and suspend the fibers. Fibers were rinsed with distilled water and collected in 10 μg/mL polyornithine in phosphate buffered saline using a 0.22μm filter. Fibers were stored in polyornithine overnight prior to filtering again and collecting the fibers in water. The cryosectioned fiber solution was then lyophilized and resuspended at a higher concentration in PBS. This fiber stock solution could then be mixed directly with macromer solution to create fiber containing hydrogels.

5.3.3 Scanning Electron Microscopy Imaging for Fiber Diameter Measurement:

A Quanta 650 scanning electron microscope (SEM) was used to obtain images of fibers produced via electrospinning. To collect fiber samples for SEM analysis, fibers were either spun directly onto a silicon wafer placed on the collector plate in the SprayBase chamber or pipetted from the cryosectioned fiber stock solution onto the silicon wafer and dried overnight under ambient conditions. (4.0), a beam voltage of (1.00 kV), and a working distance of (6.4mm). The images obtained were then analyzed using ImageJ to determine the average diameter of the fibers produced.

Fiber diameter was quantified using SEM images taken from numerous fiber web samples or a small volume of the fiber stock solution. For the fiber web diameter calculation, fibers were collected directly onto silicon wafers during the same electrospinning sessions where fiber webs were made for cell studies. Samples were obtained from 4 different spinning sessions and imaged. Two 400x images per slide were collected and all the fibers in an image were quantified to determine the average fiber diameter for a total of 8 images analyzed. For cryosectioned fibers, 10μL of the fiber stock was pipetted onto a silicon wafer and 6 regions were imaged at 400x with the SEM. 100 fibers from each of the 6 images were measured and the average diameter was calculated. Additionally for cryosectioned fibers, fiber length was calculated in the same manner using 50 fibers from each of the 6 images.

5.3.4 OPC Culture:

Two different types of cells were used in these studies. For preliminary live/dead and cell morphology analysis, glioma derived MADM OPCs expressing green fluorescent protein (GFP) were provided by the Zong laboratory [12]. MADM OPCs were maintained on tissue culture polystyrene plates coated with polyornithine. Cells were passaged with 0.25% trypsin for five minutes when roughly 90% confluent, then seeded onto new plates at a density of $1*10^4$ cells/cm^2 in OPC media. In addition to MADM OPCs, primary rat OPCS were used for maturation studies. Primary rat OPCs harvested from neonatal (day 6-8) pups were used [13]. Primary OPCs were harvested for each encapsulation and used immediately after isolation.

Both cell types and cell containing hydrogels were cultured in the same OPC media at 37°C in a tissue culture incubator with 5% CO_2 and 100% relative humidity. OPC media consists

of Dulbecco's Modified Eagle Medium (DMEM, Life Technologies, USA), with 4.5 g/L glucose, 4 mM L-glutamine, and 1 mM sodium pyruvate, supplemented with, N2 supplement (Life Technologies, USA), B27 supplement (Life Technologies, USA), 1% penicillin/streptomycin (Life Technologies), 10 ng/mL human PDGF-AA (eBioscience, USA), and 50 ng/mL human neurotrophin-3 (Peprotech, USA). Media was changed every other day in 2D MADM cultures and primary OPC gel cultures. MADM OPC hydrogel culture media was changed every other day for the first four days and then every day following to prevent acidic media conditions and depletion of nutrients due to the rapid growth rate.

5.3.5 Primary OPC Isolation:

Primary OPCs were harvested from neonatal rat pups following previously established protocols[13] and under compliance with NIH Guide for Care and Use of Laboratory Animals and the Institutional Animal Care and Use Committee at the University of Virginia. Briefly, cortices from 6-8 day old rat pups were obtained and digested to a single cell suspension in Accutase (Gibco, USA) with 50 units/mL DNAse for 45 minutes, triturating every 15 minutes. Cells were centrifuged at 1200 RPM for 5 minutes and resuspended in panning buffer consisting of Hanks Buffered Saline Solution (Gibco, USA) with calcium and magnesium, 0.02% bovine serum albumin (Fisher, USA), 50 units/mL DNAse (Sigma Aldrich, USA), and 5 μg insulin (Life Technologies, USA). 20 mL of panning buffer were added to a lectin (Vector Labs, USA) coated 15cm petri dish and incubated at room temperature for 15 minutes. Following the incubation, the supernatant cell-panning buffer was transferred to a fresh lectin coated dish and incubated at room temperature for an additional 15 minutes. Finally, panning buffer and remaining nonadherent cells were transferred to a 10cm petri dish that had previously been coated with goat anti-mouse IgM antibody and anti-O4 to select for $O4^+$ OPCs. Cells were incubated on the antibody coated plate for 45 minutes before washing three times in PBS and trypsinizing the cells with 0.25% trypsin with EDTA (Gibco, USA) for 10 minutes. An equal volume of 10% fetal bovine serum in Dulbecco's Modified Eagle Medium was added to neutralize the trypsin prior to centrifuging the cells for 8 minutes at 1200 RPM. The cell pellet was resuspended in PBS, counted on a hemocytometer to obtain the cell concentration, and encapsulated in the PEG hydrogels. On average, 50,000 cells were obtained per rat pup.

5.3.6 OPC Encapsulation in 3D Hydrogel System with Fibers:

Hydrolytically degradable poly(ethylene glycol) (PEG)-based hydrogels were used to encapsulate cells and fibers. The non-degradable monomer, PEG-dimethacrylate (PEG-DM), was produced using 8,000 kDa PEG (Sigma Aldrich, USA) functionalized with methacrylate end groups from methacrylic anhydride (Alfa Asear, USA) following a previously established microwave methacrylation method. The degradable monomer, PEG-poly(lactic acid)-DM (PEG-PLA-DM, was produced with the same 8,000 kDa PEG monomer. D,L-lactide was added to form the triblock copolymer, PLA-PEG-PLA through a polymer melt, ring opening reaction at 140°C. The intermediate macromer was purified by dissolving in dichloromethane and precipitating in ether. PLA-PEG-PLA was then dried overnight under vacuum. Methacrylate end groups were added to the PLA-PEG-PLA as above to form PEG-PLA-DM. H-NMR confirmed that approximately 2.5 PLA units/side were added to the PEG backbone to form PEG-PLA-DM. PEG-DM and PEG-PLA-DM had a methacrylation efficiency of 73% and 70%, respectively.

Hydrogels were made with cells and with or without fibers by first dissolving macromer in Dulbecco's Modified Eagle Medium at 7.5 % (wt/v) with an equal ratio of degradable to nondegradable macromer (1:1 PEG-DM: PEG-PLA-DM). The photoinitiator lithium phenyl-2,4,6-trimethylbenzoylphosphinate (LAP) was added at a 0.05:1 mole ratio with the macromer. Cells GFP^+ OPCs were encapsulated at $2.5x10^6$ cells/mL and primary OPCs were encapsulated at $0.8x10^6$ cells/mL .

Two different methods of encapsulating fibers with OPCs in the hydrogels have been explored. In one method, fibers were spun directly into silicon molds on cover slips and 80 μL of macromer solution containing cells was added directly to fiber containing molds. In the other method, a stock solution of cryosectioned fibers was diluted with the macromer solution containing cells to allow for more homogeneous distribution of fibers. Cryosectioned fiber hydrogels and fiber free hydrogels were made in inverted syringes with the tips cut off. Cryosectioned and fiber free hydrogels were made out of either 40 μL (GFP^+ OPCs) or 20 μL (primary cells) of cell-macromer solution for the different cell types due to the lower yield of primary cells. Hydrogel molds and syringes were then exposed to UV light (365 nm, $4mW/cm^2$) for ten minutes to allow photoinitiated gelation to occur. After gelation, the gels were carefully transferred to well plates and cultured as previously described.

5.3.7 Live/Dead Assay:

To assess the viability of GFP^+ and primary OPCs, gels were stained and fluorescent images were obtained using a Zeiss 510 confocal microscope. Gels were transferred to individual wells of a 24-well plate. To each well, 500 μL of PBS containing 4.5 g/L glucose (PBSG) was added, ensuring the gel was completely submerged. Live and dead cells were stained with 2 μM calcien AM (Life Technologies, USA) and 4 μM ethidium homodimer (Sigma-Aldrich, USA) in PBSG for 30 minutes. When using GFP^+ OPCs, live cells fluoresce with no stain, thus only ethidium homodimer was used to stain dead cells. After 30 min, the stain solution was aspirated from each well and gels were rinsed twice with PBSG prior to mounting the gels between two coverslips with extra PBSG.

Cell viability images were obtained on the Zeiss 510 (Live/Dead) confocal microscope at the Keck Center for Cellular Imaging at the University of Virginia and quantified using ImageJ. Briefly, ImageJ thresholding was performed on Z-stack images in conjunction with a custom macro developed in house to produce cell-particle count data. A custom Matlab script compiled the data into an Excel file displaying the number of particles in z-stack images, as well as their diameter and intensity. The number of particles per image were compared and the average viability was determined from the number of red particles compared to the green particles. Additionally, average particle diameter for the green channel was assessed to determine if differences in cell cluster size between sample types exist.

5.3.8 Phalloidin and DAPI staining:

Gels were collected for immunostaining in separate wells of a 24 well plate. Gels were fixed for 20 minutes at 4C with 500 μL of 4% paraformaldehyde and rinsed three times with PBS. At this point, gels were permeablized with 0.3% triton-X overnight. After gels were rinsed three times with PBS, gels were stained to visualize the nuclei and actin. For actin staining, 10 μL of phalloidin-alexa 355 (Life Technologies) was added to 500 μL of 1% BSA and incubated for 20 minutes. DAPI was added simultaneously as phalloidin at 1:1000. Gels were then washed three times and mounted for imaging. Gels were imaged on the Zeiss 780 microscope and the University of Virginia's Keck Center for Cellular Imaging.

5.3.9 Quantitative Real Time Polymerase Chain Reaction (qPCR) and Data Analysis:

qPCR was used to measure gene expression and determine differentiation potential. Gels were collected and homogenized in 600 μL TRIzol Reagent (Life Technologies, USA) using an electric mortar and pestle. 120 μL of chloroform was added to isolate an aqueous RNA-containing layer and the RNA was purified using the RNA purification kit from Life Technologies. RNA concentration and purity were assessed by measuring solution absorbance at 260 and 280 nm. RNA concentration was held constant across samples by dilution with RNase-free water and measuring the absorbance at 260 nm. RNA was then converted to complementary DNA (cDNA) using the cDNA synthesis kit from BioRad and a CFX96 Connect BioRad qPCR machine. qPCR was run using BioRad SYBR master mix (50% v/v) and primers shown in table 1. $\Delta\Delta C_T$ values and the corresponding gene expression levels presented were calculated from comparison to the fiber free condition and normalizing with Actinβ as the housekeeping gene. Primers for PDGFRα, NG2, SOX10, MBP, CD82, and Actinβ were ordered from Life Technologies and sequences are obtained from Liu et. al[12].

5.3.10 Statistical Analysis

All quantified results are presented as averages with error bars representing standard deviation.

5.4 Results

5.4.1 Material characterization

Electrospun fibers were used in this study to act as axon mimics in terms of geometry through which the fibers could provide topographical cues for oligodendroglial maturation. Fibers were generated through electrospinning but incorporated in hydrogels through two different methods, resulting in distinct differences between the fibers and their distribution. Fiber diameter and length were assessed through SEM for two types of fibers, fiber webs and cryosectioned fibers(Figure 5-1).In the fiber web condition, fibers were electrospun directly into hydrogel molds; this resulted in a long continuous fiber strand with an average diameter of 2.52 ± 0.35 μm (Figure 5-1). While most fibers were clear and distinct, in the fiber web condition, there was some minimal multi-fiber roping. In both fiber conditions, very little beading of the

fibers was observed through SEM. Most fibers in both conditions appeared round in topography, with limited ribbon-like, beading, or roping geometries. Cryosectioned fibers were cut on a Lyca cryostat with a set section thickness of 250 μm, however due to the loading of random fibers in the cryostat molds the average length of the fibers was measured to be 54.7 ± 14.4 μm (Figure 5-1). Cryosectioned fibers appeared round, with an average diameter of 1.76 ± 0.20 μm (Figure 5-1). These fibers could be easily separated from each other through sonication of the fiber stock solution, however some clumping of fiber aggregates was observed on SEM and confocal microscopy.

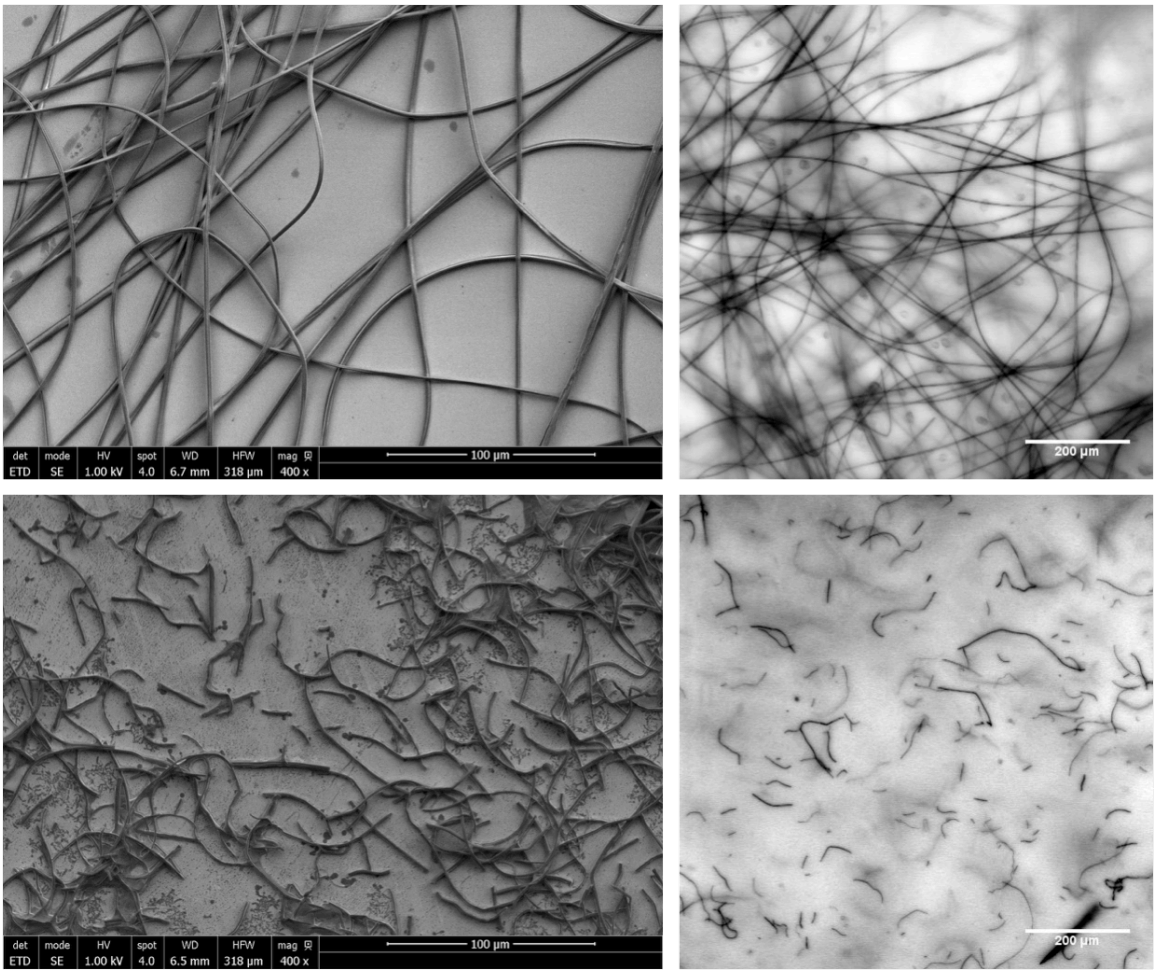

Figure 5-1 Representative SEM images of fibers (left) and representative brightfield images of fibers in 3D hydrogels (right). Top row shows fiber web condition. Bottom row shows the cryosectioned fibers. Scale bars are 100 µm and 200 µm for SEM and bright field gel images.

5.4.2 Fiber incorporation in to the hydrogel

Fibers were incorporated into the amorphous PEG hydrogels in two different methods. These two fiber methods, with different fiber concentrations and distributions were engineered to mimic different brain regions with distinct heterogeneity as a proof of concept. For instance, the pyramidal tract of the rat brainstem has a higher axon density than cervical level 2 of the corticospinal tract [14]. Additionally, Purkinje neurons have a much different axon aspect ratio than myelinated motor neurons [15]. Further studies can be designed to more closely mimic specific CNS regions. In the first fiber mold method, fibers were electrospun directly into hydrogel molds before adding the macromer solution and initiating gelation. In the second, fibers were cryosectioned and resuspended in PBS before mixing with the macromer solution and initiating gelation. The two methods yield radically different fiber-hydrogel types. In the first, long fibers extend through out a smaller z-height of the hydrogel (Figure 5-1). Fibers in the fiber web conditions were found over an average z-height of 409±151 μm and were found to cover 0.068±.015% of the 3D z-stack image volume. In the cryosectioned fiber condition, fibers were distributed throughout the entire volume of the hydrogel, while fiber web conditions were contained in a limited height of the hydrogel (Figure 5-1). Confocal microscopy z-stack images were divided into 20 μm thick sections and the number of fibers was counted in each section. Here an average of 130±8 fibers were counted in each 20 μm section. No difference in fiber concentration was observed at different z-heights indicating that polymerization occurred rapidly enough to prevent settling or floating of fibers. Additionally, cryosectioned fibers covered an average 0.14±.051% of volume.

5.4.3 GFP+ MADM response to the fibers in 3D

GFP MADM cells were encapsulated along with fibers in the 3D PEG based hydrogels for initial proof of concept studies. Viability was assessed through the Live/Dead assay (Figure 5-2,Figure 5-3). Confocal images were analyzed in the fiber free, cyrosectioned fiber, and fiber mold condition to determine if viability differences existed. Fiber containing hydrogels were found to have higher viability in comparison to the fiber free condition (Figure 5-2,Figure 5-3). Specifically, cryosectioned fibers and fiber mold conditions remained more viable than the fiber

free condition at day 1. Cryosectioned fibers were 3.2±2.1% more viable compared to 15.7±9.0% more viable for the fiber web condition (Figure 5-3). Over time, cells in the fiber web hydrogels remained 5.9±3.4% more viable at day 4 compared to the fiber free condition (Figure 5-3). After 4 days, cells in cryosectioned fibers were 17.3±10.0% more viable than the fiber free condition (Figure 5-3). At 7 days, cryosectioned fibers were 4.23±3.48% more viable, while the fiber web condition was 12.3%±3.1% more viable than the fiber free control (Figure 5-3). Additionally, it was found on average that cell clusters in the fiber web and cryosectioned fiber gels had average diameters of 20.9±11.8 and 14.8±10.6 μm, respectively. Fiber free hydrogels had a slightly larger cell cluster diameter of 24.4±11.0 μm. When GFP MADM cells were cultured in 3D PEG hydrogels with fibers cells were occasionally seen extending processes toward and along fibers. Cells in fiber free hydrogels remained more round over 7 days, despite the 50% degradable macromer.

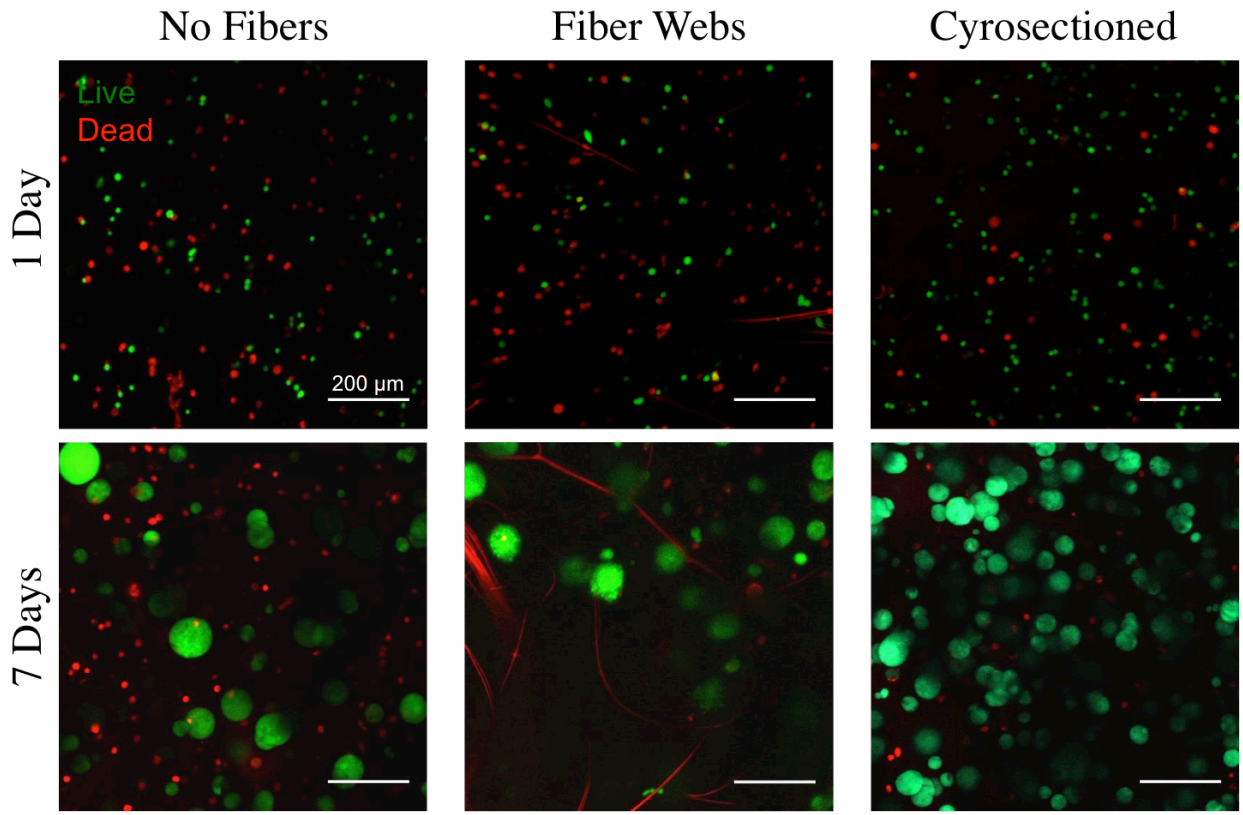

Figure 5-2 Cells in fiber containing hydrogels remain qualtiatively more viable than cells in the fiber free conditions. Fibers are visible in fiber web through the sulforhodamine dye. Cryosectioned fibers also contain the

sulforhodamine dye but are not as visible due to the smaller diameters and fluorescent intensity of ethidium homodimer. Scale bar represents 200 μm.

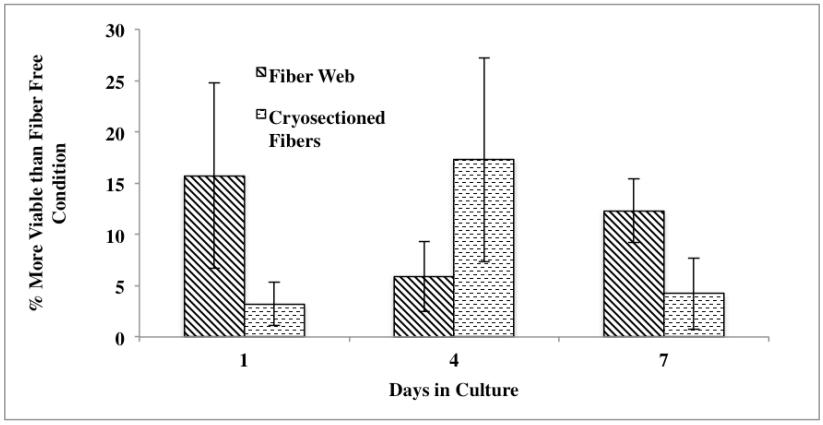

Figure 5-3 Cells in fiber containing hydrogels remain quantitatively more viable than cells in the fiber free conditions. Data presented are the average viabilities normalized to fiber free conditions. Error bars represent standard deviation.

5.4.4 Primary OPC response to the fibers

Isolated primary OPCs were encapsulated in the hydrogels at a concentration of 0.875×10^6 cells/mL and imaged one and seven days after encapsulation (Figure 5-4). Viable cells remained at both 1 day following encapsulation and 7 days after encapsulation. Qualitatively, viability at 1 day appeared significantly better in the fiber conditions compared to the fiber free condition. However, by 7 days, there was a significant decrease in the number of cells in the fiber free, fiber web, and cryosectioned fiber conditions in confocal microscopy. Additionally, cells in all conditions remained round and did not appear to extend processes toward or around fibers as was suggested by GFP^+ MADM OPC-like cells. While cells did not appear to be extending processes, some select images showed round OPCs were in contact with fibers.

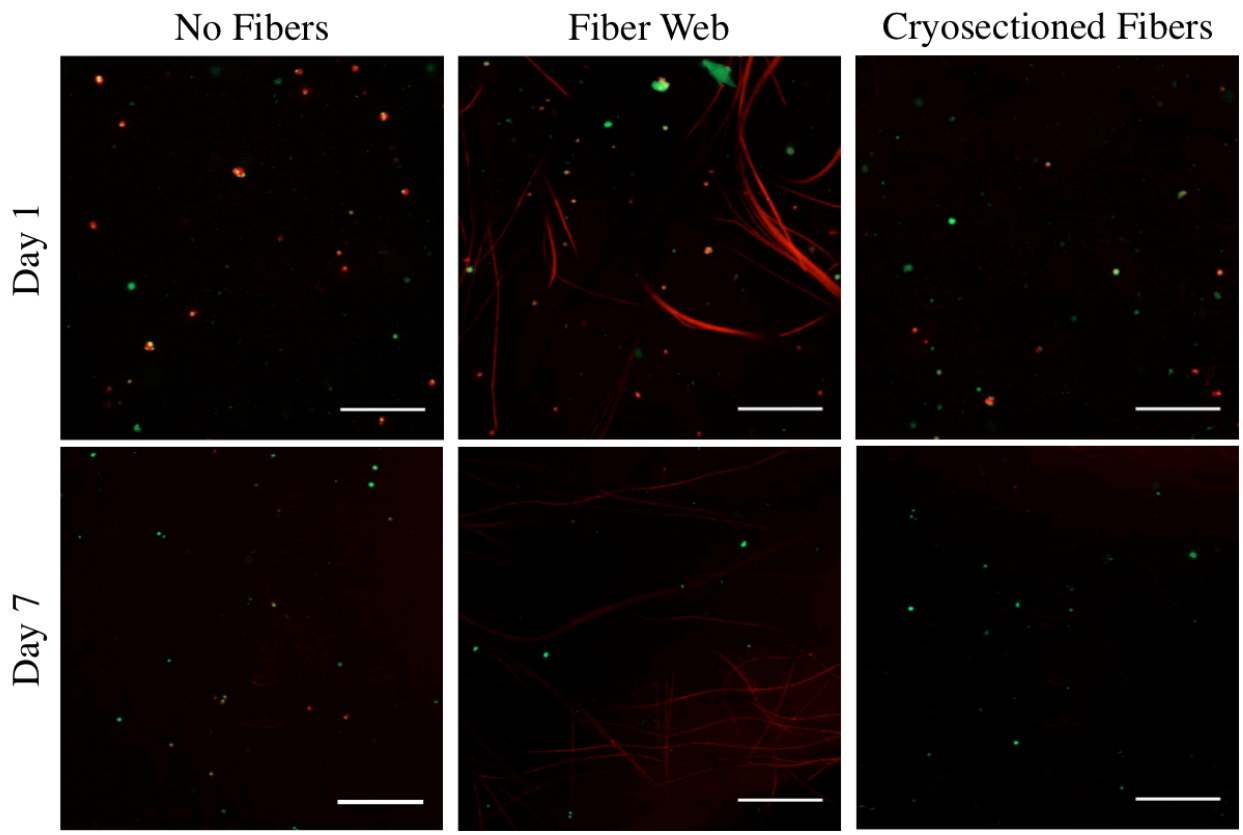

Figure 5-4 Primary OPCs in PEG hydrogels remain viable when encapsulated alongside fibers or alone. Cells remain viable after 7 days. Live cells are shown in green; red indicates dead cells or fibers. Scale bar represents 200 μm.

5.4.5 Primary OPCs do not mature with incorporation of fibers

RNA was isolated from primary OPCs cultured in gels with and without fibers and quantified for gene expression of two OPC markers (PDGFRα, NG2), an oligodendroglial marker (SOX10), and two mature markers (MBP and CD82). Due to the low cell concentration and lack of cell growth, very little RNA was collected from all encapsulated cell samples and amplification did not occur until after many cycles (>35). Gene expression was not significantly upregulated or downregulated in any of the fiber conditions for any of the primers. Relative gene expression is shown in Figure 5-5.

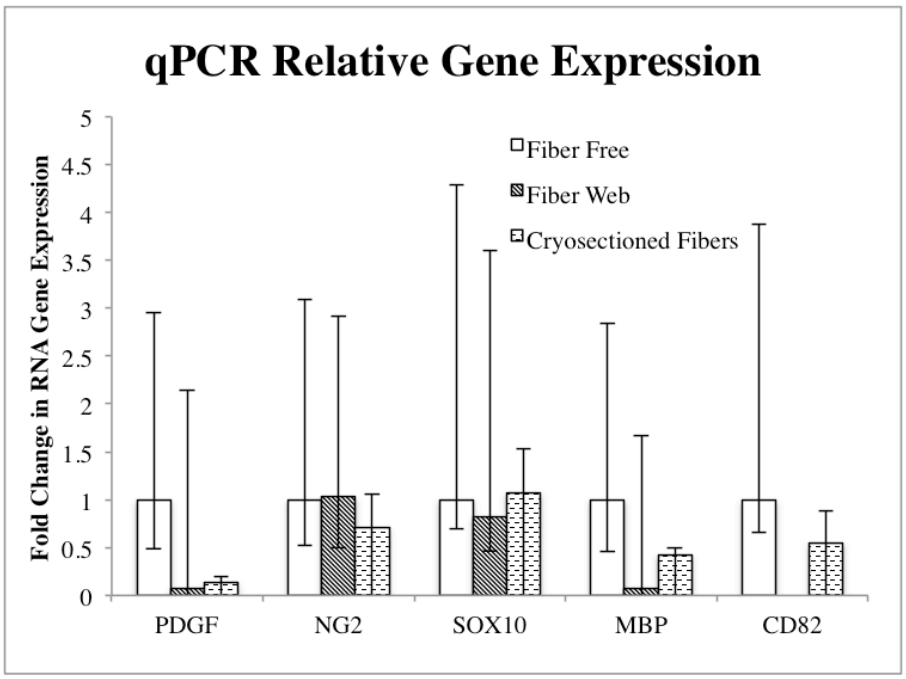

Figure 5-5 qPCR shows that cells are not maturing in gels with fibers. Neither the fiber web or cryosectioned fibers had downregulation in OPC Markers (PDGF or NG2), or upregulation in oligodendroglial markers (SOX10), or oligodendrocyte markers (MBP and CD82). 5 samples of each condition collected at day 7 are represented by the data shown.

5.5 Discussion

Fibers were designed to mimic neuronal axons in terms of topography and aspect ratio. Electrospinning polystyrene fibers resulted in fiber diameters of 1.76 ± 0.20 and 2.52 ± 0.35 μm for the cryosectioned and fiber web conditions, respectively. Additionally very little roping or beading of fibers occurred indicating that fibers closely mimic the high aspect ratio and elongation of neuronal axons[16]. These fibers were encapsulated in amorphous hydrogels where the fiber concentration, diameter, or length can be further tuned to closely mimic different brain regions. For instance, axon concentration directly correlates with the anterior to posterior location along the spinal column; fewer number of axons have been recorded in the posterior spinal cord compared to the anterior, closer to the brain stem[14]. Neuronal axon diameter size correlates with the location of the brain or spinal cord region, where thicker neurons are found in the spinal cord compared to the corpus callosum[17]. Additionally orientation is different for different types of neurons and different regions. Purkinje cells are highly branched neurons with comparatively shorter branches compared to the elongated neurons of the spinal cord[15]. Further

work remains to directly mimic specific regions of the brain, however these two models can be used as starting blocks for additional fine tuning. Furthermore, while the area made up of fibers were different in both gel conditions, 0.068±.015% and 0.14±.051% for the fiber web and cyrosectioned fiber conditions, the fiber volume is easily tunable by either through different electrospinning parameters. For instance, electrospinning for longer will provide a denser fiber web with a higher concentration of fibers. The cryosectioned fiber concentration in gels can be tuned by pipetting more or less of the fiber stock solution into the macromer solution. This difference in fiber volume percent, where cyrosectioned fiber concentration is higher than the fiber web condition, is likely due to the fact that cryosectioned fibers are dispersed through the entire z-height, while fibers in the fiber web condition cover a smaller z-height thickness. In fiber web conditions, fibers extend 409±151 μm deep along the hydrogel thickness. Further analysis needs to be done to obtain more accurate measurements for this as this data was obtained from confocal microscopy z-stack images. However, confocal microscopy limits the total height of z-stack images. Thus future experiments should cryosection hydrogels similar to tissue and image serial sections to assess the fiber height.

The ultimate goal of this project was to guide OPC maturation through the incorporation of electrospun fibers into an amorphous PEG hydrogel. Initial results with OPC-like cells showed promising results where OPC-like cells remained more viable and extended processes. OPC-like cells were found to remain significantly more viable in conditions with fibers than in the fiber free condition. This was true for the cryosectioned or fiber web conditions which remained 3.2 to 17.3% and 5.9 to 15.7% more viable, respectively. Fiber web conditions remained more viable on average compared to the cryosectioned fibers. That may be due to the fact that qualitatively more fibers were in direct contact with fibers in the fiber web condition. While these results are promising, it should be noted that OPC-like cells are significantly different from primary OPCs. In particular these OPC-like cells are glioma derived. In the CNS, gliomas and healthy brain tissue have many distinct differences in terms of their extracellular matrix, cell organization, and morphology[18]. The hydrogels used in this experiment had storage moduli of around 560 Pa while native CNS tissue measures <1 kPa[19]. Gliomas are marked by an increase in stiffness, up to an elastic modulus of 6 kPa in the optic nerve[20], of the surrounding extracellular matrix and an increase in the concentration of extracellular matrix proteins. These extracellular matrix proteins, such as fibrillar collagen, correlate with a higher amount of

topographical cues relative to areas of healthy brain tissue which is composed primarily of glycosaminoglycans, proteoglycans, and glycoproteins. Additionally, glioma cell metastasis or migration is often guided by topography[18a]. Therefore, while the results may be promising in terms of OPC potential, the results shown here with OPC-like cells can be explained by their origin. As gliomas are well characterized by their ability to remodel the extracellular matrix[18c], incorporating fibers, unaligned or aligned, in an amorphous hydrogel may better recapitulate a tumor environment and lead to better viability of OPC-like cells. Furthermore, OPC-like cell process extension is not surprising given that glioma cells preferentially migrate toward fibrous tracts and metastasize in fibrous tissue[18a].

However, primary OPC results were less promising. OPCs were found in contact with fibers, though they remained round and punctate. Additionally, while viability appeared different at the initial 1 day time point, by 7 days, cells across all conditions appeared to have a similar cell number and viability in the two fiber conditions and fiber free condition. The total cell number had decreased since day 1, however viability at day 7 was qualitatively high in the two fiber conditions and fiber free condition. Furthermore, qPCR results did not reveal an upregulation in oligodendrocyte genes or a downregulation in OPC genes in the fiber containing conditions compared to the fiber free condition. These results indicate that OPCs do not actually mature in the PEG hydrogels through the incorporation of fibrous, axon mimic topography. These results directly contradict the existing literature, which has shown that axonal topography is necessary for functional OPC maturation in 2D[4].

Contrasting results in 3D could be due to the harmful stress involved from isolating primary OPCs from rat brains and the low cell concentration in the hydrogels. This isolation process will further need to be optimized to ensure healthy, viable cells and increase the number of cells in each gel to ensure many cells are in contact with fibers. Additionally, OPCs in gels here were cultured in proliferation media, and future experiments using differentiation media might boost differentiation. *In vivo,* myelination has been shown to be a complicated process that requires many cues, both topographical and soluble[21]. Furthermore, *in vitro* OPCs were found to have a critical diameter for myelination of fibers while *in vivo* neurons are capable of myelinating neurons with axons from .1 to 10 μm[22]. While topography is certainly important in guiding OPC fate, previous myelination models that employ the use of fibrous topography further guide OPC maturation with soluble cues in differentiation media[11, 23]. Here, the volume

percentage of fibers made up of <0.2%. In addition to tuning maturation with soluble cues, more fiber topography can be incorporated. Increasing the concentration of fibers in the hydrogel increases the potential of OPC-fiber interaction and can further guide maturation.

5.6 Conclusions

In this work, fibers were incorporated in PEG based hydrogels in two ways. In the first method, fiber webs were encapsulated in the hydrogel to create distinct regions with long fibers. The second method enabled fibers to be encapsulated more homogenously, however limited the length of fibers. Both conditions had similar fiber diameters from 1-3μm in diameter. Axon diameters range from 0.1-10 μm *in vivo*, however previous results in 2D have shown that OPCs respond to critical fiber diameters of 2-4 μm for myelination *in vitro* [4, 11]. Additionally, no beading of the polymer fibers during the electrospinning sessions occurred and there was limited roping and aggregation of the fibers in the cryosectioned and fiber web conditions. These fibers were encapsulated in the hydrogel to serve as axon mimics both in terms of fiber diameter and fiber morphology. The different fiber conditions can be further tuned to more closely recapitulate different regions in the brain to learn more about myelination biology or to create models for different types of neurodegenerative diseases. In both fiber cases, OPC-like cells (GFP^+ MADM cells) remained more viable, while proliferating less than in control (fiber free) hydrogels. These results when considering the cell origin are not surprising, as the OPC-like cells are glioma-derived cells. In the CNS, gliomas express fibrous extracellular matrix proteins and preferentially migrate toward or along fibrous tissue[18a, 18c]. When primary OPCs were encapsulated in the hydrogels and maturation was investigated, qPCR revealed that no maturation occurred. However, these results were obtained through the incorporation of fibers alone. Future studies can use fibers and differentiation media with soluble factors such as ciliary neurotropic factor[24], forskolin[25], or the hormone T3[26] to enhance the differentiation capabilities of the cell. Additionally, the use of polystyrene fibers alone provide a starting block to investigate the impact of topography. The simplicity of this system allows for subsequent modification where the polystyrene fibers can be engineered to incorporate additional cues to guide oligodendroglial maturation. For instance, polystyrene fibers can be modified to recapitulate surface markers present on axons, such as neuroregulin-1, and investigate the role of surface markers on oligodendroglial maturation. While further studies and differentiation schemes remain to be

identified, the impact of fiber topography on OPC-like cells in the 3D amorphous-fibrous hydrogel suggests the potential this biomaterial may have towards developing an *in vitro* myelination model.

5.7 References

1. Snaidero, N.; Simons, M., Myelination at a glance. *J Cell Sci* **2014,** *127* (Pt 14), 2999-3004.
2. Harlow, D. E.; Honce, J. M.; Miravalle, A. A., Remyelination Therapy in Multiple Sclerosis. *Front Neurol* **2015,** *6*, 257.
3. Jarjour, A. A.; Zhang, H.; Bauer, N.; Ffrench-Constant, C.; Williams, A., In vitro modeling of central nervous system myelination and remyelination. *Glia* **2012,** *60* (1), 1-12.
4. Lee, S.; Leach, M. K.; Redmond, S. A.; Chong, S. Y.; Mellon, S. H.; Tuck, S. J.; Feng, Z. Q.; Corey, J. M.; Chan, J. R., A culture system to study oligodendrocyte myelination processes using engineered nanofibers. *Nature methods* **2012,** *9* (9), 917-22.
5. Ribeiro, A.; Vargo, S.; Powell, E. M.; Leach, J. B., Substrate three-dimensionality induces elemental morphological transformation of sensory neurons on a physiologic timescale. *Tissue engineering. Part A* **2012,** *18* (1-2), 93-102.
6. Skardal, A.; Mack, D.; Atala, A.; Soker, S., Substrate elasticity controls cell proliferation, surface marker expression and motile phenotype in amniotic fluid-derived stem cells. *J Mech Behav Biomed Mater* **2013,** *17*, 307-16.
7. (a) Moeendarbary, E.; Weber, I. P.; Sheridan, G. K.; Koser, D. E.; Soleman, S.; Haenzi, B.; Bradbury, E. J.; Fawcett, J.; Franze, K., The soft mechanical signature of glial scars in the central nervous system. *Nat Commun* **2017,** *8*, 14787; (b) Wuerfel, J.; Paul, F.; Beierbach, B.; Hamhaber, U.; Klatt, D.; Papazoglou, S.; Zipp, F.; Martus, P.; Braun, J.; Sack, I., MR-elastography reveals degradation of tissue integrity in multiple sclerosis. *Neuroimage* **2010,** *49* (3), 2520-5.
8. Murphy, N. P.; Lampe, K. J., Mimicking biological phenomena in hydrogel-based biomaterials to promote dynamic cellular responses. *J. Mater. Chem. B* **2015,** *3* (40), 7867-7880.
9. Tsai, H.-H.; Niu, J.; Munji, R.; Davalos, D.; Chang, J.; Zhang, H.; Tien, A.-C.; Kuo, C. J.; Chan, J. R.; Daneman, R.; Fancy, S. P. J., Oligodendrocyte precursors migrate along vasculature in the developing nervous system. *Science* **2016,** *351* (6271), 379-384.
10. (a) Lewicka, M.; Hermanson, O.; Rising, A. U., Recombinant spider silk matrices for neural stem cell cultures. *Biomaterials* **2012,** *33* (31), 7712-7; (b) Wang, H. B.; Mullins, M. E.; Cregg, J. M.; Hurtado, A.; Oudega, M.; Trombley, M. T.; Gilbert, R. J., Creation of highly aligned electrospun poly-L-lactic acid fibers for nerve regeneration applications. *J Neural Eng* **2009,** *6* (1), 016001.
11. Lee, S.; Chong, S. Y. C.; Tuck, S. J.; Corey, J. M.; Chan, J. R., A rapid and reproducible assay for modeling myelination by oligodendrocytes using engineered nanofibers. *Nature Protocols* **2013,** *8* (4), 771-782.
12. Liu, C.; Sage, J. C.; Miller, M. R.; Verhaak, R. G.; Hippenmeyer, S.; Vogel, H.; Foreman, O.; Bronson, R. T.; Nishiyama, A.; Luo, L.; Zong, H., Mosaic analysis with double markers reveals tumor cell of origin in glioma. *Cell* **2011,** *146* (2), 209-21.

13. Dugas, J. C.; Emery, B., Purification of oligodendrocyte precursor cells from rat cortices by immunopanning. *Cold Spring Harb Protoc* **2013,** *2013* (8), 745-58.
14. Leenen, L.; Meek, J.; Posthuma, P.; Nieuwenhuys, R., A Detail Morphometrical Analysis of the Pyramidal Tract of the Rat. *Brain research* **1985,** *359*, 65-80.
15. Barron, T.; Saifetiarova, J.; Bhat, M. A.; Kim, J. H., Myelination of Purkinje axons is critical for resilient synaptic transmission in the deep cerebellar nucleus. *Scientific reports* **2018,** *8* (1), 1022.
16. Liewald, D.; Miller, R.; Logothetis, N.; Wagner, H. J.; Schuz, A., Distribution of axon diameters in cortical white matter: an electron-microscopic study on three human brains and a macaque. *Biol Cybern* **2014,** *108* (5), 541-57.
17. Komlosh, M. E.; Ozarslan, E.; Lizak, M. J.; Horkayne-Szakaly, I.; Freidlin, R. Z.; Horkay, F.; Basser, P. J., Mapping average axon diameters in porcine spinal cord white matter and rat corpus callosum using d-PFG MRI. *Neuroimage* **2013,** *78*, 210-6.
18. (a) Agudelo-Garcia, P. A.; De Jesus, J. K.; Williams, S. P.; Nowicki, M. O.; Chiocca, E. A.; Liyanarachchi, S.; Li, P.-K.; Lannutti, J. J.; Johnson, J. K.; Lawler, S. E.; Viapiano, M. S., Glioma Cell Migration on Three-dimensional Nanofiber Scaffolds Is Regulated by Substrate Topography and Abolished by Inhibition of STAT3 Signaling. *Neoplasia* **2011,** *13* (9), 831-IN22; (b) Claes, A.; Idema, A. J.; Wesseling, P., Diffuse glioma growth: a guerilla war. *Acta neuropathologica* **2007,** *114* (5), 443-58; (c) CL, G., The Etracellular matrix of gliomas: modulation of cell function. *J Neuropathol Exp Neurol* **1999,** *58* (10), 1029-40.
19. Chatelin, S.; Constantinesco, A.; Willinger, R., Fifty years of brain tissue mechanical testing: from in vitro to in vivo investigations. *Biorheology* **2010,** *47* (5-6), 255-76.
20. Walter, C.; Crawford, L.; Lai, M.; Toonen, J. A.; Pan, Y.; Sakiyama-Elbert, S.; Gutmann, D. H.; Pathak, A., Increased Tissue Stiffness in Tumors from Mice with Neurofibromatosis-1 Optic Glioma. *Biophysical journal* **2017,** *112* (8), 1535-1538.
21. Hughes, E. G.; Appel, B., The cell biology of CNS myelination. *Curr Opin Neurobiol* **2016,** *39*, 93-100.
22. Hilderbrand, C.; Hahn, R., Relation between myelin sheath thickness and axon size in spinal cord white matter of some vertebrate species. *Journal of the Neurological Sciences* **1978,** *38*, 421-434.
23. Li, X.; Liu, X.; Cui, L.; Brunson, C.; Zhao, W.; Bhat, N. R.; Zhang, N.; Wen, X., Engineering an in situ crosslinkable hydrogel for enhanced remyelination. *FASEB journal : official publication of the Federation of American Societies for Experimental Biology* **2013,** *27* (3), 1127-36.
24. Talbott, J. F.; Cao, Q.; Bertram, J.; Nkansah, M.; L., R.; Benton; Lavik, E.; Whittemore, S. R., CNTF promotes the survival and differentiation of adult spinal
cord-derived oligodendrocyte precursor cells in vitro but fails to
promote remyelination in vivo. *Exp Neurol* **2007,** *204* (1), 485-489.
25. Shi, J.; Marinovich, A.; Barres, B. A., Purification and Characterization of Adult Oligodendrocyte Precursor Cells from the Rat Optic Nerve. *Journal of Neuroscience* **1998,** *18* (12), 4626-4636.
26. Dugas, J. C.; Ibrahim, A.; Barres, B. A., The T3-induced gene KLF9 regulates oligodendrocyte differentiation and myelin regeneration. *Mol Cell Neurosci* **2012,** *50* (1), 45-57.

6 OPC Viability in 3D vs. Traditional 2D Cell Culture

6.1 Abstract

Primary OPCs are difficult to culture *in vitro* as they will often have poor long term viability or will spontaneously differentiate and therefore necessitate the need for frequent harvests. Isolating primary OPCs from rat brains is a complicated, timely process that involves many steps that can compromise cell viability. Of these steps, there are two enzymatic digestions and numerous pipetting steps that can either disrupt the cell membrane or mechanically shear the cells. In this dissertation research, one important observation was that isolated primary OPCs appeared to remain more viable following immediate encapsulation in the PEG hydrogel versus those seeded in traditional 2D cell culture. To further elucidate some of these results, the viability of cells in the PEG biomaterial compared to traditional 2D cell culture was investigated through ATP and viability assays. Over time, as shown in previous chapters, cells remain viable in the 3D hydrogel while simple microscopy shows large amounts of cell debris in 2D culture. Additionally, the concentrations of caspase 3 and 7, markers of cell apoptosis, were found at higher levels in traditional 2D cell culture. Together, these results confirm the belief that even simple 3D hydrogel biomaterials can have a large impact on cell viability and can be further used to advance simple 2D tissue culture models to ease biological understanding of native phenomena.

6.2 Introduction

OPCs are at their highest concentration in the developing brain, after neurons and many astrocytes have already matured[1]. Because oligodendrocyte maturation occurs later in development, after many other cell types are present, isolating OPCs from brains is a complicated process that involves many steps[2]. First, the brain extracellular matrix must be degraded to obtain a single cell suspension. Next the cells are centrifuged to remove most of the enzyme before suspending in a plating buffer. The established protocol buffer lacks essential amino acids and glucose, potentially disrupting the cellular metabolism. Over the next hour and a half, cells are then transferred across three different coated plates to select and deselect primary

OPC. The final plate selects for OPCs, which adhere strongly to the antibody coated plate. Removing the final purified OPCs requires the cells to be trypsinized again, washed vigorously, and finally centrifuged to collect a cell pellet.

All these steps together pose many challenges for cell viability and increase the likelihood of cell membrane disruption and cell death. Necrosis is the sudden cell death that results in lysis of the cell. Contrastingly, apoptosis is programmed cell death characterized by an increase in caspase activation[3], that cells undergo in response to certain stimuli, such as the detachment of cells from the extracellular matrix[4]. This specific form of apoptosis is known as anoikis[4]. Numerous pipetting and trituration steps increase the risk of mechanically shearing the cell membrane. Mechanically shearing the cell membrane results in necrosis, which in turn releases reactive oxygen species and other potentially cytotoxic molecules. This increase in reactive oxygen species can further result in apoptosis as programmed cell death serves to prevent further cell damage[5]. Furthermore, the simple act of removing and digesting the brain extracellular matrix potentiate the possibility of anoikis, a particular type of apoptosis[6].

Anoikis is the induced death caused by a lack cell-ECM attachment or removal of the extracellular matrix from the cell environment[6]. Biomaterials have been shown previously to help protect cells from anoikis, however many of these biomaterials include adhesive cell sites from native extracellular matrix, such as RGD or IKVAV[7]. In relation to this, it has been shown that mechanical stimuli from the surrounding environment can cause clustering of integrin binding domains[8] on the cell surface and prevent the induction of anoikis[9]. From these ideas, we hypothesize that simply encapsulating cells in a bioinert hydrogel that mimics native ECM stiffness may help to prevent apoptosis.

Additionally, the ECM plays an important role in the localization of soluble bioactive cues, such as growth factors. Many growth factors, such as PDGF[10], are well known to interact or bind with extracellular matrix proteins and heparin sulfate, therefore enabling, to an extent, spatial localization or drug release of these proteins[11]. PDGF in particular is well known to enhance OPC viability and prevent apoptosis[12]. While bioinert hydrogels would not allow the same sorts of growth factor-ECM interactions, limited diffusion through constricted hydrogel networks may have similar impacts. Previous work in PEG hydrogels has shown that diffusion of large proteins (67 kDa) is reduced by up to 10% of that in water[13]. While this diffusion did not

hinder cell viability in the hydrogels, the decreased diffusion rates may impact the cell-cell cross talk through growth factor release or diffusion of toxic signals[13].

In addition to important ECM cues, paracrine signals play an important role of cell viability[14]. Cells secrete numerous hormones, electrical signals, and growth factors that communicate with neighboring cells to maintain proliferation or guide differentiation[14]. This cell cross talk and the resulting feedback loop is known as paracrine signaling. Furthermore, paracrine signaling has been shown to directly correlate with the cell seeding concentration[15]. However, paracrine signaling of OPC cells to OPCs is remains unclear[16]. They are well known to secrete factors that promote pericyte function and support blood-brain barrier integrity[17]. Additionally, it has been observed that OPCs extend process and are contact inhibited by neighboring OPCs to determine their spatial domains, though paracrine signaling of OPCs is not well understood. [18]

During the course of the dissertation research, an important observation suggested that sensitive primary rat OPCs remained more viable when encapsulated in the PEG hydrogel as opposed to seeded in 2D. To further elucidate these results, we quantified cell viability and apoptosis over time in both scenarios. DNA and ATP were used as simple measures of cell growth and metabolic activity, respectively. Apotox-Glo Triplex cell assay was used to measure active cell proteases, indicators of death. Finally, caspase types 3 and 7, which are upregulated in apoptosis, were measured as a direct measure of apoptosis. Together these results confirm that the bioinert PEG hydrogel helps promote cell viability and prevent apoptosis.

6.3 Materials and Methods

6.3.1 Cell culture

Primary OPCs were isolated according to the procedure outlined in chapter 5[2] and cultured in the OPC media described throughout this work. Following the trypsin digest step, a cell pellet was obtained that was resuspended in media and either encapsulated in PEG hydrogels or seeded in coated well plates. Cells were cultured in a 50% degradable PEG-PLA-DM hydrogel (7.5% wt/v) at $2x10^6$ cells/mL. 20 μL hydrogels were cultured one gel per well in 24 well plates, with 500 μL of media. Prior to seeding OPCs on 24 well plates for 2D cell culture, plates were coated in one of three ways. Poly(L-Lysine) (PLL) coated plates were incubated at 37°C with 500 μL of 150 to 300 kDa PLL hydrobromide (Millipore Sigma) solution overnight.

PLL plus laminin (PLL+L) coated plates were made by diluting laminin (Life Technologies) at 1:120 in PLL and incubating 500 μL of solution in each well of a 24 well plate overnight at 37°C. Polyornithine coated plates were prepared as before. All three 2D cell culture conditions were rinsed three times with phosphate buffered saline with calcium and magnesium prior to seeding OPCs. PLL and PLL+LN plates were allowed to air dry thoroughly prior to seeding. To seed OPCs on the plates, a 20 μL drop of OPC solution ($2x10^6$ cells/mL) was added to each well and placed in the tissue culture incubator for an hour. Following the hour incubation, 500 μL of media was added to each well.

For the UV light experiments, cells were seeded on 2D polyornithine coated plates as mentioned above. After one hour, cell media was added and the wells exposed to ultraviolet light exposure were placed under the lamp for 10 minutes (~4 mW/cm^2, 365 nm). Well plates were returned to the tissue culture incubator for another hour and 500 μL of 2X lysis buffer was added to each well.

For the cell concentration experiments, cells were seeded on polyornithine coated plates. In one condition cells were seeded at the normal concentration in a 20 μL droplet. In the 2x concentration condition, a 40 μL droplet was added to each well. Both conditions were cultured in 500 μL of media and changed every day. Three samples per condition were collected at day 7 by adding concentrated 2x lysis buffer to each well. Additionally GFP$^+$ MADM OPC-like cell concentration was varied in 3D hydrogels to determine viability. These gels were made with cells at $1x10^6$, $5x10^6$, and $10x10^6$ cells/mL. Gels were stained with the Live/Dead stain at day 1 and day 7, while media was changed according to procedures outlined in chapter 3.

In both 2D and 3D gel conditions, media was changed every two days and samples were taken at 1 day, 4 days, and 7 days by adding lysis buffer. For 2D conditions, 500μL of 2X lysis buffer was added to each well. For gels, gels were removed from media and placed in 500μL of lysis buffer. Gels were homogenized in lysis buffer using a handheld pestle as described previously. Cell lysates were stored in the -80 °C freezer until use.

6.3.2 Experimental assays

Cell lysates from 2D cultures and homogenized gels were used with the Promega CellTiter Glo ATP assay, the Promega Apotox-Glo Triplex Assay, and the Life Technologies PicoGreen DNA assay. Assays were done in that order in 3 different 384 well plates according to

the manufacturer protocol. Briefly, 10 μL of lysates were added in triplicate to wells of a 384 well plate. Assay buffer was added at an equal volume to the lysates and placed on a rocker to stir the lysates for the required activation time. Luminescence or fluorescence values were measured on the lab BMG Clariostar plate reader. The Apotox-Glo Tiplex assay is designed to measure active proteases in live cells, active proteases in dead cells, and caspase 3/7 concentrations[19]. However, since these assays were performed on cell lysates, the assay gave two measures for active cell proteases with different fluorophores and a measure of caspase 3 and 7 concentrations. ATP and DNA values were compared to a standard curve and average ATP or DNA concentrations were calculated from the CellTiter Glo and PicoGreen assays. Relative luminescence or fluorescence values were presented for the ApotoxGlo assay.

6.4 Results and Discussion

6.4.1 Ultraviolet light studies

Exposure to UV light leads to apoptosis and programmed cell death in numerous cell types[20]. Because the PEG based hydrogel is photopolymerized, it was important to determine if, and to what extent, UV light is detrimental to primary OPC viability. These studies were done without photoinitiator or PEG macromer, and occurred with cells seeded on 2D polyornithine coated plates. The same number of cells were added to each well in these studies and the DNA quantification confirms equal cell loading (Figure 6-1). DNA concentrations of the two conditions should not differ as cells were only cultured for two hours and thus no proliferation would have occurred. When cells were exposed to UV light, ATP significantly decreased (Figure 6-1). These results are consistent with previous literature, which shows that UV exposure can stimulate the intracellular production of reactive oxygen species[20a]. This imbalance of reactive oxygen species further disrupts the metabolic and energy synthesis pathways[20a].

In addition to a decrease in ATP, the active cell protease concentration decreased, indicated by a reduction in assay luminescence (Figure 6-1). Cell proteases are used in many aspects of cellular maintenance. Proteases are extensively utilized during apoptosis as a means to "recycle" cell proteins upon cell death[21]. Additionally, they are often termed the "executioners of cell death. [22]" However, it is unclear the role of proteases in other types of cell death such as necrosis. While apoptosis is generally characterized by an increase in cell proteases and caspase concentration, necrosis is instead characterized simply by cell membrane permeation,

mitochondrial swelling, or cytoplasmic vacuolation[23]. Furthermore, it has been found that high exposure to UV light can cause cellular necrosis rather than apoptosis[20b].

Here the decrease in ATP upon exposure to UV light might prevent induction of apoptosis and indicate a death by necrosis instead. Further supporting the necrosis hypothesis, the concentration of caspase 3 and 7 did not increase with exposure to UV. Necrosis is considered a caspase-independent process. While it was hypothesized that this low experimental level of UV light exposure (~4mW/cm^2) would increase the induction of apoptosis and concentration of caspase, it has also been shown that a high exposure to UV instead leads to necrosis[20b]. Previous results (Chapter 3) have shown that cells encapsulated in the PEG hydrogel remain viable, however our previous studies did not look at the effect of UV light alone. It is possible that when the photoinitiator is present, LAP absorbs most of the damaging UV rays preventing damage to the cell. Additionally, previous results have shown that cells remain more viable when exposed to UV with LAP compared to other photoinitiators such as Irgacure 2959[24].

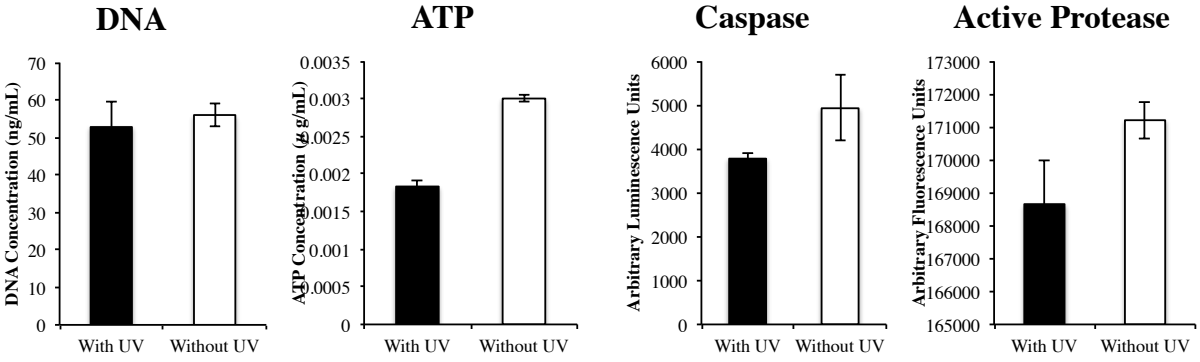

Figure 6-1 Ultraviolet light exposure causes a decrease in ATP, caspase, and active protease concentrations, indicating cellular necrosis. Data presented are averages from 3 experimental replicates, with error bars representing the standard deviation.

6.4.2 Effect of Cell Concentration on OPC viability

As seeding density of other cell types have directly correlated with cell viability[25], preliminary data was obtained to determine if OPC seeding concentration was important here as well. Previous studies in Chapters 2 and 3 were performed with GFP$^+$ MADM cells in gels at 10^7

cells/mL. When fibers were added into the hydrogels from Chapter 3 and 4, the GFP^+ MADM cell concentration was lowered as the high density of cell clusters over time hindered visibility of fiber-cell interactions. Before switching to a lower cell density, three cell concentrations (0.5, 1, and $2x10^6$ cells/mL) were tested in the hydrogel and imaged at day 1 and day 7 (Figure 6-2). Qualitatively, cell viability was not affected by the lower cell concentration.

Figure 6-2 OPC-like cell viability is not affected by encapsulation concentration. Scale bar represents 200 µm. Cell concentrations indicated at the top are in cells/mL.

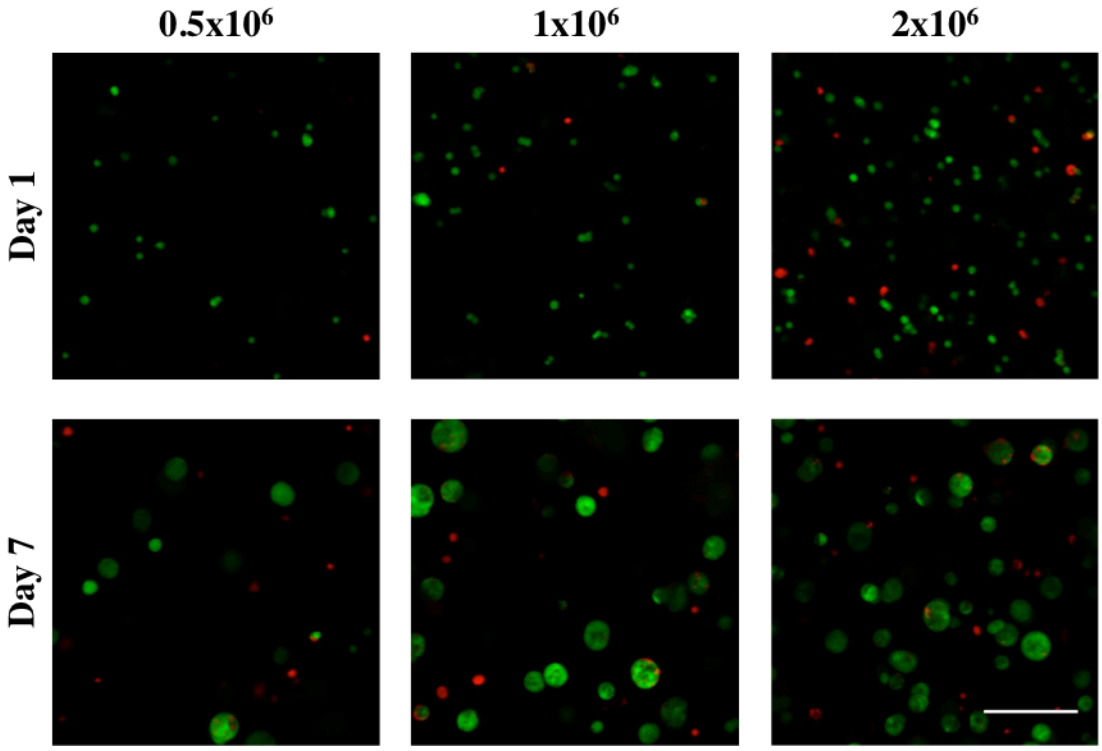

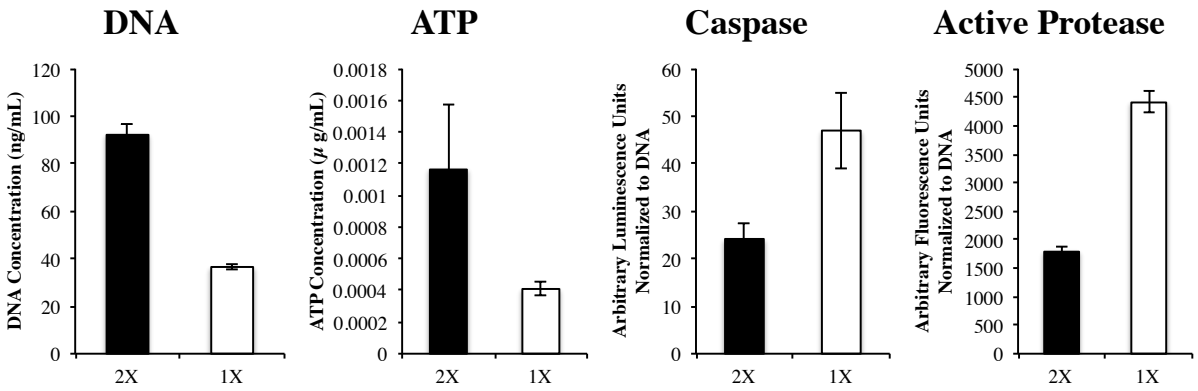

Figure 6-3 Higher number of cells in each well leads to an increase in ATP and a decrease in caspase concentration per cell. 2X indicates $3.5x10^4$ cells/well, while 1X is $1.75x10^4$ cells/well (20 or 40 microliter drops of $8.75x10^5$ cells/mL). Active protease concentration per cell decreases with increase in cell number. Data presented are averages from 3 experimental replicates, with error bars representing the standard deviation.

Upon switching to the primary rat OPC cells, the low yield of primary cells required a lower cell encapsulation concentration in order to test multiple conditions and have sample replicates. In cell studies with fibers, primary OPCs were encapsulated at $8.75x10^5$ cells/mL. This concentration is lower than previous studies where NSCs or neural cell types are often encapsulated on the order of 10^6 to 10^7 cells/mL[26]. However, it was within the range tested with OPC-like cells, which showed no difference in viability compared to higher concentrations (Figure 6-2). We wanted to determine if there was a significant impact of paracrine signaling and cell concentration on cell viability with primary OPCs. Very little is known about the factors OPCs secrete that can guide OPC fate, however it is known that OPCs in the developing brain are at much lower concentrations than neurons or NSCs. In the adult brain, OPCs and oligodendrocytes are significantly lower in cell concentration than neurons[27]. Additionally, OPCs are known to have distinct spatial requirements where they are not in contact with other OPCs or oligodendrocytes [18b].

To determine if the cell concentration impacts viability in these studies, primary OPCs were seeded on polyornithine coated plates at two concentrations (2X and 1X). These concentrations correlated to the gel encapsulation cell number or twice the encapsulation cell number. DNA was measured after 7 days to determine if cells were proliferating or dying and

coming off the plate. DNA was measured at 92.1 ± 4.4 ng/mL for the 2X condition compared to the 1X condition at 36.5 ± 1.0 ng/mL(Figure 6-3). While we would expect that the 2X concentration would measure twice the DNA compared to the 1X condition, this measurement was taken at the end of the experiment after cells have either proliferated or died, detached from the surface, and removed in any of the 3 media changes. These values of DNA where the 2X concentration is 2.5 times greater indicates that cells seeded at the higher concentration either proliferate more than the 1X condition or remain more adherent due to an increase in cell viability. The DNA results, together with the decrease in caspase and protease concentration per cell suggest that fewer cells are undergoing apoptosis when cells are cultured at higher conditions. Additionally, the raw ATP concentration is higher in the more concentrated cell well, suggesting that cells are more metabolically active (Figure 6-3). Furthermore, it has been shown previously that increased cell concentrations are beneficial to cell viability as paracrine signaling has been shown to support the surrounding cells[25]. While increasing cell concentration may be an important factor for viability, the low yield from the OPC isolation process poses a challenge in both increasing the cell concentration and maintaining a sufficient amount of sample replicates. One potential solution is to encapsulate cells at the same concentration in cell clusters rather than single cell suspensions. Cell clusters have previously been shown to enhance cell viability of certain cell types [28]. However, the impact of clusters on viability may be detrimental to OPC viability due to their territorial, spatial requirements for maturation[18b].

6.4.1 3D hydrogels vs. 2D tissue culture

We observed via brightfield microscopy that cells in our 3D PEG hydrogels remained more viable than cells in 2D. Previous data from Figure 5-4 shows that OPCs encapsulated in the 3D PEG hydrogel remained viable over 7 days. There are some dead cells however many still remain alive and stained green with calcein. This observation was surprising as cells seeded on PLL+LN well plates often appeared unhealthy in brightfield microscopy. Most of the cells in the wells remained small and round with jagged edges and cell debris increase with culture time (Figure 6-4). However, in very few instances, we observed cells that closely resembled OPCs with process extension, indicating that some cells can remain viable (Figure 6-4). These observations led us to believe that the PEG hydrogel is beneficial for cell viability and perhaps prevents cellular apoptosis.

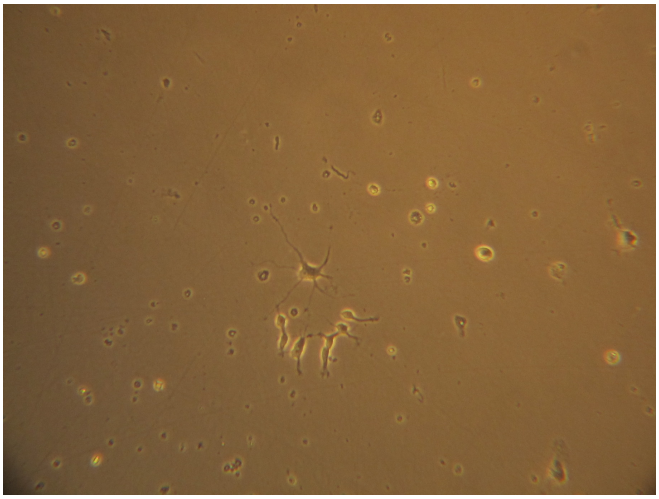

Figure 6-4 Most primary OPCs in 2D cell culture remain rounded. In rare instances, OPCs are seen extending processes. Cell debris is present in 2D.

In order to quantify cell viability of primary OPCs the ATP, DNA, and apoptosis assays were performed on cells in gels, cells in 2D on PLL-coated surfaces wells (poly-l-lysine), and cells in 2d on PLL+LN coated surfaces. DNA results were as expected: PLL and PLL+LN wells were not significantly different while DNA measured from the gel was lower (Figure 6-5). This is not surprising as results in chapter 3 encountered similar results due to the large size of DNA and small gel mesh size. Likely homogenization and sonication of the hydrogel in lysis buffer is still insufficient to completely release DNA from the small hydrogel mesh[29]. However, diffusion of smaller proteins is possible according to observed viability and previous reports[13]. In our experiments, viability did not appear to decrease along the height of the hydrogel, indicating that diffusion of important cell metabolites was unhindered. Additionally, it should be noted that while the mesh size calculated through the Canal and Peppas equation was on the order of 60-130 Angstroms in these PEG based hydrogels[29], the diffusion of large proteins still occurs in under a day in similar systems[13, 30] and the diffusivities of solutes in PEG hydrogels are similar to those in water and other hydrogels[13, 30-31]. Additionally, it should be noted that there were no significant differences between PLL and PLL+LN wells. Over time cells proliferate and DNA concentration increases approximately 2 fold in PLL and PLL+LN wells, 2.23 and 2.12 fold respectively (Figure 6-5). DNA concentrations over time in the gel condition did not change. While differences were insignificant in DNA values for PLL and PLL+L, PLL+LN values were

consistently lower. This could suggest that laminin has an effect on differentiation or regulation in cell number, which has been shown previously in literature [32]. However, previous literature found that laminin null mice had an increase in OPC numbers [33].

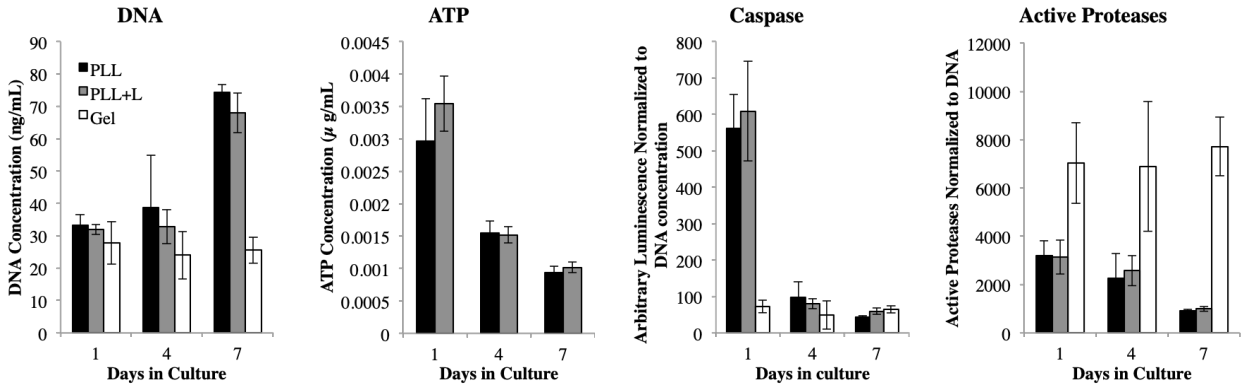

Figure 6-5 Primary OPCs in a gel have lower caspase concentration and higher concentrations of active proteases compared to traditional 2D cell culture. Data presented are averages from 3 experimental replicates, with error bars representing the standard deviation.

Despite the increases in DNA, ATP decreased in all conditions over time. Unfortunately, accurate measures for the gel conditions or day 7 PLL and PLL+LN conditions were not obtained so data from a prior experiment was used. The poor readings were due to an insufficient amount of assay buffer thawed in preparation of the experiment. This meant the readings for the gel conditions and day 7 PLL and PLL+LN conditions were obtained using an old batch of assay buffer which likely had a decrease in luminescence potential and resulted in negative ATP concentrations. This was not realized until after running the next 3 assays when ATP had likely degraded. However, ATP values for the PLL and PLL+LN condition from a prior experiment showed a similar trend for the first 4 days and gave reasonable values over time (Figure 6-5). These results indicate metabolic activity decreases over time. Additionally, PLL and PLL+LN values, while insignificant in differences, suggest that laminin might play a slight role in OPC viability, as ATP values are slightly higher in the PLL+LN condition at each time point. Furthermore, laminin presents integrin binding domains which may help mediate the cell damage and anoikis [34].

Caspase results further support the hypothesis that viability is better in the PEG hydrogel as compared to 2D cell culture (Figure 6-5). Caspase is significantly increased in 2D cell culture

compared to the 3D gel condition after one day. This timing is the first time point collected after the isolation and encapsulation. This result could suggest that encapsulation helped prevent OPCs from undergoing anoikis and becoming apoptotic. The results presented in Figure 6-5 are normalized to the DNA concentration, however it should be noted that raw values of caspase luminescence also suggest that less caspase is present in the gel conditions across 7 days. Protease concentrations were higher in the gel conditions. Cell proteases have been deemed the executioners of cell death, however caspase 3 and 7 are the "terminators of cell death. [35]" These results suggest that cells in gels are perhaps slowly undergoing apoptosis, but that the termination of cell death is delayed compared to traditional 2D culture. Additionally cell proteases are used in numerous cell processes and it is possible that these proteases are not involved in cell death. Regardless, our results suggest that encapsulation of primary OPCs in a PEG hydrogel delay the onset and culmination of apoptosis, more specifically anoikis, increasing the longevity of primary OPCs in *in vitro* culture. Laminin coated plates were hypothesized to enhance cell viability, as cell adhesive domains on laminin and resulting integrin binding directly correlate with anoikis[32]. OPCs are usually cultured on laminin-coated plates, however numerous other cell types are often seeded on laminin free plates. In these conditions, serum is often added into the media. This enables serum proteins, including ECM proteins such as laminin from the serum, to stick down to the plates, similar to the laminin coating protocol. As a result, serum concentration has been shown to directly result in cell viability in 2D and 3D cell culture and prevent anoikis.[36]

While future studies need to be done to determine the effect of laminin coating on OPC cell viability, the results of cells cultured in 2D plates and 3D hydrogels suggest that the 3D environment and resulting mechanical stimuli are more favorable than traditional 2D cell culture regardless of laminin incorporation. Previous studies have shown that mechanical stimuli can promote integrin clustering, such as focal adhesion formation[8]. Furthermore integrin clustering is shown to prevent activation of anoikis pathways[9]. Future studies can investigate the presence of focal adhesions on OPCs in 3D and 2D cell culture to further elucidate the pathway for cell death in 3D versus 2D.

6.5 Conclusion

When cells are exposed to ultraviolet light, caspase concentration decreases, active proteases decrease, and ATP decreases. These results suggest that ultraviolet light alone damages OPCs and impacts cell viability, although perhaps via necrosis rather than apoptosis. While ultraviolet light does appear detrimental to cell viability in the absence of photoinitiator, ultraviolet light with photoinitiator and macromer did not appear to effect cell viability as OPCs remain viable after encapsulations (Figure 5-4). The photoinitiator likely preferentially absorbs damaging UV radiation and initiated radicals are quickly terminated as macromer crosslinking and gelation occur.

Cells seeded at twice the concentration in well plates remain adherent in the well over numerous media changes or proliferate more, indicated by a ratio greater than 2 for the DNA concentrations of 2X: 1X. Cells cultured at a higher concentration in the wells had higher viability than those seeded at a lower concentration. However, it should be noted that OPCs actively avoid contact *in vivo* and *in vitro*[18]. Likely indicating that an upper boundary exists where cell contact is too high for every cell to survive. Cell concentration in 3D needs to be further investigated, as cell concentration in 2D does not directly correlate to 3D concentrations.

When 3D gels were compared to traditional 2D cell culture with the same number of cells, caspase concentration was found to be lower. Despite lower caspase values, higher values in active cell proteases were found from gel lysates. While proteases are used in numerous cell processes, they are employed in cellular apoptosis[35]. Together these trends suggest that encapsulating primary rat OPCs in the PEG based hydrogel may promote long term viability and delay apoptosis. Previously, mechanical stimuli have been shown to guide focal adhesion formation, which can delay anoikis and promote cell viability[7a, 8-9]. The low sample number collected in our studies were not sufficient enough to elucidate differences in PLL and PLL+LN conditions, however it has been previously found that integrin binding domains on laminin are beneficial to many cell types and prevent anoikis[37]. Additional studies should be preformed to determine if laminin incorporation in the hydrogel will further enhance cell viability. However, this was investigated in Chapter 3, where laminin incorporation resulted in minimal changes in viability or cell morphology of the OPC-like cells.

Overall these results suggest the importance simple 3D biomaterials may have on cell viability. Additional modification of the PEG hydrogel may be necessary to further protect cells

from apoptosis and cell death, such as increasing cell concentration, moving towards another gelation initiation scheme, or incorporating bioadhesive ligands.

6.6 References

1. Kessaris, N.; Fogarty, M.; Iannarelli, P.; Grist, M.; Wegner, M.; Richardson, W. D., Competing waves of oligodendrocytes in the forebrain and postnatal elimination of an embryonic lineage. *Nat Neurosci* **2006,** *9* (2), 173-9.
2. Dugas, J. C.; Emery, B., Purification of oligodendrocyte precursor cells from rat cortices by immunopanning. *Cold Spring Harb Protoc* **2013,** *2013* (8), 745-58.
3. Citron, B. A.; Arnold, P. M.; Sebastian, C.; Qin, F.; Malladi, S.; Ameenuddin, S.; Landis, M. E.; Festoff, B. W., Rapid upregulation of caspase-3 in rat spinal cord after injury: mRNA, protein, and cellular localization correlates with apoptotic cell death. *Exp Neurol* **2000,** *166* (2), 213-26.
4. Alanko, J.; Ivaska, J., Integrin "endoadhesome" signaling suppresses anoikis. *Cell Cycle* **2016,** *15* (5), 605-6.
5. Elmore, S., Apoptosis: A Review of Programmed Cell Death. *Toxicol Pathol* **2007,** *35* (4), 495-516.
6. Gilmore, A. P., Anoikis. *Cell Death Differ* **2005,** *12 Suppl 2*, 1473-7.
7. (a) Mitrousis, N.; Fokina, A.; Shoichet, M. S., Biomaterials for cell transplantation. *Nature Reviews Materials* **2018,** *3* (11), 441-456; (b) Gerard, C.; Forest, M. A.; Beauregard, G.; Skuk, D.; Tremblay, J. P., Fibrin gel improves the survival of transplanted myoblasts. *Cell Transplant* **2012,** *21* (1), 127-37.
8. Sigaut, L.; von Bilderling, C.; Bianchi, M.; Burdisso, J. E.; Gastaldi, L.; Pietrasanta, L. I., Live cell imaging reveals focal adhesions mechanoresponses in mammary epithelial cells under sustained equibiaxial stress. *Scientific reports* **2018,** *8* (1), 9788.
9. Sakamoto, S.; Schwarze, S.; Kyprianou, N., Anoikis disruption of focal adhesion-Akt signaling impairs renal cell carcinoma. *Eur Urol* **2011,** *59* (5), 734-44.
10. Smith, E. M.; Mitsi, M.; Nugent, M. A.; Symes, K., PDGF-A interactions with fibronectin reveal a critical role for heparan sulfate in directed cell migration during Xenopus gastrulation. *Proceedings of the National Academy of Sciences of the United States of America* **2009,** *106* (51), 21683-8.
11. J, T.; J, K.-O., Growth Factors in the Extracellular Matrix. *FASEB journal : official publication of the Federation of American Societies for Experimental Biology* **1997,** *11* (1), 51-59.
12. McKinnon, R.; Matsui, T.; Dubois-Dalcq, M.; Aaronson, S., FGF Modulates the PDGF-Driven Pathway of Oligodendrocyte Development. *Neuron* **1990,** *5*, 603-614.
13. Weber, L. M.; Lopez, C. G.; Anseth, K. S., Effects of PEG hydrogel crosslinking density on protein diffusion and encapsulated islet survival and function. *Journal of biomedical materials research. Part A* **2009,** *90* (3), 720-9.
14. Orellana, J. A.; Martinez, A. D.; Retamal, M. A., Gap junction channels and hemichannels in the CNS: regulation by signaling molecules. *Neuropharmacology* **2013,** *75*, 567-82.

15. Domenech, M.; Yu, H.; Warrick, J.; Badders, N. M.; Meyvantsson, I.; Alexander, C. M.; Beebe, D. J., Cellular observations enabled by microculture: paracrine signaling and population demographics. *Integrative biology : quantitative biosciences from nano to macro* **2009,** *1* (3), 267-74.
16. Marinelli, C.; Bertalot, T.; Zusso, M.; Skaper, S. D.; Giusti, P., Systematic Review of Pharmacological Properties of the Oligodendrocyte Lineage. *Frontiers in Cellular Neuroscience* **2016,** *10* (27).
17. Seo, J. H.; Maki, T.; Maeda, M.; Miyamoto, N.; Liang, A. C.; Hayakawa, K.; Pham, L. D.; Suwa, F.; Taguchi, A.; Matsuyama, T.; Ihara, M.; Kim, K. W.; Lo, E. H.; Arai, K., Oligodendrocyte precursor cells support blood-brain barrier integrity via TGF-beta signaling. *PloS one* **2014,** *9* (7), e103174.
18. (a) Kirby, B. B.; Takada, N.; Latimer, A. J.; Shin, J.; Carney, T. J.; Kelsh, R. N.; Appel, B., In vivo time-lapse imaging shows dynamic oligodendrocyte progenitor behavior during zebrafish development. *Nat Neurosci* **2006,** *9* (12), 1506-11; (b) Hughes, E. G.; Kang, S. H.; Fukaya, M.; Bergles, D. E., Oligodendrocyte progenitors balance growth with self-repulsion to achieve homeostasis in the adult brain. *Nat Neurosci* **2013,** *16* (6), 668-76.
19. Kostadinova, R.; Boess, F.; Applegate, D.; Suter, L.; Weiser, T.; Singer, T.; Naughton, B.; Roth, A., A long-term three dimensional liver co-culture system for improved prediction of clinically relevant drug-induced hepatotoxicity. *Toxicol Appl Pharmacol* **2013,** *268* (1), 1-16.
20. (a) Birch-Machin, M. A.; Swalwell, H., How mitochondria record the effects of UV exposure and oxidative stress using human skin as a model tissue. *Mutagenesis* **2010,** *25* (2), 101-7; (b) Caricchio, R.; McPhie, L.; Cohen, P. L., Ultraviolet B Radiation-Induced Cell Death: Critical Role of Ultraviolet Dose in Inflammation and Lupus Autoantigen Redistribution. *The Journal of Immunology* **2003,** *171* (11), 5778-5786; (c) Schmitt, D. A.; Ullrich, S. E., Exposure to Ultraviolet Radiation Causes Dendritic Cells/Macrophages to Secrete Immune-Suppressive IL-12p40 Homodimers. *The Journal of Immunology* **2000,** *165* (6), 3162-3167; (d) Gentile, M., Cell cycle arrest and apoptosis provoked by UV radiation-induced DNA damage are transcriptionally highly divergent responses. *Nucleic Acids Research* **2003,** *31* (16), 4779-4790.
21. Huai, J.; Jockel, L.; Schrader, K.; Borner, C., Role of caspases and non-caspase proteases in cell death. *F1000 Biol Rep* **2010,** *2*.
22. Chang, H. Y.; Yang, X., Poteases for Cell Suicide: Functions and Regulation of Caspases. *Microbiology and Molecular Biology Reviews* **2000,** *64* (4), 821-846.
23. Fink, S. L.; Cookson, B. T., Apoptosis, Pyroptosis, and Necrosis: Mechanistic Description of Dead and Dying Eukaryotic Cells. *Infection and Immunity* **2005,** *73* (4), 1907.
24. Fairbanks, B. D.; Schwartz, M. P.; Bowman, C. N.; Anseth, K. S., Photoinitiated polymerization of PEG-diacrylate with lithium phenyl-2,4,6-trimethylbenzoylphosphinate: polymerization rate and cytocompatibility. *Biomaterials* **2009,** *30* (35), 6702-7.
25. (a) Kim, K.; Dean, D.; Mikos, A. G.; Fisher, J. P., Effect of initial cell seeding density on early osteogenic signal expression of rat bone marrow stromal cells cultured on cross-linked poly(propylene fumarate) disks. *Biomacromolecules* **2009,** *10* (7), 1810-7; (b) Perera, D.; Medini, M.; Seethamraju, D.; Falkowski, R.; White, K.; Olabisi, R. M., The effect of polymer molecular weight and cell seeding density on viability of cells entrapped within PEGDA hydrogel microspheres. *J Microencapsul* **2018,** *35* (5), 475-481.
26. (a) Madl, C. M.; LeSavage, B. L.; Dewi, R. E.; Dinh, C. B.; Stowers, R. S.; Khariton, M.; Lampe, K. J.; Nguyen, D.; Chaudhuri, O.; Enejder, A.; Heilshorn, S. C., Maintenance of neural progenitor cell stemness in 3D hydrogels requires matrix remodelling. *Nature materials* **2017,** *16*

(12), 1233-1242; (b) Lampe, K. J.; Mooney, R. G.; Bjugstad, K. B.; Mahoney, M. J., Effect of macromer weight percent on neural cell growth in 2D and 3D nondegradable PEG hydrogel culture. *Journal of biomedical materials research. Part A* **2010,** *94* (4), 1162-71; (c) Leipzig, N. D.; Shoichet, M. S., The effect of substrate stiffness on adult neural stem cell behavior. *Biomaterials* **2009,** *30* (36), 6867-78; (d) Johnson, P. J.; Tatara, A.; McCreedy, D. A.; Shiu, A.; Sakiyama-Elbert, S. E., Tissue-engineered fibrin scaffolds containing neural progenitors enhance functional recovery in a subacute model of SCI. *Soft matter* **2010,** *6* (20), 5127-5137.
27. von Bartheld, C. S.; Bahney, J.; Herculano-Houzel, S., The search for true numbers of neurons and glial cells in the human brain: A review of 150 years of cell counting. *J Comp Neurol* **2016,** *524* (18), 3865-3895.
28. (a) Gong, X.; Mills, K. L., Large-scale patterning of single cells and cell clusters in hydrogels. *Scientific reports* **2018,** *8* (1), 3849; (b) McMurtrey, R. J., Patterned and functionalized nanofiber scaffolds in three-dimensional hydrogel constructs enhance neurite outgrowth and directional control. *J Neural Eng* **2014,** *11* (6), 066009; (c) Adil, M. M.; Vazin, T.; Ananthanarayanan, B.; Rodrigues, G. M. C.; Rao, A. T.; Kulkarni, R. U.; Miller, E. W.; Kumar, S.; Schaffer, D. V., Engineered hydrogels increase the post-transplantation survival of encapsulated hESC-derived midbrain dopaminergic neurons. *Biomaterials* **2017,** *136*, 1-11.
29. Russell, L. N.; Lampe, K. J., Oligodendrocyte Precursor Cell Viability, Proliferation, and Morphology is Dependent on Mesh Size and Storage Modulus in 3D Poly(ethylene glycol)-Based Hydrogels. *ACS Biomaterials Science & Engineering* **2017**.
30. Zustiak, S. P.; Boukari, H.; Leach, J. B., Solute diffusion and interactions in cross-linked poly(ethylene glycol) hydrogels studied by Fluorescence Correlation Spectroscopy. *Soft matter* **2010,** *6* (15).
31. (a) Johnson, E.; Berk, D.; Jain, R.; Deen, W., Diffusion and Partitioning of Proteins in Charged Agarose Gels. *Biophysical journal* **1995,** *68* (4), 1561-1568; (b) Nauman, J. V.; Campbell, P. G.; Lanni, F.; Anderson, J. L., Diffusion of insulin-like growth factor-I and ribonuclease through fibrin gels. *Biophysical journal* **2007,** *92* (12), 4444-50.
32. (a) Schnaper, H. W.; Kleinman, H. K.; Grant, D. S., Role of laminin in endothelial cell recognition and differentiation. *Kidney International* **1993,** *43* (1), 20-25; (b) Turck, N.; Lefebvre, O.; Gross, I.; Gendry, P.; Kedinger, M.; Simon-Assmann, P.; Launay, J. F., Effect of laminin-1 on intestinal cell differentiation involves inhibition of nuclear nucleolin. *J Cell Physiol* **2006,** *206* (2), 545-55.
33. Relucio, J.; Menezes, M. J.; Miyagoe-Suzuki, Y.; Takeda, S.; Colognato, H., Laminin regulates postnatal oligodendrocyte production by promoting oligodendrocyte progenitor survival in the subventricular zone. *Glia* **2012,** *60* (10), 1451-67.
34. (a) Kodama, K.; Ishii, G.; Miyamoto, S.; Goya, M.; Zhang, S. C.; Sangai, T.; Yoshikawa, T.; Hasebe, T.; Hitomi, Y.; Izumi, K.; Ochiai, A., Laminin 5 expression protects against anoikis at aerogenous spread and lepidic growth of human lung adenocarcinoma. *Int J Cancer* **2005,** *116* (6), 876-84; (b) Vachon, P. H.; Loechel, F.; Xu, H.; Wewer, U. M.; Engvall, E., Merosin and laminin in myogenesis; specific requirement for merosin in myotube stability and survival. *The Journal of Cell Biology* **1996,** *134* (6), 1483.
35. Cryns, V.; Yuan, J., Proteases to die for. *Genes & Dev* **1998,** *12*, 1551-1570.
36. Zvibel, I.; Smets, F.; Soriano, H., Anoikis: Roadblock to Cell Transplantation? *Cell Transplantation* **2002,** *11* (7), 621-630.

37. Gu, J.; Fujibayashi, A.; Yamada, K. M.; Sekiguchi, K., Laminin-10/11 and fibronectin differentially prevent apoptosis induced by serum removal via phosphatidylinositol 3-kinase/Akt- and MEK1/ERK-dependent pathways. *J Biol Chem* **2002,** *277* (22), 19922-8.

7 Conclusions and Future Directions

The work presented in this dissertation focused on creating an *in vitro* neural tissue model. This model utilized a PEG based hydrogel and investigated the effects of hydrogel mechanics, degradability and topography for future implications in the development of multiple sclerosis therapies. This work has implications for both neuroscientists and tissue engineers alike. The easy photopolymerization chemistry enables translatability from material scientists to physician scientists with limited equipment costs, only requiring access to a UV lamp. Neuroscientists may be able to utilize this system in the lab to replace traditional 2D cell culture or expensive *in* vivo experiments. Furthermore, while there are many current biomaterials that either focus on amorphous hydrogels or fibrous systems, very few materials have been investigated that incorporate fibrous topography in amorphous hydrogels[1]. While this idea was designed to mimic the central nervous system and be utilized for multiple sclerosis research, the tunability of our amorphous-fibrous system can be tuned to recapitulate other tissue types or disease states as well.

In this work, PEG-DM hydrogels were made over a range of stiffnesses and mesh sizes, which enabled the encapsulation of two types of OPC-like cells and primary OPCs. Previously, OPCs have rarely been encapsulated in 3D biomaterials[2] and *in vitro* OPC experiments used traditional 2D cell culture methods[3]. These 2D models fail to fully recapitulate many aspects of native tissue, and have substantial limitations in recreating normal CNS tissue[3b]. While the tunability of the PEG hydrogel can ease the investigation of numerous properties, this work focused on three: (1) the effect of hydrogel mechanics, (2) the release of lactic acid and associated degradability of a PEG-PLA-DM hydrogel and (3) the incorporation of electrospun fibers as topographical axon mimics.

First this work elucidated the role of stiffness and mechanical properties of a PEG hydrogel on the proliferation of two OPC-like cell likes. PEG-DM hydrogels were made in the range of 290 to 1560 Pa. OPC-like cells were encapsulated in hydrogels of differing stiffnesses and OPC-like cells were found to proliferate more in the more compliant materials. In the more compliant materials with the largest mesh sizes, cells

formed larger clusters and maintained higher percentages of EdU^+ cell nuclei. Additionally ATP concentrations in gels with the largest mesh size and more compliant storage moduli showed the largest increase over time for both OPC-like cells.

Furthermore, the impact of degradability was investigated in the PEG based hydrogel. PEG-PLA-DM was incorporated into the hydrogel to investigate the effects of lactic acid as an antioxidant and the potential of degradability on cell morphology. Degradability was found to enable cell process extension as the hydrogel mesh is degraded and crosslinking density decreases. Regardless of the potential lactic acid has as a mild antioxidant, neither OPC-like cells and primary rat OPCs showed significant differences in intracellular redox state. These results were confirmed with soluble lactic acid and through the slow release of lactic acid from the hydrogel for OPC-like cells. Because primary rat OPCs are harder to obtain in large quantities, and theoretically more sensitive to reactive oxygen species, these were tested with lactic acid release from the slowly degrading PEG hydrogel. When OPC-like cells were cultured with 1mM of hydrogen peroxide in 3D, OPC-like cells had a more oxidized intracellular redox state measured through the glutathione concentration and mitochondrial staining. However, minimal metabolic differences with exposure to hydrogen peroxide were observed with primary rat OPCs, likely due to poor starting cell viability.

A large portion of this dissertation's studies sought to determine the effect of electrospun fibers as axon mimics on OPC maturation. Fibers were engineered to mimic the diameter and geometry of native neuronal axons. These fibers were incorporated in the hydrogel through two distinct methods that can each be further tuned to mimic different brain or spinal regions. In one method, short cryosectioned fibers were homogeneously incorporated in the degradable PEG hydrogel. In the other, long fiber webs were incorporated. Both fiber conditions were found to increase OPC-like cell viability. In the cryosectioned fiber condition, OPC-like cell proliferation appeared to slow, as noted by smaller cell clusters. In both fiber conditions, cells extended processes towards and potentially around fibers. These results suggest the potential for OPCs to create myelin around the fibers in the 3D hydrogel. However, when qPCR was used to determine if OPCs were maturing, no maturation was evident.

An important observation throughout the course of this thesis work was that while primary rat OPCs generally had poor viability, viability appeared to be enhanced when encapsulated in our PEG hydrogels. We sought to investigate potential factors leading to poor viability and found that exposure to UV light and cell concentration may be critical in increasing cell viability. That being said, viability in 3D hydrogels was noticeably elevated compared to traditional 2D cell culture; cells in 3D had a significantly lower concentration of caspase 3/7 compared to cells in 2D.

Toward the ultimate goal of creating an *in vitro* myelination model, further experiments need to be performed. First and foremost, OPC-like cells behave very differently from primary OPCs and subsequent experiments should be performed with primary cells. The OPC-like cells used in most of these cells are derived from a glioma mouse model[4]. It should be noted that glioma cells behave very different from primary OPCs and are influenced differently by extracellular matrix stiffness, topography, and lactic acid. OPCs secrete low levels of matrix proteins[5], while glioma cells actively secrete many matrix proteins that stiffen the surrounding environment[6]. This suggests that differences in proliferation rate resulting from the stiffness and mesh size of the hydrogel might be different between primary OPCs and OPC-like cells. Cancer cells are known to favor anaerobic respiration resulting in high levels of lactic acid in the cell[7]. Because of this, metabolic and intracellular redox state differences from the release of lactic acid evaluated in chapter 4 were nonexistent with OPC-like cells, while primary OPCs suggested a slight protective effect from the lactic acid in the degradable hydrogel. Further studies can be designed to clarify this trend and should. Cancer cells are known to migrate toward and along fibrous tissue, often migrating along myelinated axons in the CNS [8]. We noticed in earlier work with the OPC-like cells and fiber containing hydrogels when cells were encapsulated at much higher concentrations, the cells appeared to proliferate or migrate down the length of fibers. This apparent growth along the length of fibers is seen with cancer cells [8], while OPCs should instead extend processes toward and wrap around fibers[9]. Though these results predict the ability of OPCs to extend processes in the hydrogel, significant work needs to be done enhancing the viability and response of primary OPCs to the fiber hydrogels.

The main drawbacks of using primary OPCs are the low yield and low viability relative to the time and cost. Subsequent troubleshooting needs to be done to further increase cell viability in the hydrogels. A large reason why qPCR results were inconclusive is likely due to the poor cell viability. Enhancing cell viability is critical before small differences in maturation can be observed. As well as enhancing overall cell viability, OPC viability is highly variable from isolation to isolations. Few samples can be obtained from each batch requiring a significant amount of repeated isolations, which consistently result in large differences in viability. While preliminary data suggested that cells were maturing in the hydrogel, lumping data in from subsequent isolations voided this hypothesis due to the significant cell death. Additionally, topography alone may not adequately guide cell maturation and biochemical factors may need to be incorporated[10]. These experiments were all done in OPC proliferation media, however maturation media with ciliary neurotropic factor[11], forskolin[12], or the hormone T3[13] may enhance maturation.

While this project did not reach the ultimate goal of creating an *in vitro* myelination model, significant strides have been made toward that effect. The poly(ethylene glycol) based hydrogel is a promising biomaterial for neural regeneration as it adequately recapitulates many properties of native brain tissue[14]. Furthermore, the PEG-PLA-DM hydrogel may pose significant advantages in mediating oxidative stress and protecting OPCs. This current setup offers a blank slate with many tunable properties to further enhance maturation and guide myelination. Electrospun fibers can be engineered to release soluble factors[15], or incorporate neuronal surface proteins and bioactive sites[16] to enhance maturation while the PEG hydrogel can be further engineered to incorporate additional degradation or drug release schemes[17]. Fiber concentration or diameter tunability using the incorporation schemes investigated here enables the hydrogels to more closely mimic specific regions of the brain or spinal cord.

Upon creating a valid *in vitro* myelination model, numerous studies can be run to further elucidate (1) the biology and pathology of healthy tissue and neurodegenerative diseases such as multiple sclerosis or (2) develop novel therapies to facilitate regeneration of the myelin sheath. One of the main drawbacks of the widely used multiple sclerosis model, experimental autoimmune encephalomyelitis, is that it affects the CNS

homogeneously rather than displaying the focused, disease lesions prominent in multiple sclerosis. In a hydrogel model system, mechanical stresses or toxin release schemes can be designed to more closely model the disease lesions[18]. With a successful model, potential therapeutics can be investigated at a much cheaper price to determine their role on OPC maturation or extracellular matrix formation.

Further optimization of the hydrogel biomaterial may be necessary to fully recapitulate the CNS microenvironment and develop an adequate tissue model; this material has the possibility of being used in place of expensive *in vivo* models. Many of the current myelination models either occur in vivo or involve coculturing numerous cell types. This model has the potential to decouple cell-cell signaling between different cell types to more easily determine the influence of single parameters without special cell lines or knockout mice. Together, results explained in the dissertation highlight the possibility of our PEG-hydrogel in the development of a novel *in vitro* myelination model. This model has the potential to expand our knowledge on basic OPC maturation biology or develop advanced therapeutics for CNS disease or injury.

7.1 References

1. Mi, H. Y.; Jiang, Y.; Jing, X.; Enriquez, E.; Li, H.; Li, Q.; Turng, L. S., Fabrication of triple-layered vascular grafts composed of silk fibers, polyacrylamide hydrogel, and polyurethane nanofibers with biomimetic mechanical properties. *Mater Sci Eng C Mater Biol Appl* **2019,** *98*, 241-249.
2. (a) Lourenco, T.; Paes de Faria, J.; Bippes, C. A.; Maia, J.; Lopes-da-Silva, J. A.; Relvas, J. B.; Graos, M., Modulation of oligodendrocyte differentiation and maturation by combined biochemical and mechanical cues. *Scientific reports* **2016,** *6*, 21563; (b) Li, X.; Liu, X.; Cui, L.; Brunson, C.; Zhao, W.; Bhat, N. R.; Zhang, N.; Wen, X., Engineering an in situ crosslinkable hydrogel for enhanced remyelination. *FASEB journal : official publication of the Federation of American Societies for Experimental Biology* **2013,** *27* (3), 1127-36.
3. (a) Lee, S.; Chong, S. Y. C.; Tuck, S. J.; Corey, J. M.; Chan, J. R., A rapid and reproducible assay for modeling myelination by oligodendrocytes using engineered nanofibers. *Nature Protocols* **2013,** *8* (4), 771-782; (b) Jarjour, A. A.; Zhang, H.; Bauer, N.; Ffrench-Constant, C.; Williams, A., In vitro modeling of central nervous system myelination and remyelination. *Glia* **2012,** *60* (1), 1-12.

4. Liu, C.; Sage, J. C.; Miller, M. R.; Verhaak, R. G.; Hippenmeyer, S.; Vogel, H.; Foreman, O.; Bronson, R. T.; Nishiyama, A.; Luo, L.; Zong, H., Mosaic analysis with double markers reveals tumor cell of origin in glioma. *Cell* **2011,** *146* (2), 209-21.
5. Yang, Z.; Suzuki, R.; Daniels, S. B.; Brunquell, C. B.; Sala, C. J.; Nishiyama, A., NG2 glial cells provide a favorable substrate for growing axons. *The Journal of neuroscience : the official journal of the Society for Neuroscience* **2006,** *26* (14), 3829-39.
6. CL, G., The Etracellular matrix of gliomas: modulation of cell function. *J Neuropathol Exp Neurol* **1999,** *58* (10), 1029-40.
7. Strickland, M.; Stoll, E. A., Metabolic Reprogramming in Glioma. *Front Cell Dev Biol* **2017,** *5*, 43.
8. Claes, A.; Idema, A. J.; Wesseling, P., Diffuse glioma growth: a guerilla war. *Acta neuropathologica* **2007,** *114* (5), 443-58.
9. Pfeiffer, S. E.; Warrington, A. E.; Bansal, R., The oligodendrocyte and its many cellular processes. *Trends in cell biology* **1993,** *3* (6), 191-7.
10. (a) Mitew, S.; Hay, C. M.; Peckham, H.; Xiao, J.; Koenning, M.; Emery, B., Mechanisms regulating the development of oligodendrocytes and central nervous system myelin. *Neuroscience* **2014,** *276*, 29-47; (b) Snaidero, N.; Simons, M., Myelination at a glance. *J Cell Sci* **2014,** *127* (Pt 14), 2999-3004; (c) Hughes, E. G.; Appel, B., The cell biology of CNS myelination. *Curr Opin Neurobiol* **2016,** *39*, 93-100.
11. Talbott, J. F.; Cao, Q.; Bertram, J.; Nkansah, M.; L., R.; Benton; Lavik, E.; Whittemore, S. R., CNTF promotes the survival and differentiation of adult spinal cord-derived oligodendrocyte precursor cells in vitro but fails to promote remyelination in vivo. *Exp Neurol* **2007,** *204* (1), 485-489.
12. Shi, J.; Marinovich, A.; Barres, B. A., Purification and Characterization of Adult Oligodendrocyte Precursor Cells from the Rat Optic Nerve. *Journal of Neuroscience* **1998,** *18* (12), 4626-4636.
13. Dugas, J. C.; Ibrahim, A.; Barres, B. A., The T3-induced gene KLF9 regulates oligodendrocyte differentiation and myelin regeneration. *Mol Cell Neurosci* **2012,** *50* (1), 45-57.
14. (a) Zustiak, S. P.; Pubill, S.; Ribeiro, A.; Leach, J. B., Hydrolytically degradable poly(ethylene glycol) hydrogel scaffolds as a cell delivery vehicle: Characterization of PC12 cell response. *Biotechnology Progress* **2013,** *29* (5), 1255-1264; (b) Lampe, K. J.; Mooney, R. G.; Bjugstad, K. B.; Mahoney, M. J., Effect of macromer weight percent on neural cell growth in 2D and 3D nondegradable PEG hydrogel culture. *Journal of biomedical materials research. Part A* **2010,** *94* (4), 1162-71.
15. Johnson, C. D.; D'Amato, A. R.; Gilbert, R. J., Electrospun Fibers for Drug Delivery after Spinal Cord Injury and the Effects of Drug Incorporation on Fiber Properties. *Cells Tissues Organs* **2016,** *202* (1-2), 116-135.
16. Kim, I. L.; Khetan, S.; Baker, B. M.; Chen, C. S.; Burdick, J. A., Fibrous hyaluronic acid hydrogels that direct MSC chondrogenesis through mechanical and adhesive cues. *Biomaterials* **2013,** *34* (22), 5571-80.
17. (a) Pinezich, M.; Russell, L.; Murphy, N.; Lampe, K., Encapsulated oligodendrocyte precursor cell fate is dependent on PDGF-AA relesae kinetics in a 3D microparticle-hydrogel drug delivery system. *Journal of biomedical materials research. Part A* **2018,** *106A*, 2403-2411; (b) Janse van Rensburg, A.; Davies, N. H.; Oosthuysen,

A.; Chokoza, C.; Zilla, P.; Bezuidenhout, D., Improved vascularization of porous scaffolds through growth factor delivery from heparinized polyethylene glycol hydrogels. *Acta biomaterialia* **2016**.
18. Tissue-engineered disease models. *Nature Biomedical Engineering* **2018,** *2* (12), 879-880.

8 Appendix A: Chapter 3 Supplemental information

Supplemental information for: LN Russell, KJ Lampe, "Oligodendrocyte Precursor Cell Viability, Proliferation, and Morphology is Dependent on Mesh Size and Storage Modulus in 3D Poly(ethylene glycol) Based Hydrogels," *ACS Biomater. Sci. Eng.* (2017).

Supporting Information. S1:Similar to MADM OPCs, N20.1 OPCs grown in 7.5% (wt/v) PEGDM gels remain viable immediately after encapsulation and for up to 7 days in culture. S2: GFP MADM OPCs grown in hydrogels with laminin occasionally extend short processes or have less rounded clusters (arrows) than when laminin is not incorporated.

S1

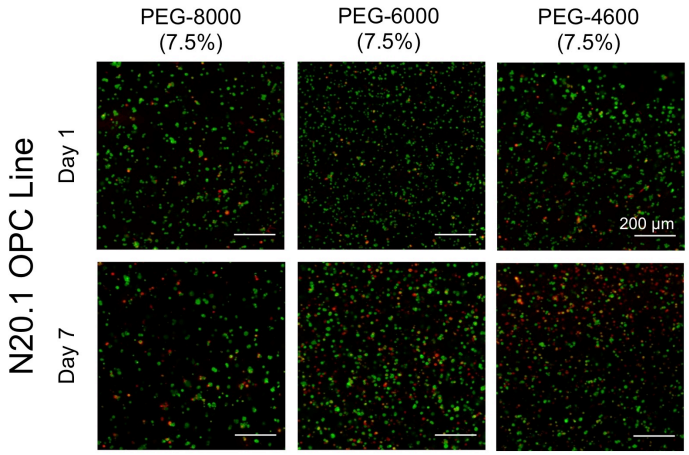

Supplemental 1: Similar to MADM OPCs, N201.1 OPCs grown in 7.5 % (w/v) PEGDM gels remain viable immediately after encapsulation and for up to 7 days in culture. Live (green)/dead (red) Images are max projections of 100µm confocal images.

S2

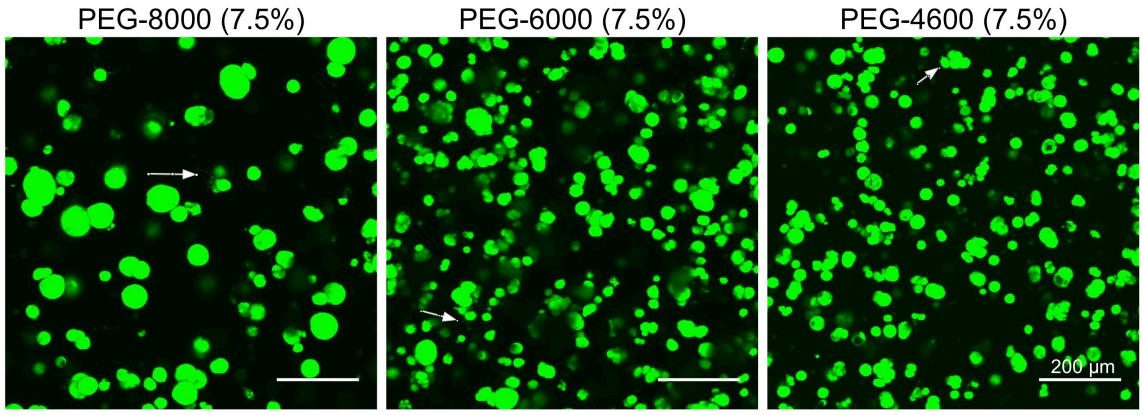

Supplemental 2: GFP+ MADM OPCs grown in hydrogels with laminin occasionally extend processes or have less rounded clusters (arrows) than when laminin is not incorporated. Images are max projections of 100µm think confocal images.

9 Appendix B: List of Publications

MR Pinezich, **LN Russell**, NP Murphy, KJ Lampe, "Encapsulated oligodendrocyte precursor cell fate is dependent on PDGF-AA release kinetics in a 3D microparticle-hydrogel drug delivery system," *Journal for Biomedical Materials Research Part A* 106(9): 2402-2411.

LN Russell, KJ Lampe, "Oligodendrocyte precursor cell viability, proliferation, and morphology is dependent on matrix mechanics in 3D poly(ethylene glycol) based hydrogels," *ACS Biomaterials, Science, and Engineering* 3: 3459-3468 (2017).

LN Russell, KJ Lampe, "Engineering biomaterials to influence oligodendroglial growth, maturation, and myelin production," *Journal of Cells, Tissues, and Organs* 202: 85-101 (2016).

In addition to the above publications, another paper is in the works with collaborators at the Baylor College of Medicine in the department of Thoracic Surgery. This work was presented at the Annual American Association of Thoracic Surgery conference in May 2018. The conference abstract is attached.

Injectable Supraphysiologic PEG Hydrogels Reduce Infarct Strain and Improve Remote Myocardial Function Following Ischemic Injury

Ravi K. Ghanta, MD, Yunge Zhao, MD, PhD, Aarthi Pungazethi, MS, Lauren N. Russell, BS, Kyle J. Lampe, PhD

Objective: Injectable acellular biomaterials may limit adverse ventricular remodeling by thickening or stiffening the infarct region. The relationship of biomaterial mechanical properties on regional ventricular mechanics remains undefined. Consequently, rational biomaterial mechanical design criteria have not been determined. In this study, we hypothesized that a supraphysiologic stiffness material would reduce infarct strain and improve remote ventricular function in an acute and chronic rat infarction model.

Methods: Injectable methacrylated poly(ethylene glycol) (PEG) hydrogels were fabricated using reduction/oxidation polymerization at 3 different mechanical stiffnesses as determined by storage moduli: 4.9 ± 0.3 kPa (Low stiffness; similar to most prior injectable materials), 24.6 ± 1.0 kPa (Normal stiffness; similar to normal rat myocardium), and 249 ± 74 kPa (Supraphysiologic stiffness). All PEG conditions gelled within three minutes of initiation. We evaluated the mechanical effects of intramyocardial injection of the 3 PEG mechanical doses or saline control into the anterior LV wall after LAD ligation in a rat model (n = 20 total; 5 per group). Regional mechanics, LV volume, and cardiac output were measured using sonomicrometry at baseline, 30 minutes after LAD ligation, and 30 minutes after PEG injection. We then utilized Cardiac MRI and DENSE imaging to measure chronic regional strain 1 week post injection of saline or supraphysiologic stiffness PEG. (n=4; 2 per group)

Results: Following infarction, all subjects demonstrated increased LV EDP, decreased cardiac output, and rightward shift of the end-systolic pressure-volume relationship (ESPVR). Infarct areas demonstrated passive stretch instead of contraction during systole. PEG hydrogel injection reduced infarct strain and increased remote myocardial strain dependent on the mechanical dose administered (Figure). Only supraphysiologic PEG reduced infarct area stretch (+0.15 ± 0.01 control vs 0.00 ± 0.001 PEG; $p<0.05$) and

improved remote area strain (-0.93 ± 0.02 control vs -1.31 ± 0.01 PEG; p<0.05). Furthermore high stiffness PEG gel shifted the ESPVR leftward, indicating improved pump function. After 1 week, high stiffness PEG sustained prevention of infarct stretch (+0.10 ± 0.02 control vs 0.00 ± 0.01 PEG; p<0.05) and improvement in remote myocardial function (-0.12 ± 0.01 vs 0.20 ± 0.02; p<0.05).

Conclusions: Low stiffness injectable biomaterials do not affect post-infarct regional mechanics. High supraphysiologic stiff materials eliminate infarct strain and improve remote myocardial mechanics. Injectable biomaterials with mechanical properties that exceed the stiffness of native myocardium may maximize efficacy of therapy.

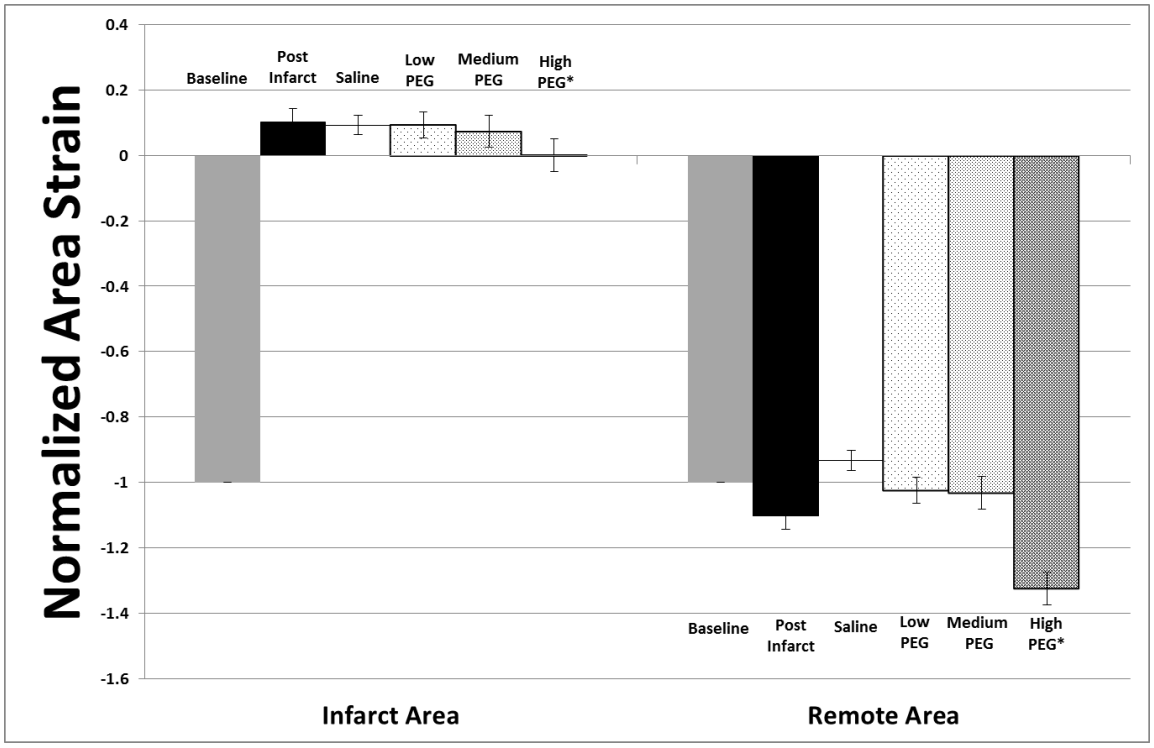

Figure 1. Changes in Infarct Area and Remote Area Systolic Strain. *p<0.05 for change from Post Infarct